ISTANBUL TECHNICAL UNIVERSITY ★ INSTITUTE OF SCIENCE AND TECHNOLOGY

CONSTRUCTION OF GFP BASED DESIGNER PROTEINS

Ph.D. Thesis by
Esra YÜCA

Department : **Advanced Technologies**

Programme : **Molecular Biology-Genetics and Biotechnology**

Thesis Supervisor: **Prof. Dr. Candan TAMERLER**

DECEMBER 2010

ISTANBUL TECHNICAL UNIVERSITY ★ INSTITUTE OF SCIENCE AND TECHNOLOGY

CONSTRUCTION OF GFP BASED DESIGNER PROTEINS

Ph.D. Thesis by
Esra YÜCA
(521042213)

Date of submission : 21 September 2010
Date of defence examination: 23 December 2010

Supervisor (Chairman) : **Prof. Dr. Candan TAMERLER (ITU)**
Members of the Examining Committee : **Assoc. Prof. Dr. Ayten YAZGAN KARATAŞ (ITU)**
Prof. Dr. Mehmet SARIKAYA (UW)
Prof. Dr. Mustafa ÜRGEN (ITU)
Assoc. Prof. Dr. Nevin GÜL KARAGÜLER (ITU)
Assis. Prof. Dr. Fatma Neşe KÖK (ITU)
Assis. Prof. Dr. Şenay VURAL KORKUT (YTU)

DECEMBER 2010

İSTANBUL TEKNİK ÜNİVERSİTESİ ★ FEN BİLİMLERİ ENSTİTÜSÜ

GFP BAZLI TASARIM PROTEİNLERİNİN OLUŞTURULMASI

DOKTORA TEZİ
Esra YÜCA
(521042213)

Tezin Enstitüye Verildiği Tarih : 21 Eylül 2010
Tezin Savunulduğu Tarih : 23 Aralık 2010

Tez Danışmanı : Prof. Dr. Candan TAMERLER (İTÜ)
Diğer Jüri Üyeleri : Doç. Dr. Ayten YAZGAN KARATAŞ (İTÜ)
Prof. Dr. Mehmet SARIKAYA (UW)
Prof. Dr. Mustafa ÜRGEN (İTÜ)
Doç. Dr. Nevin GÜL KARAGÜLER (İTÜ)
Yrd. Doç. Dr. Fatma NEŞE KÖK (İTÜ)
Yrd. Doç. Dr. Şenay VURAL KORKUT (YTÜ)

ARALIK 2010

FOREWORD

First and foremost I would like to express my deepest and sincere gratitude to my advisors Professor Candan TAMERLER and Associate Professor Ayten YAZGAN KARATAŞ, for their excellent guidance, valuble suggestions, caring and patience. I would never have been able to finish my dissertation without their comments and criticisms. I am deeply indebted to them.

I would like to take an opportunity here to acknowledge Professor Mehmet SARIKAYA for giving me the opportunity to visit his labs and providing me expert advice and guidance. It has been a great experience to work in his labs.

I would like to thank to Professor Mustafa ÜRGEN and Assistant Professor Fatma Neşe KÖK for participation as my committee members and for their time to review my dissertation.

I would like to express my gratitude to Yildiz Technical University for their great support.

I am thankful to Günseli GÜR, Öykü İRİGÜL, Ebru KÖROĞLU, for being great and supportive lab mates.

I would like to thank to Dr. Urartu ŞEKER, Dr. Turgay KAÇAR and Mustafa GÜNGÖRMÜŞ for their help and support both in and outside the lab. I would also like to thank to Dr. Marketa HNILOVA and Carol JIA for their help on the immobilization study. I am also very thankful to my colleagues Deniz ŞAHİN, Sibel ÇETİNEL, Hilal YAZICI, Emel ORDU. I would like to send my special thanks to Dr. Şermin UTKU for her support.

I would like to thank to the funding agencies for their financial support: GEMSEC (Genetically Engineered Materials and Engineering Center) through NSF-MRSEC at the UW, ITU Institute of Science and Technology through Turkish State Planning Organization and TUBITAK/NSF-IRES joint project 107T250.

Last but not the least, I would like to acknowledge and deeply thank to my parents for their love, support and confidence.

September 2010

Esra Yüca

Molecular Biologist

TABLE OF CONTENTS

Page

ABBREVIATIONS

AgBP	**:** Silver binding peptide
AuBP	**:** Gold binding peptide
E. coli	**:** Escherichia coli
FM	**:** Fluorescence miroscopy
GFP	**:** Green fluorescent protein
GEPI	**:** Genetically engineered polypeptides for inorganics
GFPuv-HABP	**:** Genetic fusion of GFPuv and HABP
GFPuv-AgBP2c	**:** Genetic fusion of GFPuv and AgBP2c
HABP	**:** Hydroxyapatite binding peptide
IPTG	**:** Isopropyl B-D-1-thiogalactopyranoside
MBP	**:** Maltose binding protein
MBP-GFPuv	: Genetic fusion of MBP and GFPuv
MBP-GFPuv-AgBP	**:** Genetic fusion of MBP, GFPuv and AgBP
MBP-GFPuv-AuBP	**:** Genetic fusion of MBP, GFPuv and AuBP
PDMS	**:** Polydimethylsiloxane
QCM	**:** Quartz crystalline microbalance

LIST OF TABLES

Page

LIST OF FIGURES

Page

CONSTRUCTION OF GFP BASED DESIGNER PROTEINS

SUMMARY

In nanotechnological applications, peptide and protein related materials are exploited as smart building blocks. In nature, molecular recognition based functions are a key role in evolution, sequential cycles of mutation and selection are part of improved progeny. In nature there are various examples of functional biological materials and systems that proteins control the formation and the morphology of inorganics.

In recent years, not only in hard tissue engineering but also in producing advance materials and systems, biomimetic synthesis and formation of inorganics using biological routes have attracted a great interest. In this study, we focus on addressing biological routes for materials labelling and assembly using genetically engineered proteins. We designed multifunctional proteins that can target inorganic materials specifically and still carry their biological functionality. Here, we selected two different case study based on calcium phosphate mineral, and metal surface/NP interactions through designing engineered green fluorescence proteins.

Calcium phosphate based biomineralization is studied extensively due to its key role in the bone and dental hard tissue formation. We therefore, designed a protein based system that can target calcium phosphate minerals and allows monitoring of biomineralization, namely GFPuv-HABP. Fluorescence and binding activities of bi-functional proteins were characterized using fluorescence microscopy and spectroscopy, and quartz crystal microbalance system, respectively. The utility of GFPuv-HABP1 fusion protein was assessed for both time-wise mineralization monitoring and visualization of mineralized tissues.

In biotechnology, site-specific protein immobilization is required for the fabrication of efficient tools such as protein chips, biosensors and microarrays. The conventional methods, including physical and chemical immobilizations are also applicable for protein immobilization. However, these approaches may cause a decrease in protein activity due to the uncontrolled assembly following interaction between functional groups of the protein and the surface. Here we employed peptide based assembly where inorganic binding peptides were used for the directed immobilization of a functional protein GFPuv on silver and gold substrates with different forms, as flat surfaces and nanoaprticles. The correlation between the binding of bifunctional proteins to nanoparticles and fluorescence quenching/enhancement efficiency was evaluated.

Finally, we demonstrated that genetically engineered peptides for inorganics (GEPI) can be inserted into functional proteins and GEPI-GFP can be used in diverse areas from labelling minerals to quenching flurorescence activity in a controlled manner.

GFP BAZLI TASARIM PROTEİNLERİNİN OLUŞTURULMASI

ÖZET

Nanoteknolojik uygulamalarda, peptit ve proteinlerle ilgili malzemeler akıllı yapıtaşları olarak kullanılırlar. Doğada moleküler tanımaya dayalı işlevler evrimde anahtar bir rol alırlar, ardışık mutasyon ve seçilim döngüleri iyileştirilmiş neslin bir parçasıdır. Doğada proteinlerin anorganiklerin oluşumunu ve morfolojisini kontrol ettiği pek çok işlevsel biyolojik malzeme ve sistem örneği vardır.

Son yıllarda, yalnızca sert doku mühendisliğinde değil, aynı zamanda ileri malzeme ve sistemlerin üretiminde, anorganiklerin biyolojik yolla biyobenzetimsel sentez ve oluşumu oldukça ilgi çekmektedir. Bu çalışmada, genetik mühendisliği ile iyileştirilmiş proteinlerin malzemenin etiketlenmesi ve kurulumu için biyolojik yollara yönelmeye odaklandık. Anorganik malzemeyi özgül olarak hedefleyen ve biyolojik fonksiyonlarını hala sürdüren multifonksiyonel proteinler tasarladık. Burada, genetik mühendisliği uygulanmış yeşil floresan proteinlerinin tasarlamasıyla, kalsiyum fosfat mineral ve metal yüzey/nanopartikül etkileşimlerine dayalı iki farklı durum çalışması seçtik.

Kalsiyum fosfat bazlı biyomineralizasyon, kemik ve diş sert dokularının oluşumundaki anahtar rolü nedeniyle yaygın olarak çalışılmıştır. Bu nedenle, kalsiyum fosfat minerallerini hedefleyen ve biyomineralizasyonun görüntülenmesini mümkün kılan protein bazlı bir sistemi yani GFPuv-HABP'yi tasarladık. Çift fonksiyonlu proteinlerin floresan ve bağlanma aktiviteleri, sırasıyla floresan mikroskopi ve spektroskopi ile kuartz kristal mikrobalans sistemi kullanılarak karakterize edilmiştir. GFPuv-HABP1 füzyon proteinin kullanımı, zamansal mineralizasyonu izleme ve mineralleşen dokuların görüntülenmesi açısından değerlendirilmiştir.

Biyoteknolojide, bölgeye özgül protein immobilizasyonu protein çipleri, biyosensörler ve mikroarrayler gibi etkin araçların üretiminde gereklidir. Fiziksel ve kimyasal immobilizasyonu kapsayan geleneksel yöntemlerin, protein immobilizasyonu için de uygulanabilirliği vardır. Ancak, bu yaklaşımlar, proteinin fonsiyonel gurupları ile yüzey arasındaki etkileşimleri izleyen kontolsüz toplanma sebebiyle protein aktivitesinde düşüşe neden olabilir. Burada, anorganiklere bağlanan peptidlerin, fonksiyonel protein GFPuvnin düz yüzey ya da nanopartikül şeklinde farklı formlardaki gümüş ve altın substrata immobilizasyonunda kullanılmasında, peptit bazlı kurulumdan faydalanılmıştır. Bifonksiyonel proteinlerin nanopartiküllere bağlanması ve floresan sönüm/artma etkinliği arasındaki korelasyon değerlendirilmiştir.

Son olarak, genetik mühendisliği ile iyileştirilmiş anorganiklere bağlanan peptitlerin (GEPI) fonksiyonel proteinlere yerleştirilebileceğini, GEPI-GFP'nin kontrollü biçimde, minerallerin etiketlenmesinden floresan sönme aktivitesine kadar çeşitli alanlarda kullanılabileceğini gösterdik.

1. INTRODUCTION

1.1 Nano- and Bionanotechnology

Nanotechnology was first introduced by Nobel laureate Richard P. Feynman (1959) in his lecture, “There’s Plenty of Room at the Bottom”. Since his consideration for the possibility of direct manipulation of individual atoms, there have been many critical developments in physics, chemistry, and biology that have represented Feynman’s vision. This vision also paved the way first towards biomimetic material processing, then using biology as a guide to realize nanotechnology (Sarikaya and Aksay, 1995, Mann, 1996, Sarikaya, 1999, Whaley et al., 2000).

The specificity and the recognition funcions of peptide and protein based materials are exploited as building blocks in nanotechnology to fabricate useful functional structures and devices (Woodbury et al., 1998, Sarikaya, 1999, Brown, 2001, Sarikaya et al., 2003, Sarikaya et al., 2004, Kacar et al., 2009a). Nanotechnology has been commonly defined as “the understanding, control, and restructuring of matter on the order of nanometers to create materials with fundamentally new properties and functions”. “Topdown” and “bottom-up” approaches are the two main approaches in nanotechnology . There is not any atomic level control for topdown approach. In this approach, structures are reduced to nanoscale size and the original properties of matter are maintained. The “bottom-up” approach is also called as molecular nanotechnology or molecular manufacturing. In this approach, materials are engineered by assembly or self-assembly mechanism from atoms or molecules (Drexler, 1995, Sanchez and Sobolev, 2010). Bionanotechnology is the integration of biology and nanotechnology. Molecular biomimetics, proposed by Sarikaya et al., can be considered as a promising path to realizing nano- and bionanotechnology. In molecular biomimetics, hybrid technologies are developed by using the tools of molecular biology and nanotechnology (Sarikaya, 1999, Sarikaya et al., 2003, Tamerler et al., 2010).

Engineering materials at molecular level is possible by exploiting molecular biomimetics. Short amino acid sequences that can specifically bind to inorganics and be selected using combinatorial techniques can be further engineered. These small peptides can be synthesized easily by chemical and genetic engineering procedures and they became an important component of the bionanotechnological studies (Sarikaya, 1999, Sarikaya et al., 2003, Tamerler and Sarikaya, 2009a).

1.2 Lessons From Nature

Proteins are the major building blocks of biological systems from the simplest forms to mammalian species. Specific interactions of these building blocks sustain the viability of organisms. Formation of controlled structures at all scales in the system depends on biomolecule-material interaction which is accomplished with molecular specificity and efficiency (Sarikaya et al., 2003, Tamerler and Sarikaya, 2009b, Tamerler et al., 2010).

In traditional materials science engineering, materials are produced using a group of methods, including melting and solidification, thermomechanical treatments, solution/vacuum deposition and growth. In nature, molecular recognition and functions are tested, improved and developed by evolutionary selection process, sequential cycles of mutation and selection (Sarikaya et al., 2003).

There are many examples in nature of functional biological materials and systems that proteins control the formation (Tamerler et al., 2010). A magnetotactic bacterium Aquaspirillum magnetotacticum which can sense the Earth's magnetic field has a magnetic nanoparticle system (Figure 1.1A) incorporating aligned magnetosomes, protein and lipid based membrane compartments (Sarikaya et al., 2004, Tamerler et al., 2010).

The second example is mother of pearl, nacre, of seashells (Figure 1.1B). Nacre is a segmented laminated composite of aragonite (orthorhombic calcium carbonate) and biomolecules in the interior with superior mechanical properties. It is now possible to understand, engineer, and control peptide molecular recognition and peptide-material interaction (Tamerler et al., 2010).

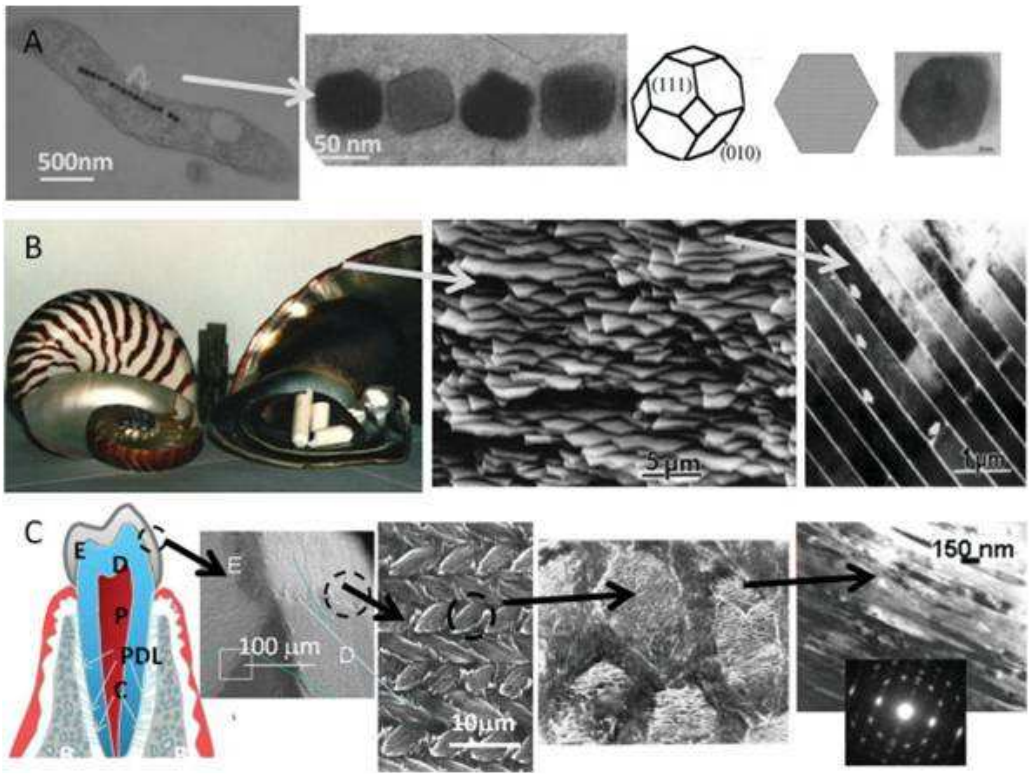

Figure 1.1 : Functional biological materials systems. A) A magnetotactic bacterium Aquaspirillum magnetotacticum has a magnetic nanoparticle system B) Nacre of seashells. C) Mammalian tooth composed of enamel (E), dentin (D), pulp (P), cementum (C) and periodontal ligaments (Tamerler et al., 2010).

The third example is enamel, the hardest material in the body, protecting the dental tissues. Enamel is integrated to the softer tissue dentin. Tougher bone-like tissue, enamel, prevents premature fracture or failure through absorbing energy during mastication and cutting. Hierarchically ordered woven structure of mammalian tooth enamel is controlled by proteins. This structure consist of thousands of 30 nm-diameter, mm-long hydroxyapatite (HA) crystallites (Figure 1.1C). More than 40 different proteins are known to take part in the enamel formation. Studies on these proteins and understanding their effects on biofabrication of dental tissues would provide developments for regeneration or restoration of hard tissues including enamel (Fong et al., 2003, Tamerler et al., 2007a, Tamerler et al., 2010).

Another example is an deep-sea sponce Rosella racovitzea which has silica based spicules that collect and transmit light effectively. The spicules' star shaped tips collect light and the silica based optical fiber shaft transmits light 200 m under the ocean (Figure 1.2). Both parts of the spicules are composites of silica and proteins

that makes possible the structural and functional properties of the system (Tamerler et al., 2007b; Tamerler and Sarikaya, 2009a).

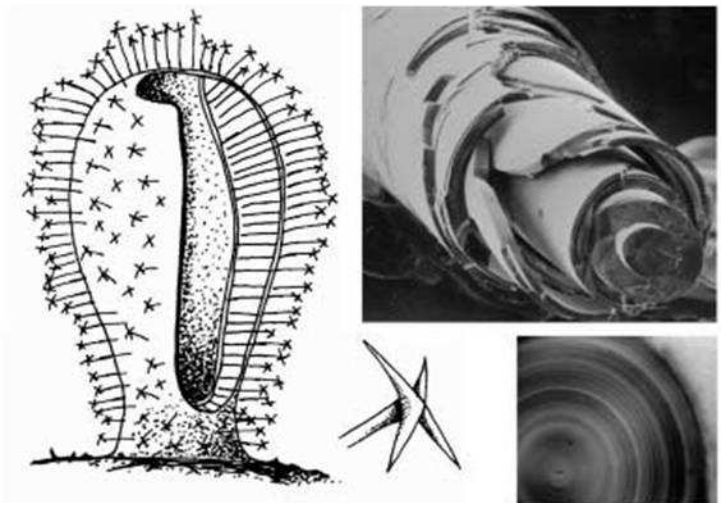

Figure 1.2 : Spicules of Rosella rocavitzea are made of layered amorphous silica. The tip of the spicule is a star shaped lens (Tamerler and Sarikaya, 2009a).

1.3 Designing and Engineering of Proteins

The diverse interactions between a variety of hydrophobic, polar and ionizable side chains of proteins cause their structural and functional complexity. Therefore it is difficult to predict the structure and function of a protein from its primary sequence.

The high amount of sequence information obtained from genome projects is available and it has been shown that abnormal protein structures give rise to certain diseases. The progress in protein structure and function research including these examples has led to new studies on designing proteins with desired properties. Research areas including knowledge-based structure prediction, protein stability, protein–protein and protein–ligand interactions, enzyme catalysis and protein design provide information about structure-function relationship and lead to new developments in protein science (Lilie, 2003).

It is important to purify proteins in high amount for most applications ranging from biotechnology to medicine by using recombinant methods or by peptide synthesis as many kinds of proteins in their native sources are not aboundant enough to be extracted.

In the recombinant production approach, cloning strategies should be carefully chosen in order to make designed recombinant proteins which are well expressed in the host organism. In addition to this, proteins should be soluble form without any loss in original activity. Using Escherichia coli as a recombinant host is cost effective and provides the scalable and fast expression The process for obtaining a synthetic peptide starts with designing. Following this are the chemical synthesis, evaluation and purification steps (Grant, 2002).

Creating designed interfaces using solid-binding peptides between biological and material sciences may provide opportunities for the fabrication of novel practical systems (Tamerler and Sarikaya, 2009a). Model of mutant pIII protein of M13 phage, representing a functional protein containing a solid binding peptide (quartzbinding peptide) binding to the surface (quartz (100)) is shown in Figure 1.3.

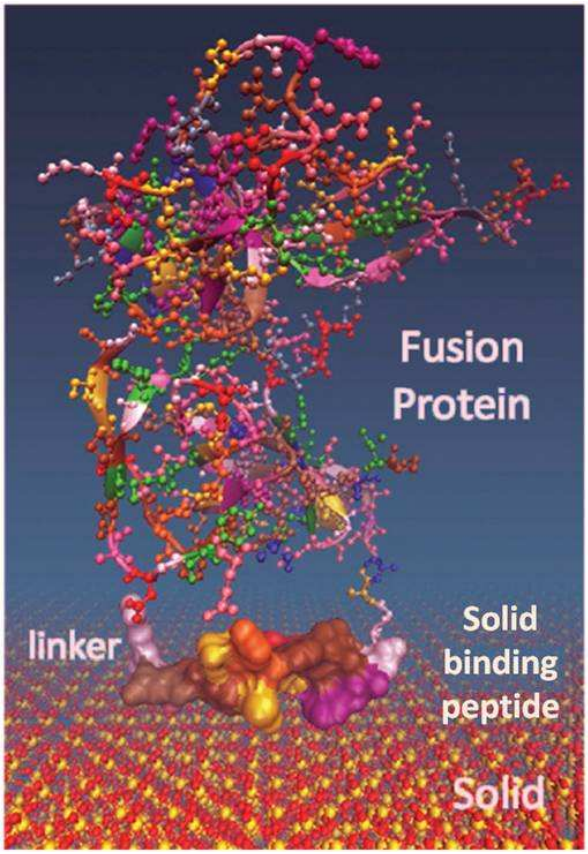

Figure 1.3 : Model of a designed peptide. Mutant pIII protein of M13 phage, representing a functional protein containing a solid binding peptide (quartzbinding peptide) binding to the quartz (100) surface (Tamerler and Sarikaya, 2009a).

1.4 Molecular Biomimetics

Biomolecules, mainly proteins and inorganic components are essential for synthesis, assembly and function of the section 1.2 given examples and other biological materials and hard tissues. Proteins control nucleation, growth and assembly of biological tissues at the nano, meso and macroscales. For understanding the biochemical and biophysical nature and the practical utilization of these proteins, studies on simple polypeptides with specific functions could be carried besides the genomic and proteomic research. With the new emerging field, molecular biomimetics, peptides can be selected and engineered to molecularly recognize the specific inorganic surface (Mayer and Sarikaya, 2002, Fong et al., 2003, Sarikaya et al., 2003, Sarikaya et al., 2004, Tamerler et al., 2007a, Tamerler and Sarikaya, 2009b).

With their highly controlled nonastructures, biocomposites have advantages over the synthetic structures (Lowenstam et al., 1984, Sarikaya, 1999, Ball, 2001). Researchers have been emulated or inspired from nature to design useful materials and systems generally using synthetic components and conventional methods in the traditional biomimetics approach (Mann, 1993, Seeman and Belcher, 2002). Molecular biomimetics, a promising route for material assembly, fabrication and application of technologically exquisite materials, has been an emerging field based on recent advances in molecular biology and engineering and physical sciences. In addition to traditional biomimetics aspects emulating or duplicating biosystems, it can be possible to engineer materials at molecular level based on molecular biomimetics approach (Sarikaya 1999, Seeman and Belcher, 2002, Sarikaya et al., 2003, Tamerler et al., 2010).

1.4.1 Inorganic binding peptides

It is now possible to understand, engineer, and control peptide molecular recognition and peptide-material interaction. The utilization of combinatorial screening techniques has recently led to development of a large number of novel peptides that can specifically bind with inorganic substrate (Sarikaya et al., 2003, Tamerler et al., 2010).

Short peptides with specificity to a variety of materials have been selected through both cell surface or phage display methods. After selection, further experiments have

been applied to determine the binding kinetics and surface stability of these short peptides called as genetically engineered peptides for inorganics, i.e., GEPIs (Sarikaya et al., 2003, Tamerler et al., 2010).

Peptide sequences that are specific to a myriad of inorganic materials including noble metals, e.g., gold (Brown et al., 2000, Huang et al., 2005, Hnilova et al., 2008), silver (Naik et al., 2002, Nam et al., 2008, Hnilova et al., unpublished data), and platinum (Seker et al., 2007)), oxides, e.g., SiO_2 (Oren et al., 2007; Tamerler, 2007a), ZnO (Thai et al., 2004), Cu_2O (Thai et al., 2004), TiO2 (Sano and Shiba 2003; Sano et al., 2005, Dickerson et al., 2008), minerals, hydroxyapatite (Gungormus et al., 2008, Roy et al., 2008), calcite (Gaskin et al., 2000)), sapphire (Krauland et al., 2007)) and semiconductors (e.g., GaAs (Whaley et al., 2000), ZnS and CdS (Lee et al., 2002)) have been identified.

1.4.1.1 Combinatorial selection

Combinatorial selection techniques such as phage display (Smith 1985, Hoess, 2001) and cell surface display (Wittrup, 2001) have been exploited for various biological applications including identifying the ligands, mapping the molecular recognition site of the antibodies and indicating the affinity and specificity for a certain molecule in the design of new drugs and agents (Smith and Petrenko 1997, Petrounia and Arnold 2000, Benhar, 2001, Rosander et al., 2002).

Combinatorial selection protocols can be used to select polypeptides that bind to the inorganics that have unique physical properties in nano and biotechnology. Oligonucleotides encoding random sequences of aminoacids are inserted into phage genomes or into bacterial plasmids for the generation of phage and cell surface display libraries. The randomized aminoacid sequences which are incorporated with proteins like the coat protein of the phage or the outer membrane or flagellar protein of a bacterium are expressed on the surface of the organism. Eventually, each organism produces different and random peptide (Brown et al., 2000; Whaley et al., 2000).

The mixture of recombinant cells or phages are exposed to the inorganic surface of interest. Following washing cycles to eliminate non-binder phages or cells, binders are eluted from the material surface. Weak interactions with the surface are disrupted during the washing step. After this step, phages and cells are amplified and a round

of biopanning is completed. To obtain strong binders three to five rounds are repeated (Tamerler and Sarikaya, 2008). After the biopanning rounds, clons carrying the peptides binding to the inorganic material are sequenced to obtain the DNA sequences (Figure 1.4).

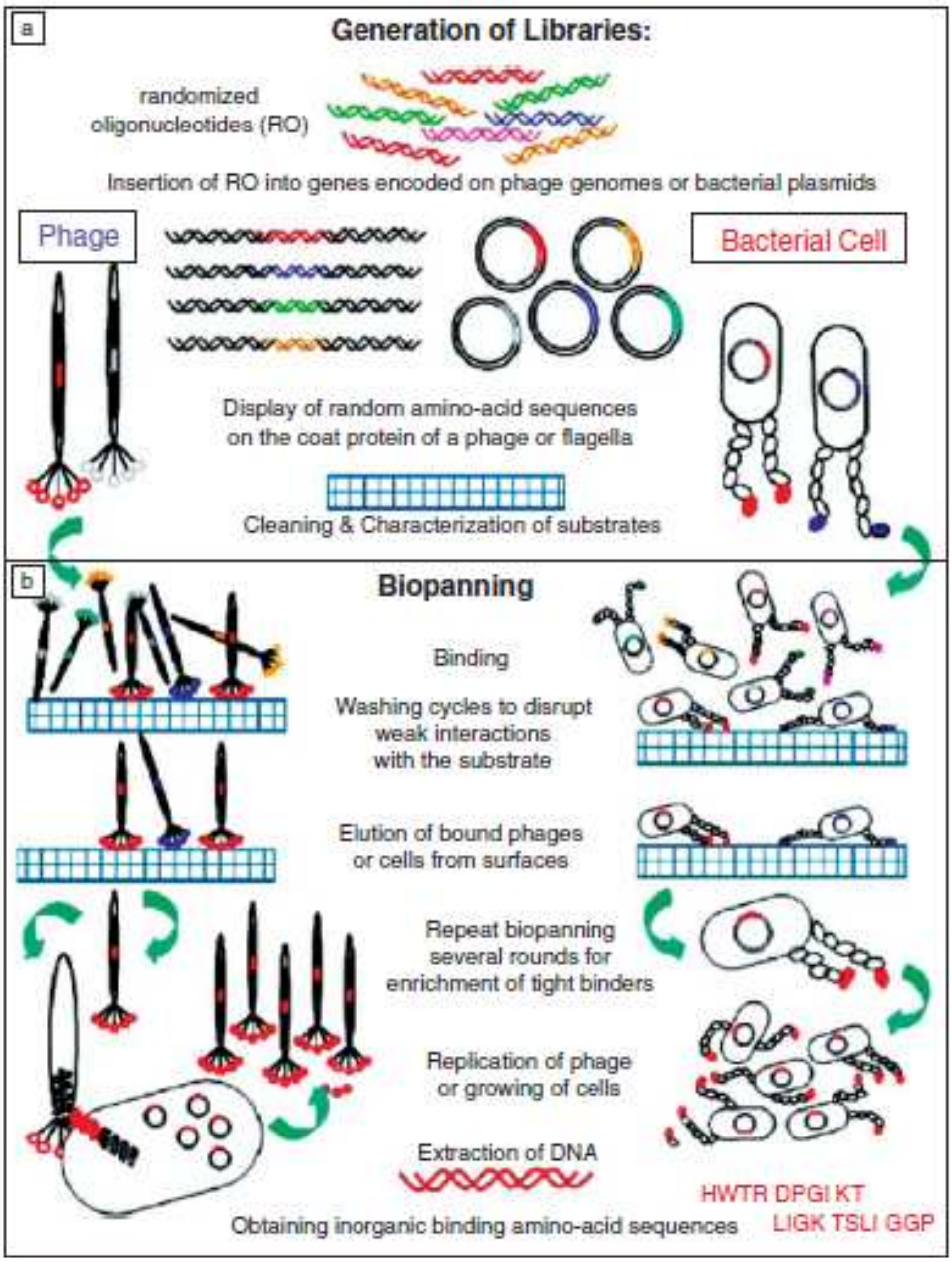

Figure 1.4 : Combinatorial selection of GEPIs (Tamerler and Sarikaya, 2008).

Outer membrane proteins, lipoproteins,fimbria and flagellar proteins have been used for cell surface display while coat proteins are used for the phage display.

1.4.1.2 Molecular characterization of GEPIs

Binding characteristics of GEPIs can be tested by microscopic or spectroscopic analyses such as fluorescence microscopy or surface plasmon resonance spectroscopy (SPR) and quartz crystal microbalance (QCM). SPR and QCM determine the specificity and kinetics of the molecular binding of peptides to certain surfaces (Tamerler et al., 2006b, Seker et al., 2007, Tamerler et al., 2007a). These methods may have limitations for the studies on small molecules (Bailey et al., 2002). The detailed molecular structure of the inorganic binder peptides can be characterized by circular dichroism (CD) and nuclear magnetic resonance (NMR) spectroscopy (Kulp et al., 2004). In the Figure 1.5, CD and NMR data are shown for hydroxyapatite binding peptides, HABP1, HABP2 and 3 repeat gold binding peptides, 3rGBP1, respectively (Tamerler and Sarikaya, 2008). Another step for molecular characterization is computational modelling to understand the molecular conformation and mechanism of crystallographic surface recognition in the absence of the structural experimental data (Barth et al., 2005, Oren et al., 2007, Tomasio and Walsh, 2007). Supramolecular selfassembly and surface coverage of GEPIs can be visualised by atomic force microscopy (AFM). Quantitative data and nanostructure images obtained by AFM is important for specific application of GEPIs (Tamerler and Sarikaya, 2007a).

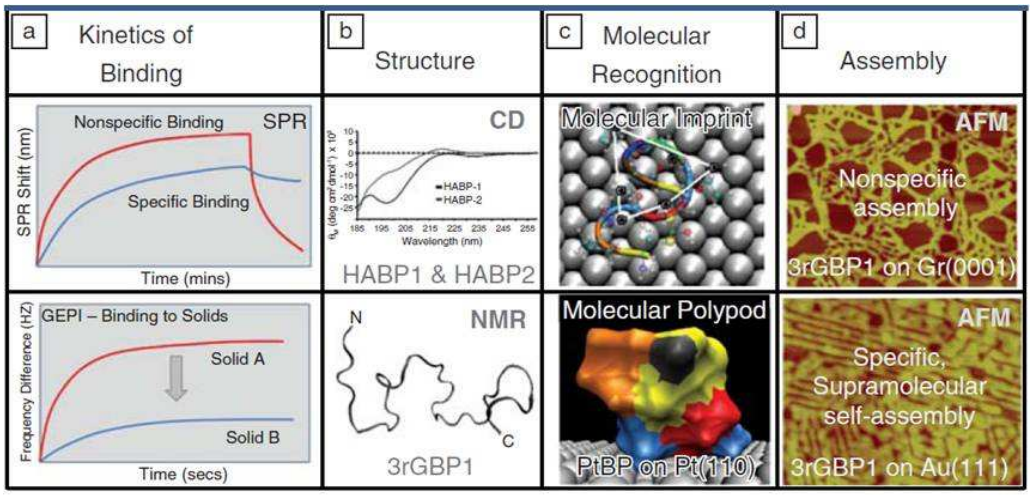

Figure 1.5 : Molecular characterization of GEPIs. a) SPR and QCM determine the specificity and kinetics of the binding. b) The detailed molecular structure of the peptides. c) Computational modelling of GEPIs is necessary for understanding the molecular conformation and mechanism of crystallographic surface recognition. d) Supramolecular self assembly of gold binding peptide on graphite and Au (Tamerler and Sarikaya, 2008).

1.4.1.3 GEPI based bionanotechnological systems

Binding, assembling, synthesizing and growing of the materials on the solid surfaces under desired conditions are important for many technological and medical applications ranging from biosensors to nanophotonics (Ginger et al., 2004, Chen et al., 2008, Wei et al., 2009). At this point, selection and optimization of the linking conditions for binding functional structures to a variety of different surfaces such as metals, oxides and semiconductors have come into prominence (Wei et al., 2009).

There are a range of small molecules used in functionalizing of the surfaces, such as thiols for gold, silanes for silica or other oxides, and phosphonic acids for metal oxides. In recent years, the utility of peptides as a promissing technique for surface functionalization have become common (Hnilova et al., 2008; Kacar et al., 2009b).

There is only limited understanding for the fundamental mechanisms of molecular binding to solids, assembly and the organization in spite of the recent developments and the extensive reports (Sarikaya, 1999, Evans et al., 2008, Tamerler et al., 2010). However, the data obtained from techniques like NMR spectroscopy (Kulp et al., 2004), computational modeling (Braun et al., 2002, Oren et al., 2005), and experiments with geometrically constrained peptides (Dai et al., 2005) have provided an oppurtunity for making suggestions about the mechanisms. In the light of these data it has been suggested that the secondary structures of the engineered peptides in solution can play an important role in their solid-binding and selectivity (Wei et al., 2009).

Many techniques including pin printing, inkjet printing, nanoimprint lithography, electron beam lithography, focused ion beam lithography, soft lithography, photolithography, scanning probe microscopy, and dip-pen nanolithography have been exploited for the patterning of biomolecules (Wilson et al., 2001; Noy et al., 2002; Agarwal et al., 2003; Lee et al., 2003; Ginger et al., 2004; Cho and Ivanisevic 2006). However, these biomolecules are not engineered for specific binding to target surface. Functions of the biomolecules are generally lost in the case of nonspecific binding. Solution-phase secondary structure of the solid binding peptides has a possible role in the affinity or selectivity for the given suface. Engineered solid binding peptides can be used as “viable inks” for a variety of immobilization approachs (Kacar et al., 2009b; Wei et al., 2009).

Further tailoring of the selected solid-binding peptides to improve their affinity and material-selectivity properties so that they can be used in biofunctionalization of nanoparticles and flat substrates can be achieved by using molecular biology protocols (Tamerler et al., 2006a; Kacar et al., 2009a).

Solid-binding peptides can also be fused to proteins (Dai et al., 2005) and other peptides (Slocik and Naik 2006), conjugated to functional small molecules or attached to quantum dots (Zin et al., 2005; Ma et al., 2007; Zin et al., 2007) to develop molecular building blocks or multifunctional molecular entities for various applications including efficient immobilization of enzymes, conjugation of nanoentities, nanoparticle synthesis with controlled size (Kramer et al., 2004; Krauland et al., 2007; Kacar et al., 2009b; Park et al., 2009), selective immobilization of fluorescent proteins (Yokoo et al., 2010) and for direct assembly or in situ synthesis of other functional inorganic nanostructures (Brown 2001; Pender et al., 2006; Sano et al., 2006; Slocik and Naik 2006).

1.4.1.4 Fabrication of multifunctional micropatterned substrates using GEPI

Protein microarrays are fabricated by spatial immobilization of proteins on desired inorganic surfaces through several lithography techniques including soft lithography, dip-pen lithography and photolithography (Xia and Whitesides 1998; Revzin et al., 2001; Lee et al., 2002).

Immobilization provides a physical support to the protein, making the reuse of the protein possible by separating the protein from solution easily (Bornscheuer 2003). The surface is generally functionalized by self-assembled monolayers (SAMs) of bifunctional molecules for the immobilization of biomolecules on glass or metal surfaces (Mrksich and Whitesides 1996; Ostuni et al., 1999). These bifunctional molecules have some limitations.

Bifunctional molecular constructs including inorganic substrate binding capability and certain functionalities can be designed using genetic engineering techniques (Sarikaya et al., 2003). In a recent alternative technique solid binding peptides with strong binding affinity to inorganics are exploited for the immobilization of nanoparticles and biomolecules. Beside their high inorganic binding capability, high substrate and biomolecular specificity of GEPIs is an advantage for protein immobilization. In the previous studies, functional proteins and nanoparticles were

immobilized on inorganic surface (Woodbury et al., 1998; Park et al., 2006; Kacar et al., 2009b; Yokoo et al., 2010) and SiO2, Ag and Au nanoparticles and protein-Cu2O nanostructures were sytnhesized by exploiting inorganic peptides (Brown et al., 2000; Brott et al., 2001; Naik et al., 2002; Zin et al., 2005).

Polydimethylsiloxane (PDMS) stamping is a common soft-litography technique for constructing protein patterns (Bernard et al., 2000; Yang and Chilkoti 2000; Inglis et al., 2001; Tan et al., 2002; Pla-Roca et al., 2007). The original master template is used for the fabrication of PDMS mold. Following coating with proteins, the mold contacts the substrate surface. Afterwards, the mold leaves a protein pattern on the surface (Figure 1.6).

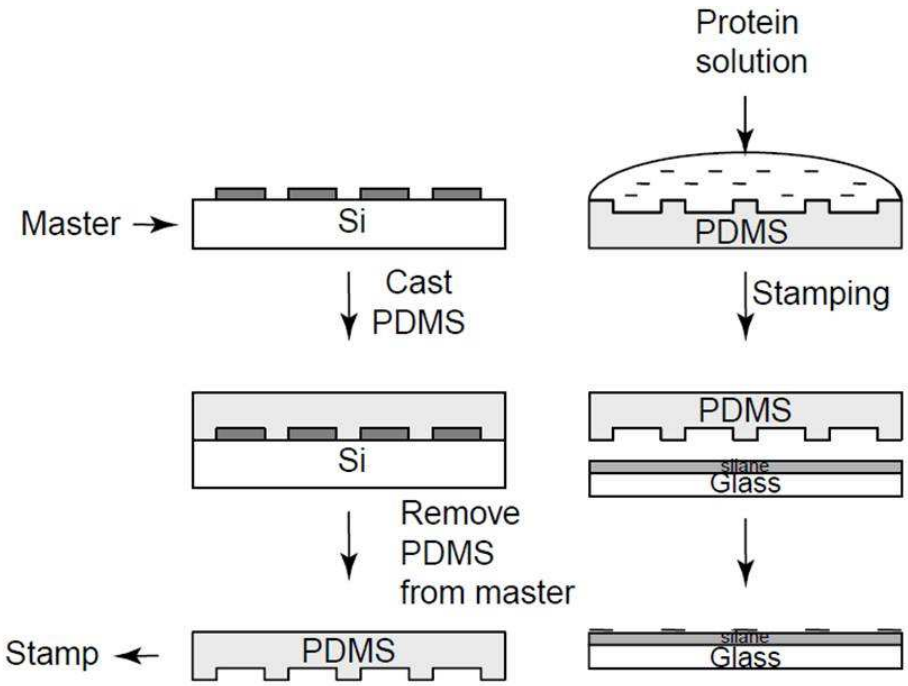

Figure 1.6 : Schematic illustration for PDMS patterning of proteins. The original master template is used for the fabrication of PDMS mold. Following the coating with the proteins, the mold contacts the surface of the substrate. Afterwards, the mold leaves a protein pattern on the surface (Truskett and Watts 2006).

Gold nanoparticles, streptavidin functionalized quantum dots and functional proteins have been directly immobilized on gold surface by microcontact printing of gold binding peptides in previous studies (Zin et al., 2005; Park et al., 2006; Zin et al., 2007). Kacar et al. (2009b) have demonstrated micropatterning of fluorescent quantum-dot nanocrystals and fluorescein, on quartz surface, immobilized through a quartz-binding peptide.

1.4.1.5 Attachment of nanoentities on the substrate

In nanotechnological and biological material science and engineering applications controlled binding and assembly of proteins onto inorganic substrates is a key issue (Drexler 1994; Ryu and Nam 2000; Niemeyer 2001; Tamerler et al., 2010).

With their structure, composition, size and surface related optical, magnetic and electronic properties, nanoparticles have importance in nanotechnology (Alivisatos 1996; Hines and Guyot-Sionnest 1996; Lewin et al., 2000; Santra et al., 2001; Daniel and Astruc 2004). Gold and silver nanoparticles which have been used for labelling in immunoassay studies (Schultz et al., 2000; Nam et al., 2003) and in cytologic imaging (Loo et al., 2005; Lee et al., 2007), absorb and scatter light, and can be detected by optical microscopy (Wiley et al., 2006; Chen et al., 2007; Anker et al., 2008). With the ability of converting minute changes in the refractive index into spectral shifts in the spectral data, gold and silver nanoparticles can be used for determining the binding of molecules on particles (Nath and Chilkoti 2002; Yonzon, et al., 2004).

Zin et al have demonstrated utility of GEPIs in the controlled organization of gold nanoparticles on the surface. Three repeats of GBP-1 (Brown et al., 2000) gold-binding protein (42 amino acids, [MHGKTQATSGTIQS]3) have been physically and chemically patterned by microcontact printing. Obtained patterns functioned as templates for the direct the assembly of gold nanoparticles (Zin et al., 2005).

1.4.1.6 Studies on the mechanism of molecular recognition of GEPIs

The structural effect of originally selected Pt-, Au-, and Cu_2O-binding peptides on their binding to inorganic surfaces have been studied in recent reports. All these inorganic binding peptides were selected from constraint peptide libraries (Choe et al., 2007; Seker et al., 2007; Hnilova et al., 2008).

Hnilova et al have selected two gold-binding peptide (AuBP1 and AuBP2) sequences using a FliTrx random peptide display library. Following the synthesis of cyclic, as displayed on the bacteria, and linear dodecapeptides, adsorption behavior of the peptides were analiyzed. After performing CD spectra and molecular dynamics analyses, they have found that the cyclic AuBPs have mainly random coil structures, on the other hand the linear versions also have some degree of polyproline type II (PPII) rigid structures in addition to the random coil (Figure 1.7).

They have demostrated that the circular and linear forms of AuBP1 retained the molecular conformation and had similar adsorption behavior. On the contrary AuBP2 have revealed different molecular structures in the circular and linear forms. Consequently the two peptides had different gold binding affinities (Hnilova et al., 2008).

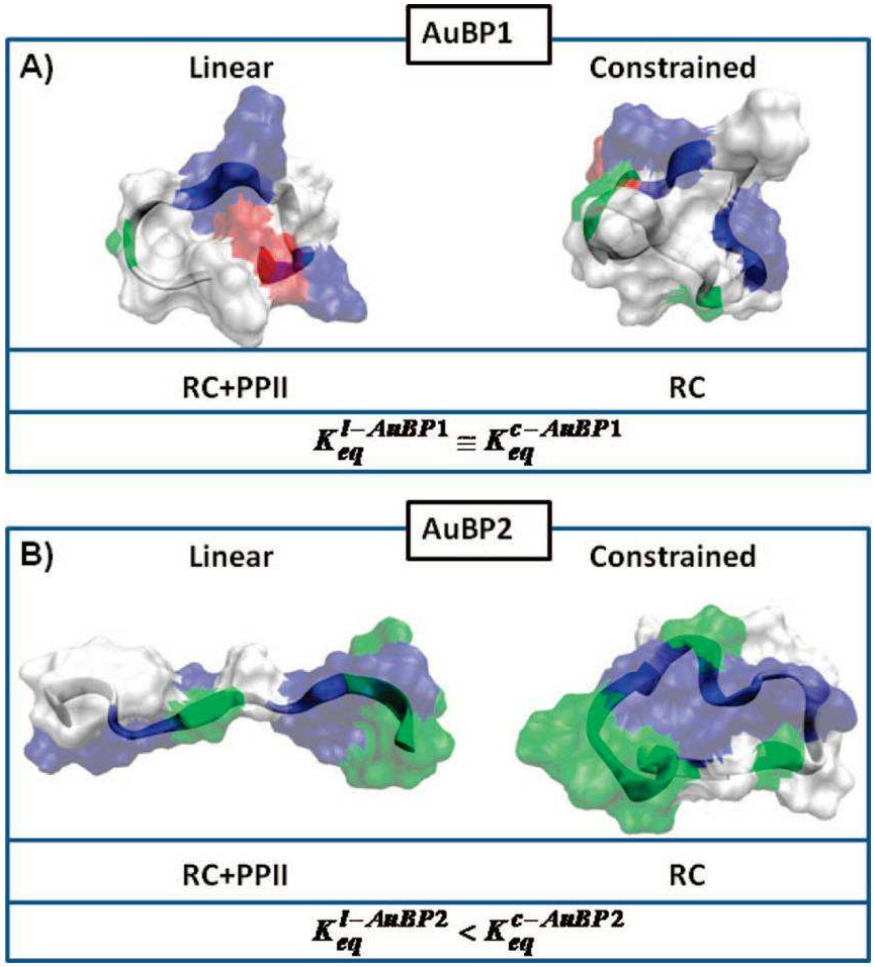

Figure 1.7 : Predicted molecular structures of the linear and cyclic version of AuBP1 (A) and AuBP2 (B). Ribbon and transparent surface models of the structures were overlapped. The percentage of PPII structure in linear AuBP2 is greater than that in linear AuBP1. RC: Random coil, PPII: polyproline type II structure (Hnilova et al., 2008).

Choe et al have used a derivative of the DNA binding protein TraI mutated with a cuprous oxide binding peptide called CN225 to show the influence of sequence composition and conformation on the binding affinity. They have demonstrated that the presence of disulfide constrained loop is crutial for binding (Choe et al., 2007).

Seker et al, have used circular and linear form of high-affinity seven amino acid Pt-binding sequence and analyzed them for their a adsorption behavior on Pt thin films

by surface plasmon resonance spectroscopy and for their conformational properties by circular dichroism. They have concluded that circularization affects both the conformation and binding behavior of the Pt-binding peptide (Seker et al., 2007).

In the light of these data, it has been found that when the inorganic binding peptide retains its molecular conformation in both cyclic and linear forms, it also preserves similar adsorption behavior on the surfaces. However, when the molecular structure of the respective sequence in the linear forms differs from their cyclic, a decrease is observed in the solid-binding affinities (Tamerler et al., 2010).

1.5 The Fluorescence Phenomenon

Fluorescence, as the most sensitive spectroscopic technique available, is a phenomenon that comprises two stages, excitation and emission. A fluorophore, the fluorescent chromophore, absorbs a photon, for a few nanoseconds remains in this state called as excited state and then emits a lower energy photon. Hence the intensity of a fluorescent molecule depends upon both the absorption of light and the emission of photon from the excited fluorescent chromophore (Johnson 2005).

Herschel has reported a visible emission from a natural source, an aqueus quinine solution in 1845 (Herschel 1845). In 1852 Stokes reported that this fact was because of the absorbtion and then emission of light by the first defined small molecule fluorophore quinine. Stokes called this process as fluorescence (Lavis and Raines 2008; Stokes 1852). After this progress the fluorometer was developed. The intrinsic fluorescence of quinine is responsible for developing of the first spectrofluorometers which were needed to monitor antimalarial drugs, including quinine during World War II (Lakowicz 2006). Today numerous other fluorophores are available including genetically encoded fluorophore GFP.

In the Figure 1.8, Jablonski Diagram illustrates the process of molecular fluorescence. S0 is the singlet ground state which is the nonexcited state of a molecule, S1 and S2 are first and second singlet excited states and T1 is the triplet state. The fluorophore molecule in a S0 state absorbs light energy and this promotes the fluorophore from S0 to S1 or S2. The relaxation of excitated state can occur with radiative way, by releasing energy in the form of light (fluorescence) or with

nonradiative way including bond rotation or vibration, molecular collision and photoinduced electron transfer (PeT) (Lavis and Raines 2008; Lakowicz 2006).

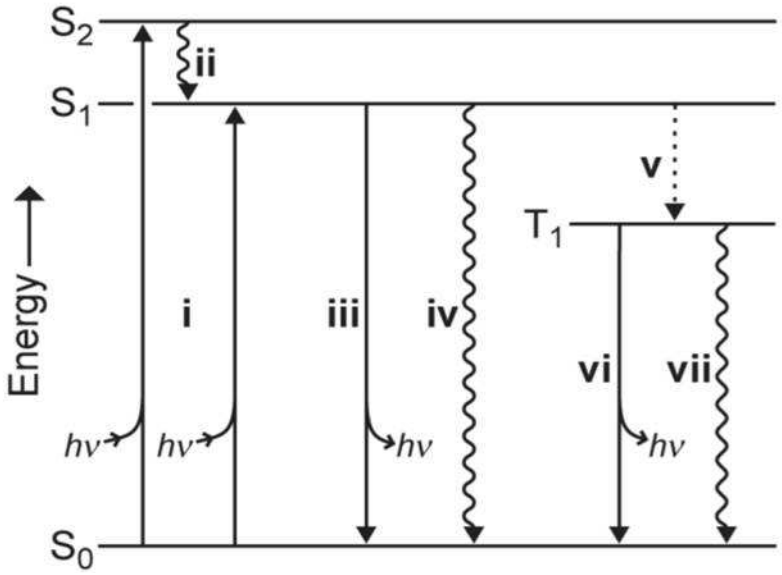

Figure 1.8 : Jablonski Diagram (Lavis and Raines 2008).

In a less common way, excited state can transit to T1 by intersystem crossing. The decay of the excited state can occur with radiative way, by photon emission (phosphorescence) or with nonradiative way. In the radiative transition process, energy of the emission is lower than the absorbed energy, due to loss of energy during the excited state. During fluorescence process emitted light is at a lower energy and has longer wavelength (Figure 1.9). This is named as the Stokes shift (Lavis and Raines 2008; Lakowicz 2006). Fluorophores have different Stokes shifts. Large shifts make it possible to separate the exciting alight easily (Lichtman and Conchello 2005).

Emission spectrum is generally used for presenting the fluorescence spectral data. This spectrum can be determined using a fluorescence measuring device after exciting the fluorophore at a convenient wavelength (Lichtman and Conchello 2005; Lakowicz 2006). Obtained spectrum is a plot of the fluorescence intensity versus wavelength or wavenumber. In the cases of wavelength and wavenumber nanometers and cm-1 units are used respectively (Lakowicz 2006).

Quantitavely reproducible signals come from the fluorescently labeled samples containing less than even 1 nM concentration of fluorescent chromophore. This concentration is much lower than those required for other spectral techniques. The signal can be analyzed using fluorescence intensity, lifetime, wavelength and

polarization or anisotropy to have knowledge of a structure, interaction, mechanism or process (Heuck et al., 2000; Ramachandran et al., 2004; Woolhead et al., 2004).

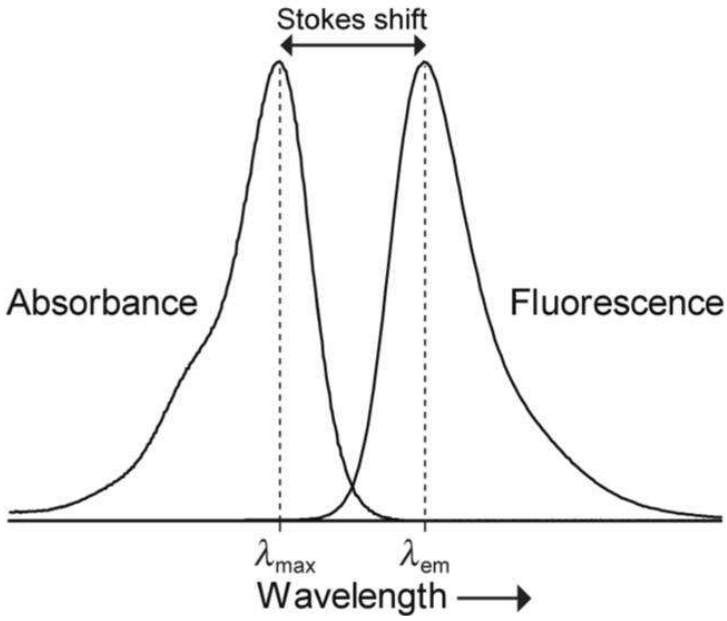

Figure 1.9 : Absoption and emission spectra showing Stokes shift (Lavis and Raines 2008).

In addition, because of its nondestructiveness, signal change in the fluorescent molecule can be analized as a function of time to reveal its kinetics propeties (Johnson 2005).

1.6 Fluorescence Detection Technology

Fluorescent detection technology is used by many disciplines including biological science. With recent progresses, extensive use of highly sensitive fluorescence detection techniques have become more eligible. These techniques do not reqauire use of any radioactive tracers for the measurement of most biological measurements (Lakowicz 2006).

There are several fluorescent detection techniques including measurement of intensity, fluorescent polarization anisotropies, Förster resonence energy transfer (FRET) and fluorescence lifetimes available for the investigation of biomolecules or biomolecular processes.Fluorescence intensity which can be measured using fluorescence microscopy is generally used for qualitative data. On the other hand, ratiometric methods which are based on the measurement of at least two parameters

are used for quantitative identification (Deniz et al., 2001; Tinnefeld and Sauer 2005; Li et al., 2008; Walla 2009).

Fluorescence polarization assay which gives a quantitative data for binding affinities is based on the measurement and comparison of the horizontal and vertical components of the fluorescence polarization. Using fluorescently labeled components, this assay can be exploited for receptor-ligand binding, proteolysis, protein-DNA interactions and membrane fluidity (Kim et al., 2006; LiCata and Wowor 2008; Xi and Deprez 2010).

FRET technique describes nonradiative energy transfer between two fluorescence chromophores. Small donor-acceptor distances are needed for effective energy transfer in this technique. If the acceptor and door fluorescent molecules are in close vicinity, energy transfer is observed between excited donor and the acceptor through dipole-dipole coupling. Many investigations including receptor-ligand binding interactions, conformational transitions of biomolecules, lipid membrane transformation can be performed using FRET technique. It also provides a nm scale molecular ruler to measure the distance between fluorescently labeled biomolecules. Another fluorescent technique is the measurement of fluorescence kinetics which change during biomolecular processes. However, it is hard to predict an incident that gives fluorescent kinetic data based on biomolecular changes (Jares-Erijman and Jovin 2003; Piston and Kremers 2007; Walla 2009).

Fluorescence Recovery after photobleaching (FRAP) based on the photochemical bleaching of fluorescence molecules in the sample. After the bleaching pulse has been applied, the fluorescence recovery kinetics are observed. This technique is used to figure out molecular diffusion of labeled agents in the sample for the membrane structure and cytoskeletal dynamics studies. Fluorescence recovery data gives knowledge about mobility of the fluorescence molecule (Trugnan et al. 2004; Sprague and McNally 2005; Walla 2009).

1.6.1 Fluorescence microscopy

In the absorption techniques, samples are stained with dyes that absorb light. In this case, the amount of light absorbed by the small parts of the samples has a very small difference from the background. One can see only parts of the sample that have fluorescence by filtering the exciting light without blocking the emitted light. At this

point, Stokes shift becomes one of the most important characteristics of fluorescence. Using fluorescence techniques it is possible to visualise even single molecules (Lichtman and Conchello 2005; Gell et al., 2010).

In fluorescence microscope system, the sample is illuminated with specific wavelength and the returned light is filtered to see only longer wavelength by seperating the emitted light from the excitation light. In modern fluorescence microscopy generally epi-fluorescence illumination technique which exploites incident-light (i.e., episcopic) is used. In epi-fluorescence illumination approach, the objective of the microscope serves as a conderser in addition to its imaging and magnifying role. The numerical aperture (NA) of the objective is an important parameter which has critical effects on the resolving power and light efficiency of the objective. An objective with a high NA is preferable for an ideal fluorescence microscope (Stanley 2003; Lichtman and Conchello 2005).

Development of the wide range of fluorophore molecules has multiplied the usage of fluorescent microscope as an essential tool. Although in both system, samples are exicitated equivalently, epi-fluorescence microscopy has advanteges over diascopic fluorescence microscopy. In diascopic fluorescence system exciting light comes through the condenser after passing through an excitation filter and the objective collects the fluorescence emission (Lichtman and Conchello 2005). In this approach brightfield and darkfield condensers are used. With brightfield condenser the maximum intensity is limited by the optical filters capacity. Darkfield condenser of the diascopic fluorescence system prevents entering most of the excitation light to objective. In this way the requirement of the optical filters is reduced, but at same time, the objective requires a smaller NA and the final efficiency of the illumination and the brightness are reduced (Reichman 2007).

In epi-fluorescence approach emitted fluorescence passes through a barrier and in this mode of fluorescence microscopy only the small amount of exciting light needs to be suppressed by barrier filter (also called emission filter or emitter). This filter passes the longer wavelengths and blocks the remaining shorter wavelength (excitation). To prevent the overlapping the exciting light passed by excitation filter and the fluorescence, a kind of filter, dichroic mirror splitter is used (Lichtman and Conchello 2005; Reichman 2007).

The dicroic mirror reflects excitating light (short wavelength) comes from the light source and passes the emitted fluorescence (longer wavelength). The primary filtering component of the epi-fluorescence microscopy is a unit composed of three filters which are held in a fluorescence filter cube (small block shaped filter holders). This fluorescence filter cube is a set of excitation filter, barrier filter and the dichroic beamsplitter. The cubes can be fitted into a circular carousels or linear blocks carrying seperate cubes thar can be moved into desired positions (Lichtman and Conchello 2005; Reichman 2007). Other advanced fluorescence based techniques such as confocal, multiphoton, stimulated emission depletion (STED), structured illumination, total internal reflection fluorescence (TIRF), FLIM, FRET, fluorescence recovery after photobleaching (FRAP) and fluorescence correlation spectroscopy (FCS) are also available to study fluorescent molecules (Gurunathan and Levitus 2008; Masi et al., 2010; Wessels et al., 2010).

1.6.2 Spectrofluorophotometer

The wavelengths affect the efficiency of monochromotors and detector tubes in spectrofluorometers. In addition to this and the other instrumental factors like the polarization or anisotropy of the emitted light, the optical properties of the specimens like optical densitiy and turbidity effect the excitation and emission spectra. The wavelength distribution of an emission measured at a certain excitation wavelength represents an emission spectrum (Hart and JiJi 2002; Lakowicz 2006). In an excitation spectrum different wavelength of excitation light is scanned at a constant emission wavelength. The spectral data can be given on a wavelength scale (nanometer) or wavenumber scale (cm-1). The units of wavelengths and wavenumbers can be interconverted.

The spectrofluorometer in the Figure 1.10 has a xenon lamp that has high intensity at all wavelenghts as a exciting light source. For the selection of the excitation and emission wavelengths the instrument has both excitation and emission monochromators. There are two concave gratings in this spectrofluorometer as shown in the figure. Wavelengths different from the desired one is decreased by these gratings. It is possible to scan wavelengths automatically using the monochromators. After the detection of the fluorescence by photomultiplier tubes (PMT) the quantified data is commonly presented in graphical form (Lakowicz 2006; Sharma and Schulman 1999).

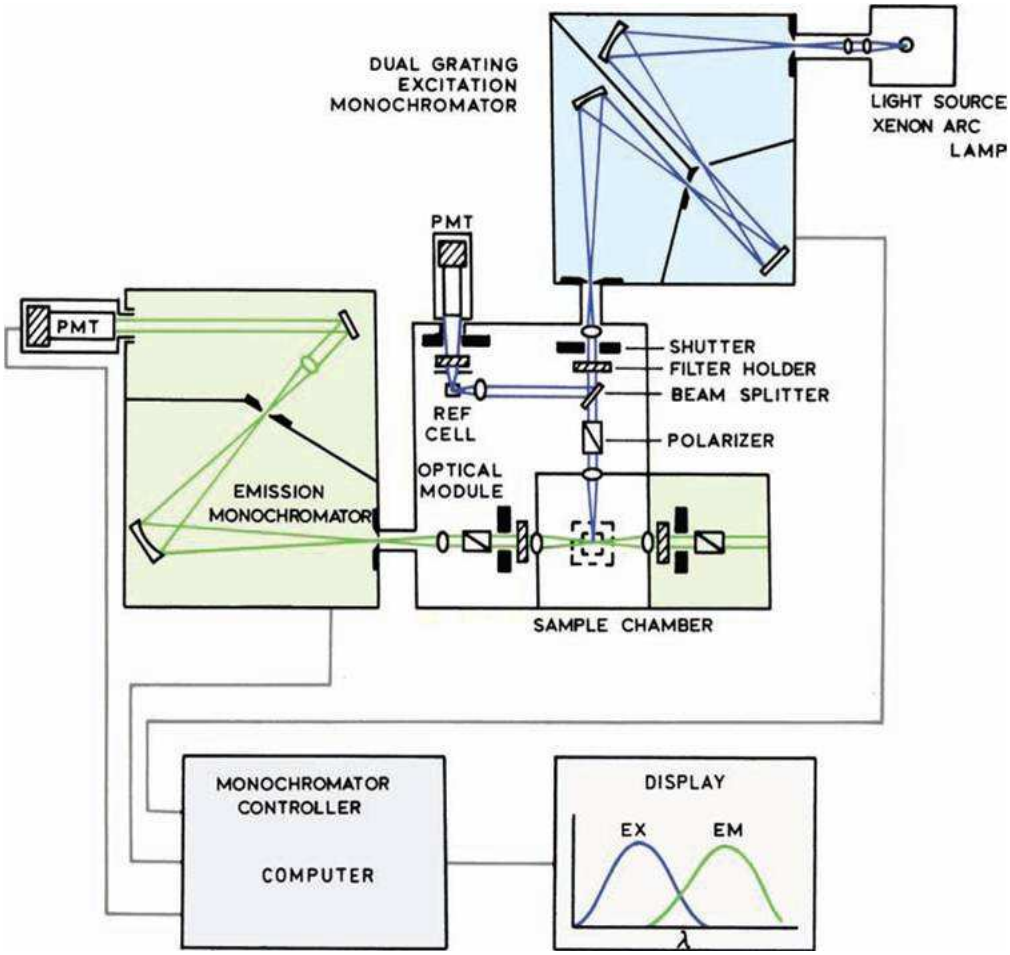

Figure 1.10 : Schematic diagram of a spectrofluorometer (Lakowicz 2006).

The sample holder is shown in the middle of the optical module containing different components such as shutters, filter holders, beam splitter, polarizer and reference cell. Shutters eliminate the exciting light or close the emission channel (Lakowicz 2006; Sharma and Schulman 1999).

The beam splitter in the excitation light path reflects some part of the excitation light to reference cell containing a reference fluorophore for correction of the effects of instrumental factors and optical properties of the sample. Polarizers provided to select for particular polarized components of the emission or excitation are usually removable components of the spectrofluorometer. In addition to other components in the figure, there is an additional optical path which allows measurement of fluorescence anisotrophy. In the present design of the instrument there is generally no need to use this kind of additional path for fluorescence anisotrophy measurement. Fluorescence microplate readers provide measurement of numerous samples rapidly using multiwell plates instead of the individual cuvettes . They are

generally used for intensity measurements. There are some differences between the spectrofluorometers designed for single sample and for multisample in respect to optics used in the design. Multiwell plates are placed horizontally. The main difference is use of the mirror with a hole which transmits the excitation.

1.7 An Introduction to Fluorescent Probes

Fluorescent probes that combine fluorescent properties and molecular recognition have been used to visualize biological events at many levels from molecules to an organism (Finney 2006; Giepmans et al., 2006). There are thousands of fluorescent probes available. Properties of the probs and the fluorophores are considered for designing. Fluorescence instruments need the information on spectral properties of the fluorophores which can be divided into two classes, intrinsic and extrinsic. While intrinsic fluorophores including the aromatic amino acids, NADH, flavins and chlorophyl occur naturally, extrinsic fluorophores are added to the sample to provide fluorescence or change the spectral properties (Lakowicz 2006). It is important to choose a suitable fluorescence probe to visualize, describe and analyse a biochemical or biological process (Figure 1.11).

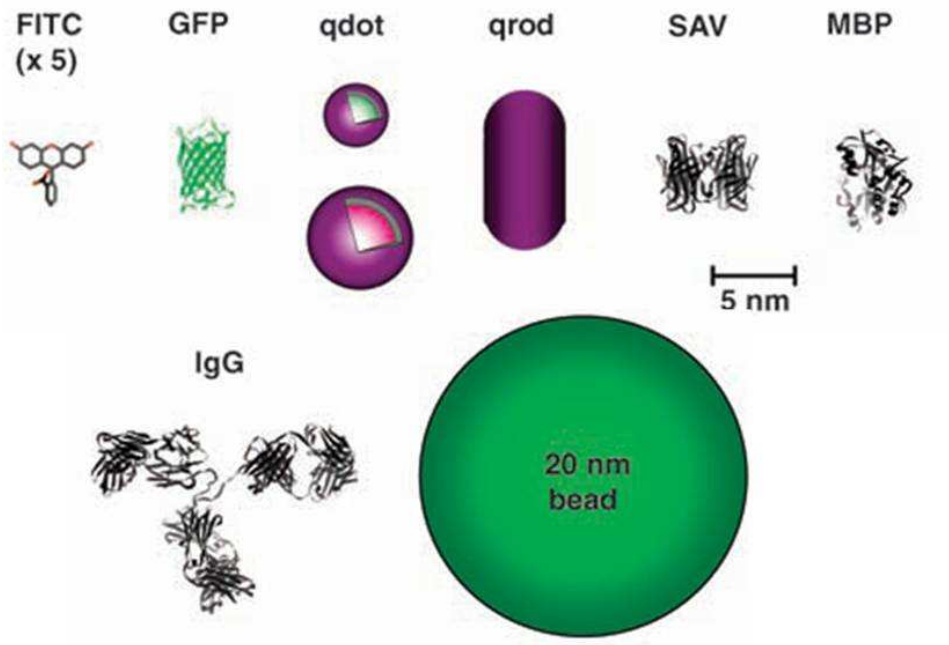

Figure 1.11 : Size comparison of green and red qdots, FITC, fluorescein isothiocyanate; GFP; CdSe/ZnS qdot; qrod, rod-shaped qdot, streptavidin (SAV), maltose binding protein (MBP), and immunoglobulin G, IgG (Michalet et al., 2005).

1.7.1 Small organic dyes for fluorescence detection

Small organic dye molecules, which are commercially available from many sources (Haugland 2002), are used for covalent labeling of macromolecules. They have been implemented for optimization of wavelength range, brightness, photostability and reduction in quenching. However, due to their unspecificity for any particular protein, antibodies are used for many applications.

Small organic dyes are attached to the protein of interest with antibodies. On the other hand, targeting of the antibody in the intracellular compartments requires fixation and permeabilization of the cells (Giepmans et al., 2006).

1.7.2 Quantum dots as fluorescence probe

Quantum dots (QDs) have sharp and discrete fluorescence wavelengths depending on their size. These inorganic nanocrystals have 10 to 100 times higher extinction coefficient than those of small organic dyes and fluorescent proteins. QDs those have good quantum yields contain a CdSe or CdTe core and ZnS shell (Giepmans et al., 2006). It is a challenging step the development of coatings for QDs that make them water soluble, prevent quenching in water and make it possible to conjugate to protein targeting molecules (Jaiswal and Simon 2004; Alivisatos et al., 2005; Gao et al., 2005; Michalet et al., 2005).

1.7.3 Fluorescent protein paintbox

Antenna pigment proteins, phycobiliproteins introduced in 1982 as the first fluorescent proteins used in cell biology, were exracted from cyanobacteria. Photosynthetic pigment protein (antenna) complex containing organisms such as red algae and cyanobacteria has the significant range of spectral variation in their antenna pigments (Oi et al., 1982; Glazer 1989). Each phycobiliprotein macromolecule contains multiple chromophores encapsulated in a matrix. This provides minimized quenching and higher brightness to the macromolecules than small organic dyes. With its size of 200 kD, applications of phycobiliprotein has a diffusion limitation. Labeled proteins or probes can not diffuse properly into cell compartments, tissues and other region of interest. Therefore, they have been used for surface labelling in flow cytometry and enzyme-linked immunosorbent assay, ELISA (Giepmans et al., 2006; Waggoner 2006).

Phytochromes containing nonfluorescent chromophores are light sensitive proteins present in photosynthetic organisms. Some phytochromes spontaneously binds phycoerythrobilin and become fluorescent. Murphy et al designated these phytochromes as phytofluors (Murphy and Lagarias 1997). Apophytochrome can be expressed recombinantly (Gambetta and Lagarias 2001). A recent report has shown that a tyrosine to histidine mutation made the phytochrome fluorescent (Fischer and Lagarias 2004).

1.7.3.1 The structure and function of green fluorescent protein

Green Fluorescent Protein (GFP) is a commonly used biological marker in molecular biology, medicine and cell biology. Its chromophore structure is formed in an autocatalytic cyclization process. Because of its stability and the fact that its chromophore formation does not require a cofactor GFP can be use in living systems (Zimmer 2002).

GFP and Aequorin protein containing coelenterazine are involved in the bioluminescence in Aequorea (Figure 1.12). Following the binding, three calcium ions, aequorin oxidizes the coelenterazine molecule. The resulting protein complex emits blue light. Instead of emitting blue light, Aequorea transfer this energy to GFP (Zimmer 2002).

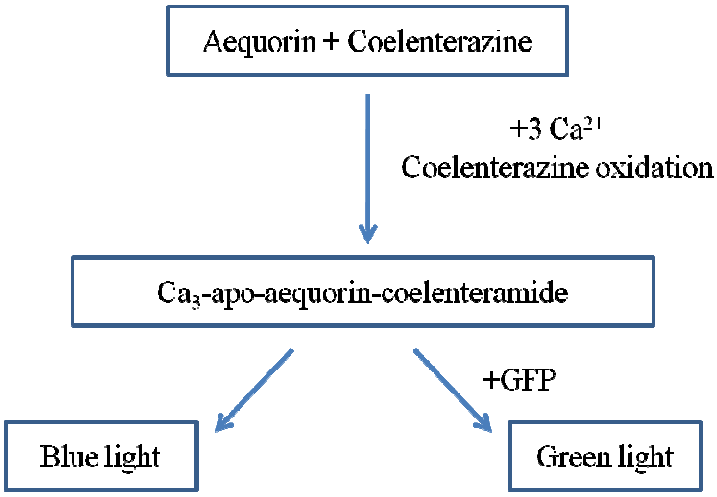

Figure 1.12 : Bioluminescence mechanism in Aequorea victoria (Adapted from Zimmer 2002).

Studies with molecular basis for the fluorescence of Aeuqorea were started by Shimomura (1962). After denaturation and digestion of GFP, he isolated a peptide fragment containing the chromophore and he proposed the structure of GFP

chromophore. Following the first cloning Aequorea GFP by Pracher in 1992, GFP was expressed in bacteria by Chalfie et al in 1994 (Shimomura et al., 1962; Prasher et al., 1992; Chalfie et al., 1994).

Jellyfish Aequorea victoria GFP is a 238-amino acid long polypeptide with a unique, rigid β-sheet barrel structure (Figure 1.13). A variety of variants of GFP with improved fluorescent roperties, have been produced recently (Chudakov et al., 2005; Miyawaki et al., 2005; Day and Davidson 2009).

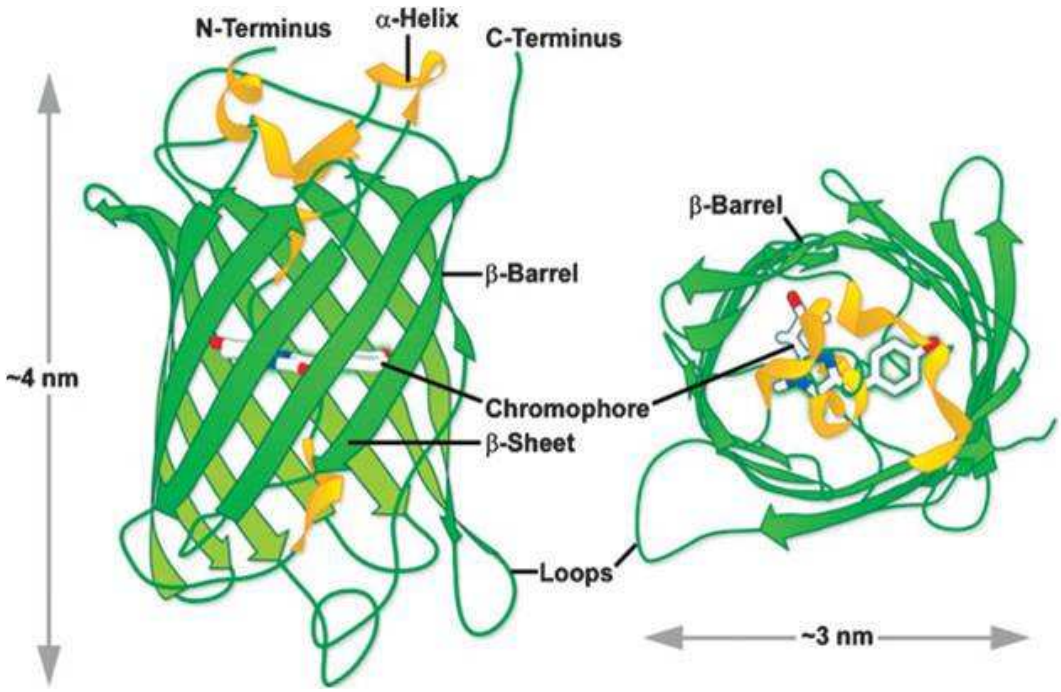

Figure 1.13 : Three-dimensional structure (β-can) of wild-type green fluorescent protein (GFP) and approximate dimensions (Day and Davidson 2009).

Spectral variants of EGFP emitting blue (EBFP), cyan (ECFP) and yellow (EYFP) fluorescence were also created by several mutations (Schmid and Neumeier 2005). GFP variants became commonly used tools in molecular and cellular biology as biological markers due to their robust biological and fluorescence properties (Lippincott-Schwartz and Patterson 2003). A GFPuv variant carrying the cycle 3 mutations has an emission maximum at 509 nm and an excitation maximum at 395 nm was reported by Crameri et al (Crameri et al., 1996).

In addition to Aequorea GFP, cloning of a red fluorescent protein DsRed from Discosoma sp. has made it possible to extend the range of fluorescence further into the red part of the spectrum (Du et al., 2006). After creating the first monomeric red

fluorescent protein mRFP1(Campbell et al., 2002), mFruits fluorescent proteins were introduced by Tsien group (Shaner et al., 2004; Wang et al., 2004).

Information about detection of the promoter activity, protein localization, motility and interactions with other proteins in living cells or various cellular parameters in living animals can be obtained by exploiting fluorescent protein variants (Hoffman 2002; Chudakov et al., 2005; Wiedenmann et al., 2009).

1.7.4 Fluorescent tagging for labeling

Immunolabeling and genetic tagging are general techniques for tagging of proteins. Using labelling techniques researchers can combine fluorescent techniques and biomolecules. For the detection of endogenous proteins the sample is labeled with a primary antibody and then amplified with a secondary antibody conjugated to a small organic dye or a QD. In an alternative way, primary antibody can be conjugated directly to fluorescent molecule. The specificity of the primary antibodies is very important for the accuracy of protein recognition.

In some applications there are some disadvantages and restrictions for immunolabeling technique. Fluorescence molecule-targeting complexes can have a size over 200kD and might prevent the recognition of multiprotein in protein complexes. Immunolabelling can be applied for permeabilized cells or extracellular or endocytosed proteins. In the other approach, the protein of interest is genetically tagged with fluorescent proteins (Giepmans et al., 2006).

Covalent fusion of the fluorescence molecule is very advantageous for targeting of the sample. In addition to these techniques, some hybrid systems in which small molecules are covalently targeted to specified proteins of living cells, via spontaneous attachment or enzymatic ligation are used.

The most studied one is the tetracysteine-biarsenical system. Fusion proteins carrying the tetracysteine tag can be labeled covalently using this system. Tetracysteine tag specifically binds to biarsenical compaunds such as a fluorescein derivative green F1AsH and a resorufin derivative red dye ReAsH. Inspite of their relatively small size, biarsenical fluorophores can couse unspecific binding (Griffin et al., 1998; Gronemeyer et al., 2005; Giepmans et al., 2006).

Developments in fluorescent probs and imaging approaches make imaging brighter, more stable and more informative, additionaly provide higher resolution and greater tissue penetration. It is important to understand biological systems and to get knowledge about biological events from molecule to organism level in life science. Fluorescent imaging make it possible to measure biological events such as gene expression, protein localization, activation and interaction (Du et al., 2006).

1.8 Quenching of Fluorescence

Fluorescence life time and quantum yield are informative characteristicts for a fluorophore molecule. Fluorescence lifetime determines the information available from emission of the fluorophore. The fluorophore interacts with or diffuse in the environment in time. The fluorescence quantum yield is measured as ratio of number of the emitted photons to the number of absorbed photons. Higher quantum yield increases the intensity (Lakowicz 2006; Lichtman and Conchello 2005).

In many dyes such as NBD (7-nitro-benz-2-oxa-1,3-diazole) the intensity primarily depends on the alterations in the efficiency of photon emission (Crowley et al., 1993). On the other hand, in other dyes like fluorescein, the intensity changes result from changes in the absorbance that depends on the pH, environment or other effects (Mercola et al., 1972; Adkins et al., 1983).

Quenching is the decrease in the intensity of the fluorescence by a variety of mechanisms. Deactivation of the excited state fluorophore upon contact with the quencher molecule is called as collisional quenching. Molecules such as oxygen, halogens, amines, and electron deficient molecules can act as collisional quenchers. Formation of nonfluorescent complex by the fluorophore and the quencher molecule is another quenching process. Non molecular mechanisms can also cause quenching (Lakowicz 2006).

The location of probes on macromolecules can be determined by use of the fluorophore and quencher pairs (Lakowicz 2006).

1.8.1 Quenchig by metallic nanoparticles

In the quenching mechanism by metallic nanoparticles the distance is larger than the mechanism for molecular quenchers and FRET (Algar et al., 2009). Dulkeith et al.

have shown that fluorescent dyes quenched at distance as large as 16 nm (Dulkeith et al., 2002; Dulkeith et al., 2005). In addition, it has been found that QDs quenched at 21 nm distance (Pons et al., 2007).

It has been suggested that the efficiency of quenching by gold nanoparticles depends on the size and shape of the nanoparticle, distance from the fluorophore, spectral overlap and dipole orientation (Dulkeith et al., 2002; Dulkeith et al., 2005; Algar et al., 2009). On the other hand, the exact mechanism for the quenching has not been exhibited yet (Algar et al., 2009). Pons et al (2007) have found that gold NPs provide the additional nonradiative decay pathway like energy transfer for quenching of QDs. However, Dulkeith et al (2005) have demonstrated that changes in the radiative rate of the fluorophore induces more significant quenching than energy transfer. It has been also shown that surface bound dye have a 10 fold decrerease in radiative rate while there is a 10 fold increase in non radiative rates (Dulkeith et al., 2002). This study also suggested that 5-10 nm diameter gold NPs are optimal quenchers (Algar et al., 2009). Gold nanoparticles mostly used as quencher for molecular beacons exploiting fluorophores or QDs in nucleic acid analysis (Dubertret et al., 2001; Cady et al., 2007).

1.9 Biomineralization and Proteins

Biomineralization is the process by which organisms produce minerals with controlled hierarchical structures across the dimensional scales from the nanometer and up resulting superior properties compared to synthetic materials with similar phase compositions (Lowenstam 1981; Addadi and Weiner 1985).

There is a major interdisciplinary interest on biomineralization among geologists, biologists, materials scientists and bioengineers in both the fundamental understanding and mimicking to develop hybrid materials with controlled structures and functions with technological and medical interests. Different types of minerals, ranging from silicates, carbonates, phosphates, metals and metal oxides, have been identified in a variety of species (Lowenstam 1981; Addadi and Weiner 1985).

Biological hard tissues are dynamic, complex, self healing and multifunctional and have a highly controlled architectural organization from nanoscales to macroscales, often in a hierarchical manner (Sarikaya et al., 2003; Tamerler et al., 2010).

In the formation of biogenic minerals in living organisms, proteins have a key role for the regulation the mineralization process. Proteins participate the biomineralization and influence nucleation, crystallography, polymorphism and morphology of biogenic inorganics (Addadi and Weiner 1985; Sarikaya 1995; Mann 1996). Biomimetic approach can be applied to utilize these proteins in designing and engineering of functional materials. Proteins can also be obtained by extracting from hard tissues. Following the isolation, purification and cloning steps (Cariolou and Morse 1988; Glimcher and Nimni 1992; Paine and Snead 1997; Liou et al., 2000) such biomineralizing peptides can be used in the synthesis of certain inorganics (Berman et al., 1988; Belcher et al., 1996; Cha et al., 1999). However, hard tissues usually contains many proteins with a complex spatial and temporal distribution that makes their extraction and purification from hard tissues difficult. As a more practical approach, the combinatorial selection of peptides through display techniques is efficient for selection of peptides that specifically bind to inorganic surfaces (Brown et al., 2000; Sarikaya et al., 2003).

1.9.1 Combinatorially selected hydroxyapatite binding peptides

Hydroxyapatite (HA), being the principal inorganic component of the hard tissues in mammalian organisms, such as bone and teeth, has been one of the most extensively studied biominerals. HA is widely utilized in hard tissue repair, replacement and implant surface coating. In addition to these fields, HA has also been reported as a potential gene/drug and cell delivery agent (Dash and Cudworth 1998; Liu et al., 2005; Tan et al., 2007; Ma et al., 2008; Braux et al., 2009) and regulator of cell bioactivity (Oh et al., 2005; Kasaj et al., 2008).

Phage-display selected hydroxyapatite-binding peptides (HABP1 and HABP2) have been reported by Gungormus et al. Binding and molecular structural properties of HABPs have been provided (Gungormus et al., 2008).

Among the selected peptides, a high affinity HA binding heptapeptide, with the amino acid sequence of CMLPHHGAC, was also demonstrated to have mineral-forming capabilities. It has been observed that the addition of HABP1 into the reaction, slowed the rate of initial mineralization and formed the larger particles compered to weak binder HABP2 (CNPGFAQAC) and control no-peptide sample (Figure 1.14). On the other hand, the rate of transformation of the amorphous phase

to the crystalline phase has been increased upon addition of HABP1 (Gungormus et al., 2008).

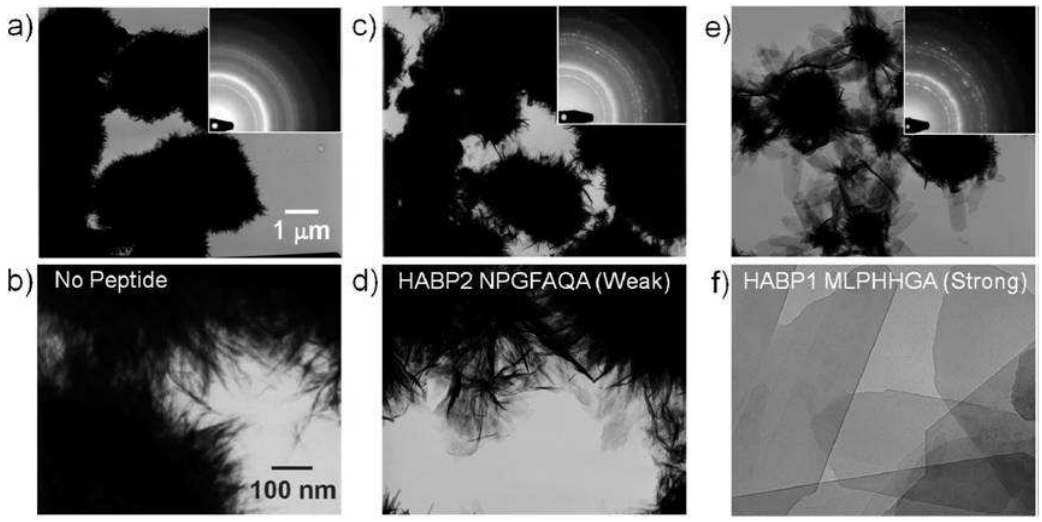

Figure 1.14 : The morphology of the minerals formed in the presence of a,b) no binder, c,d) weak binder HABP2 and e,f) strong binder HABP1 at 96 h (Gungormus et al., 2008).

A twenty-seven residue peptide containining a heptapeptide (MLPHHGA) at the C-terminal has been designed that directs the formation of hydroxyapatite. It has been reported that the peptide folded and assembled to form a hydrogel network and the peptide gels were capable of directing the formation of hydroxapatite (Gungormus et al., 2010).

1.9.2 Labelling HA formation

Tracking of HA formation, via efficient labeling is very important in biomedical application, e.g., gene/drug delivery, bone and teeth formation/remodeling, and in nano-technological implementations, e.g., nano-particle composites. HA can be labelled via several ways. Alizarin red S (Lipman 1935) and von Kossa staining (Meloan 1985) are the golden standards for in vitro staining of HA. However, both of these methods are only applicable in the ex vivo labeling of HA.

The methods for potential applications of HA labeling include synthesizing HA particles doped with fluorescent ions(de Araujo et al., 2007; Yang et al., 2008), synthesizing HA-quantum dot composites (Guo et al., 2008; Hsieh et al., 2009) or modifying the surface of the HA using chemical coupling agents such as bisphosphonates (Zaheer et al., 2001; Zhang et al., 2008). On the other hand, existing methods have complex chemistries required for labeling and the dopants or the

composites can couse a toxicity. For instance, although quantum dots have great potential in many research and diagnostic applications, they are still considered toxic when they are used in studies involving living systems (Alivisatos et al., 2005; Hardman 2006). Moreover, bisphosphonates, used as a chemical linker, because of their high affinity to hard tissues, have the risk for disrupting bone turnover due to their inhibitory effects on osteoclasts (Boonekamp et al., 1986; Weinstein et al., 2009).

2. MATERIALS AND METHODS

2.1 Cloning Construction, Expression and Analyses of Histidine Tagged GFPuv Fusion Proteins

2.1.1 Oligonucleotide primers for GFPuv-HABP constructs

Primers were designed for constructing original phage selected constraint HABP1 and HABP2 fusion proteins, GFPuv-HABP1 (C-MLPHHGA-C), GFPuv-HABP2 (C-NPGFAQA-C), and linear HABP1 fusion GFPuv-HABP1Met (MLPHHGA), linear reverse HABP1 fusion GFPuv-HABP1Ala (AGHHPLM) proteins and control GFPuv protein encoding expression vectors (Table 2.1).

Table 2.1: Oligonucleotide primers used in PCR reactions for GFPuv, GFPuv-HABP1, GFPuv-HABP2, GFPuv-HABP1Met, GFPuv-HABP1Ala constructs.

Primer Name	Sequence
HAP1	5’-CGGGCATGCTATGAGTAAAGGAGAAGAACTT-3’
HAP2	5’-GCCAAGCTTTTATTTGTAGAGCTCATCCATGCC-3’
HAP3	5’-GCCAAGCTTTTAACAAGCACCATGATGAGGTAACAT GCAACCTCCACCCGATTTGTAGAGCTCATCCATGCC-3’
HAP4	5’-GCCAAGCTTTTAACAAGCACCATGATGAGG-3’
HAP5	5’-GCCAAGCTTTTAACAAGCCTGAGCAAAACCAGGATT GCAACCTCCACCCGATTTGTAGAGCTCATCCATGCC-3’
HAP6	5’-GCCAAGCTTTTAACAAGCCTGAGCAAAACC-3’
HAP7	5’-GCCAAGCTTTTAAGCACCATGATGAGGTAACATACC TCCACCCGATTTGTAGAGCTCATCCATGCC-3’
HAP8	5’-GCCAAGCTTTTAAGCACCATGATGAGGTAA-3’
HAP9	5’-GCCAAGCTTTTACATTAAAGGATGATGACCAGCACC TCCACCAGATTTGTAGAGCTCATCCATGCC-3’
HAP10	5’-GCCAAGCTTTTACATTAAAGGATGATGACC-3’

2.1.2 Polymerase chain reaction for GFPuv-HABP DNA fragments

The vector pGFPuv (Figure 2.1) was obtained from Clontech (Takara Bio Inc. USA) and used as a template in all polymerase chain reactions (PCR). The PCR experiments were performed using a high fidelity enzyme, pfu DNA polymerase (Fermentas International INC., Ontario, Canada).

GFPuv encoding sequence was amplified using the forward HAP1 and the reverse HAP2 primers containing extra residues including a *PaeI* or *HindIII* site at their 5' ends, respectively. The DNA fragment encoding GFPuv-fused HABP1 (GFPuv-HABP1) was obtained in a two PCR reactions.

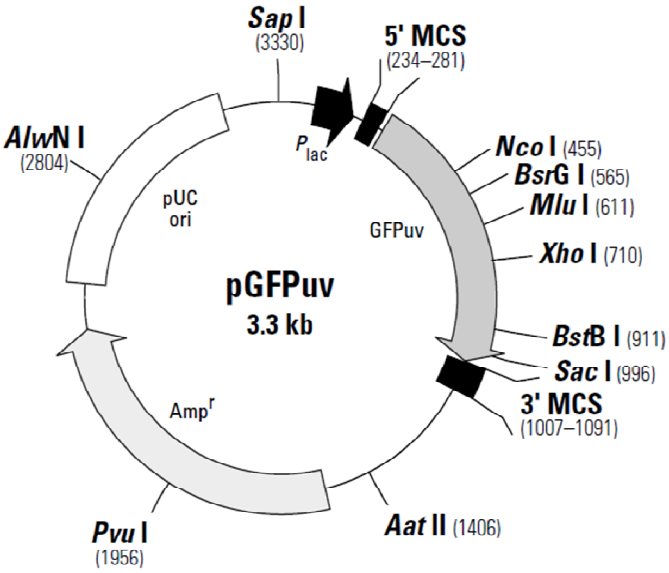

Figure 2.1 : pGFPuv vector map (Url-1).

The first PCR reaction was kept in 15 cycle and performed using the forward primer HAP1 and the reverse primer HAP3 bearing the strong hydroxyapatite binding peptide (HABP1) coding sequence with HindIII cleavage site (Table 2.2).

Table 2.2: First step PCR conditions for GFPuv-HABP constructs.

Temperature	Time	Cycle
95 °C	3 min	1
95 °C	1 min	15
50 °C	1 min	
72 °C	4 min	
72 °C	10 min	1

The second PCR reaction was kept in 30 cycle and performed by using the forward primer HAP1 and the reverse primer HAP4 and the first PCR product as a template (Table 2.3). Using the same PCR strategy described above, the DNA fragment encoding GFPuv fused HABP2 (GFPuv-HABP2) was obtained by using the forward primer HAP1 and the reverse primer HAP5 with the control peptide (HABP2) coding sequence with HindIII cleavage site in the first PCR reaction and the reverse primer HAP6 in the second PCR reaction. Linear and reverse linear HABP1 constructs, GFPuv-HABP1Met and GFPuv-HABP1Ala, were also obtained through the same strategy above. HAP1 and HAP7 were used in the first, HAP1 and HAP8 were used in the second PCR reaction for GFPuv-HABP1Met. HAP1 and HAP9 was used in the first, HAP1 and HAP10 were used in the second PCR reaction for GFPuv-HABP1Ala.

Table 2.3: Second step PCR conditions for GFPuv-HABP constructs.

Temperature	Time	Cycle
95 ^{o}C	3 min	1
95 ^{o}C	1 min	30
55 ^{o}C	1 min	
72 ^{o}C	2.5 min	
72 ^{o}C	10 min	1

2.1.3 Agarose gel electrophoresis of PCR products

1% agarose gel was prepared using 1XTAE (40 mM Tris-base, 20 mM Glacial acetic acid, 1 mM EDTA, pH: 7.6) buffer for analyzing the PCR product.

Samples and the DNA marker (Appendix A1) □X174 DNA/HinfI, Marker 10 (Fermentas) were pipetted into the gel. After gel electrophoresis, EtBr stained samples were visualized by UV trans-illuminator. Following excising DNA fragment from the agarose gel with a scalpel MinElute kit (Qiagen) was used for the gel extraction.

2.1.4 Cloning PCR products into PJET cloning vector

Extracted DNA fragments were cloned into 1.2/Blunt Cloning Vector pJET (Figure 2.2). Blunt-ended PCR products generated with the pfu DNA polymerase were

ligated directly into the cloning vector using CloneJET PCR cloning kit (Fermentas). The reaction set up is given in Table 2.4.

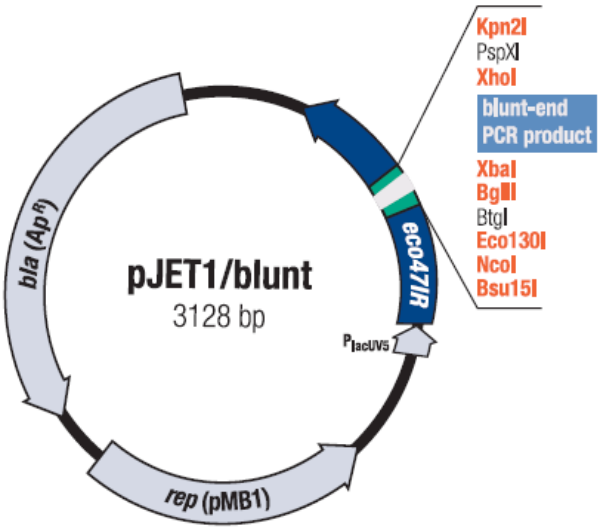

Figure 2.2 : pJET1/blunt vector map (Url-2).

The ligation mixture was incubated at room temperature for 15 min. The pJET ligation mixture was used for bacterial transformation.

Table 2.4: Components of the pJET ligation reaction.

Component	**Volume**
2X Reaction Buffer	10 µL
PCR product	1 µL
pJET vector	1 µL
Water, nuclease-free	7 µL
T4 DNA Ligase	1 µL
Total	**20 µL**

2.1.4.1 Preparation of electrocompetent E. coli TOP10

pJET plasmid clonings were carried out in *E.coli* Top10F' with the following genotype [lacIq Tn10(Tetr)], mcrA _(mrrhsdRMS-crBC), f80lacZ_M15 _lacX74, deoR,recA1, araD139_(ara-leu)7697, galU, galK,rpsL (Strr), endA1, nupG . After streaking out the glycerol stock of *E.coli* Top10F' (Invitrogen) cells onto LB-agar medium (10g/L Bacto-Tryptone, 5g/L Bacto-Yeast Extract, 10g/L NaCl, 15g/L agar pH: 7) plate, the plate was grown over night. A single colony was selected for the starter culture. 10 mL starter culture was grown overnight in 2XYT broth at 37°C.

Over night culture was inoculated into 500 ml broth containing 20 μg/ml tetracycline with a 1/100 dilution rate and placed into 37°C shaker until OD_{600} reached 0.6. After incubation, *E.coli* Top10F culture was removed and placed on ice for 30 min. Cells were centrifuged at 4000 rpm for 15 minutes. Then, supernatant was removed and pellet was gently resuspended in 40 mL of cold dH_2O and centrifuged at 4000 rpm for 15 min. The supernatant was removed again and the pellet was resuspended in 20 ml of cold dH_2O. After the centrifugation, the supernatant was discarded and cells were gently resuspended in 1 mL of ice cold 10 % glycerol. 50 μL aliquots of cells were prepared in 1.5 mL eppendorf tubes and frozen in liquid N_2, and stored at -80 °C.

2.1.4.2 Transformation of pJET plasmids into E. coli TOP 10

Electrocompotent *E.coli* top 10 cells were thawed on ice. 3 μL of the pJET ligation mixture for each sample was added to the tube containing competent cells. This mixture was transferred into the Gene-Pulser electroporator tube (Bio-Rad), which was placed into the MicroPulser electroporator (Figure 2.3) and treated at 1800V for 2-3 seconds. The reaction mixture was transferred gently to a 2 mL eppendorf tube containing 300 mL 2XYT and incubated at 37 °C for 1 h on a shaker. Then, 100 μL of culture was spread on LB plate containing 100 μg/mL ampicillin. The LB plate was incubated at 37°C over night.

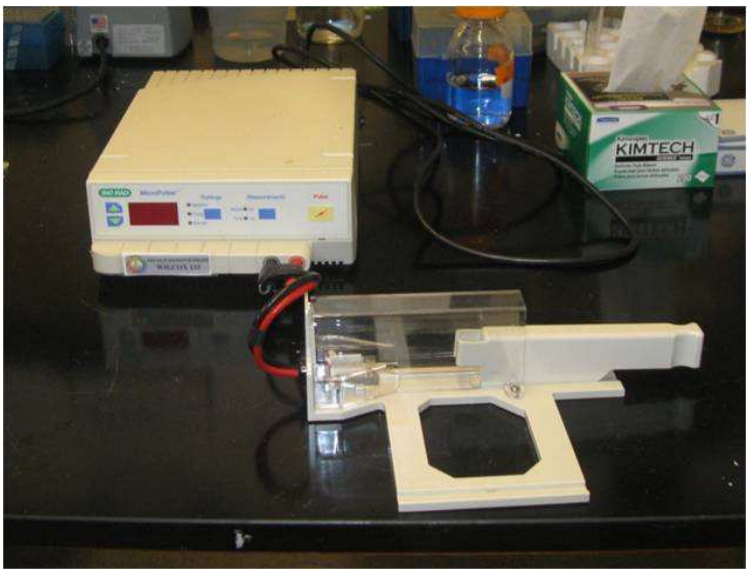

Figure 2.3 : MicroPulser electroporator (Bio-Rad).

2.1.5 Colony screening for pJET constructs

pJET cloning vector contains the gene for a restriction endonuclease which is lethal for the *E.coli* strains used for cloning. Ligation of a PCR product into the cloning site disrupts this lethal gene. Thus, only cells with recombinant plasmids are able to propagate (Url-2). All the vectors in this study contained ampicillin gene as a selection marker, therefore media and agar plates with ampicillin were used to grow and select the transformed colonies. With the help of positive selection system of pJET, only the recombinant colonies are able to grow on the plate. Colonies were analysed for the presence and orientation of the DNA inserts using the restriction analysis.

2.1.5.1 Plasmid isolation

Colonies were selected and inoculated into LB broth (10g/L Bacto-Tryptone, 5g/L Bacto-Yeast Extract, 10g/L NaCl, pH: 7) with 100 µg/mL ampicillin. Bacterial cells were harvested by centrifugation at 13000 x g for 5 min. QIAquick Plasmid DNA Isolation Kit (Qiagen) was used for plasmid DNA isolation.

2.1.5.2 DNA restriction endonuclease digestion

The *HindIII* and *PaeI* restriction enzymes and Buffer G (Fermentas) were used for the digestion of cloned fragment in pJET (Table 2.5). The pJet plasmid constructs were digested in a 40 µL reaction volume for three hours. The digestion reaction products were analyzed through agarose gel electrophoresis.

Table 2.5: Components of the DNA restriction endonuclease digestion reaction.

Component	**Volume**
G Buffer	4 µL
Plasmid	6 µL
HindIII	2 µL
PaeI	1 µL
Water, nuclease-free	27 µL
Total	**40 µL**

2.1.6 Cloning into expression vector pQE1

2.1.6.1 Preparation the insert and pQE vector for cloning

pQE1 expression vector (Qiagen) was also digested with the same restriction enzymes and the same conditions as described in section 2.1.5.2. After gel electrophoresis and excision from an agarose gel, the digested insert and pQE1 vector (Figure 2.4) were extracted as described in 2.1.3.

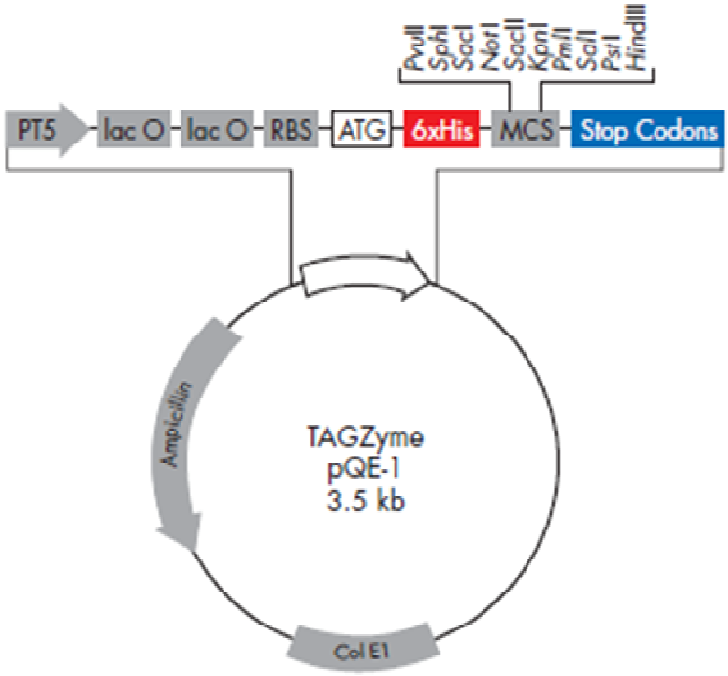

Figure 2.4 : pQE1 vector for N-terminal His tag constructs (Url-3).

2.1.6.2 Ligation and transformation

2 µL linearized pQE1 expression vector and 8 µL insert from each discrete eppendorf tubes containing DNA fragments including GFPuv, GFPuv-HABP1, GFPuv-HABP2, GFPuv-HABP1Met and GFPuv-HABP1Ala were added into 500 µL eppendorf tubes. Each tubes containing vector and DNA fragment as insert incubated at 65 ^{o}C 5 minutes. After cooling down on ice, 2µL of ligation 10 X buffer, 2µL of T4 DNA ligase (Roche), 6µL of dH_2O were added into the same reaction tube. Following the incubation at 16°C for 16 hours, heat inactivation was carried out at 65°C for 10 minutes. The same ligation reaction conditions were applied for all GFPuv-HABP constructs. Transformation was performed as desribed in 2.1.4.2.

2.1.7 Colony screening for pQE1 constructs

Colonies were analysed for the presence and orientation of the inserts using the restriction and DNA sequence analyses. After selecting and inoculating the bacterial colonies, plasmid isolation and resctriction enzyme digestion were done as described in 2.1.5.1 and 2.1.5.2 respectively.

2.1.7.1 DNA sequence analyses

Plasmids carrying the insert fragments were analyzed with ABI 3300 DNA Sequencer (Applied Biosystems). The BigDye Terminator v3.1 Cycle Sequencing Kit (Applied Biosystem) was used for sequence PCR. The reaction set up and the reaction conditions are given in Table 2.6 and Table 2.7 respectively.

Table 2.6: Sequence PCR components.

Component	**Volume**
Ready reaction mix	2 µL
Plasmid	1 µL
BigDye Terminator Sequencing Buffer	2 µL
Promoter Region/Reverse Primer	1 µL
Water, nuclease-free	4 µL
Total	**10 µL**

Table 2.7: Sequence PCR conditions.

Temperature	**Time**	**Cycle**
95 ^{o}C	5 min	1
95 ^{o}C	10 sec	15
50 ^{o}C	30 sec	
60 ^{o}C	4 min	

1 µL of 3M sodium acetate (pH 5.5) and 25 µL 95 % ethanol were added into each sequence PCR product. The tubes were incubated on ice for 15 minutes and centrifuged for 15 minutes at 14000 rpm . Supernatant was discarded and DNA pellet was washed with 250 µL cold 70 % ethanol. Samples were centrifuged for 15 minutes at 14000 rpm. Ethanol was discarded and the DNA pellet was dried at 37 ^{o}C. 20 µL di-formamide was added to each tube. Samples were incubated at 95 ^{o}C for 3

minutes for denaturating. After vortexing, the samples were keeped at 4^{o}C until the loading.

2.1.8 Expression of histidine tagged GFPuv protein and GFPuv-HABP1, GFPuv-HABP2, GFPuv-HABP1Met, GFPuv-HABP1Ala fusion proteins in E. coli TOP10 bacteria

2.1.8.1 Overnight culture preparation and inoculation

Glycerol stock of recombinant *E. coli* Top10F' strains harboring pQE1GFPuv, pQE1GFPuv-HABP1, pQE1GFPuv-HABP2, pQE1GFPuv-HABP1Met and pQE1GFPuv-HABP1Ala expression constructs were streaked out onto LB-agar medium plates containing ampicillin (100 µg/mL). The plates were grown overnight at 37 °C. A single colony was selected for the starter culture. 10 mL starter cultures were grown overnight in LB medium supplemented with ampicillin (100 µg/mL) at 37 ^{o}C by shaking at 200 rpm.

2.1.8.2 Expression conditions for pQE1 constructs

Expression of each protein construct was performed according to PQE vector instructions (Qiagen). 100 ml of prewarmed LB medium was inoculated with 5 ml of the overnight culture, and grown at 37 ^{o}C by shaking at 200 rpm, until an OD_{600} of 0.5-0.7 was reached. Expression was induced by adding IPTG to a final concentration of 1 mM. The culture was grown for an additional 4 h.

2.1.9 Preparation of glycerol stock for transformant colonies

2 mL of overnight culture was spun down with 5000 rpm and the supernatant was removed. Cell pellet was resuspended in LB medium containing 15 % Glycerol. After transferring to a sterile screw cap microcentrifuge tube, the stock was stored at -80 ^{o}C.

2.1.10 Fluorescence microscopy imaging of GFPuv protein and GFPuv-HABP1, GFPuv-HABP2, GFPuv-HABP1Met, GFPuv-HABP1Ala fusion proteins

The GFPuv, GFPuv-HABP1, GFPuv-HABP2, GFPuv-HABP1Met and GFPuv-HABPAla expressing cells were monitored using an epifluorescence microscope (BX60, Olympus Corp. Japan (Figure 2.5)) equipped with a U-MWIB filter cube (Olympus Corp. Japan).

Figure 2.5 : The setup for fluorescence microscope.

Induced culture samples were centrifuged at 5,000xg for 2 min and the pellets were washed several times with phosphate-buffered saline (PBS) solution (137 mM NaCl, 2.7 mM KCl, 10 mM Na_2HPO_4, 2 mM KH_2PO_4). The pellets were then gently suspended in PBS solution, and the suspension was deposited on a glass slide to observe the fluorescence activity of the samples. A cooled CCD camera (Diagnostic Instrument) and Spot Advanced software were used to capture the images of samples.

2.1.11 Purification of histidine tagged proteins

2.1.11.1 Preparation of E. coli lysates under native conditions

The grown culture was transferred to centrifuge tubes. Cells were harvested by centrifugation for 1 minute at 15.000xg, and the supernatant was discarded. Harvested cells were resuspended in 5 ml of lysis buffer (50 mM NaH_2PO_4, 300 mM NaCl, 10 mM imidazole, pH: 8.0). Lysozyme was added to 1 mg/mL, and the sample was incubated on ice for 30 minutes. Then, the lysate was sonicated six times for 10 s with 10s pauses at 200 W. Samples were kept on ice at all times.

2.1.11.2 Batch purification of histidine tagged proteins

Bacterial lysate was centrifuged at 10.000xg at 4 ^{o}C for 20 minutes and the supernatant was decanted. 2 mL of a 50% slurry of Ni-NTA resin (Qiagen) was added to supernatant and the tube was mixed gently for 30 minutes at 4 ^{o}C. The mixture was centrifuged for 10 s at 1000xg to pellet the resin and supernatant was discarded. The resin was washed twice with 100 µL wash buffer (50 mM NaH_2PO_4, 300 mM NaCl, 20 mM imidazole pH:8.0) and the protein was eluted three times with 20 µL elution buffer (50 mM NaH_2PO_4, 300 mM NaCl, 250 mM imidazole pH:8.0). Protein assay was performed by Bradford assay (Sigma) according to the manifacturer's instructions.

2.1.11.3 SDS-Polyacrylamide gel electrophoresis

Protein samples were analyzed by SDS-polyacrylamide gel electrophoresis (SDS-PAGE) with a discontinuous buffer system. Seperating and stacking gel parts were prepared by mixing the components stated in Tables 2.8 and 2.9.

Seperating gel acrylamide mix was poured into the gap between the glass plates and sufficient space was left for the stacking gel solution. After polimerization, stacking gel solution was poured and a comb was inserted.

10 µL of each sample was mixed with 4 µL of loading dye (Fermentas) and denaturated at 95 °C for 5 minutes. Protein samples and the molecular weight marker (Appendix A2, Fermentas) were run at 80 volt for stacking gel and 150 volt for seperating gel.

Table 2.8: Components for preparing 12% resolving gel for SDS-PAGE.

Component	**Volume**
ddH_2O	1.6 µL
30% acrylamide mix	2.0 µL
1.5 M Tris (pH 8.8)	1.3 µL
10% SDS	0.05 µL
10% ammonium persulfate	0.05 µL
TEMED	0.002 µL
Total	**2 µL**

Table 2.9: Components for preparing 5% stacking gel for SDS-PAGE.

Component	Volume
ddH_2O	0.68 µL
30% acrylamide mix	0.17 µL
1.5 M Tris (pH 8.8)	0.13 µL
10% SDS	0.01 µL
10% ammonium persulfate	0.01 µL
TEMED	0.001 µL
Total	**1 µL**

2.1.12 Spectrofluorophotometric and physicochemical analyses of GFPuv and GFPuv-HABP proteins

The excitation, emission wavelengths and fluorescence properties of the proteins were compared with a control GFPuv using Shimadzu RF-5301 PC spectrofluorophotometer (Figure 2.6), with the wavelength range of 220 to 750 nm.

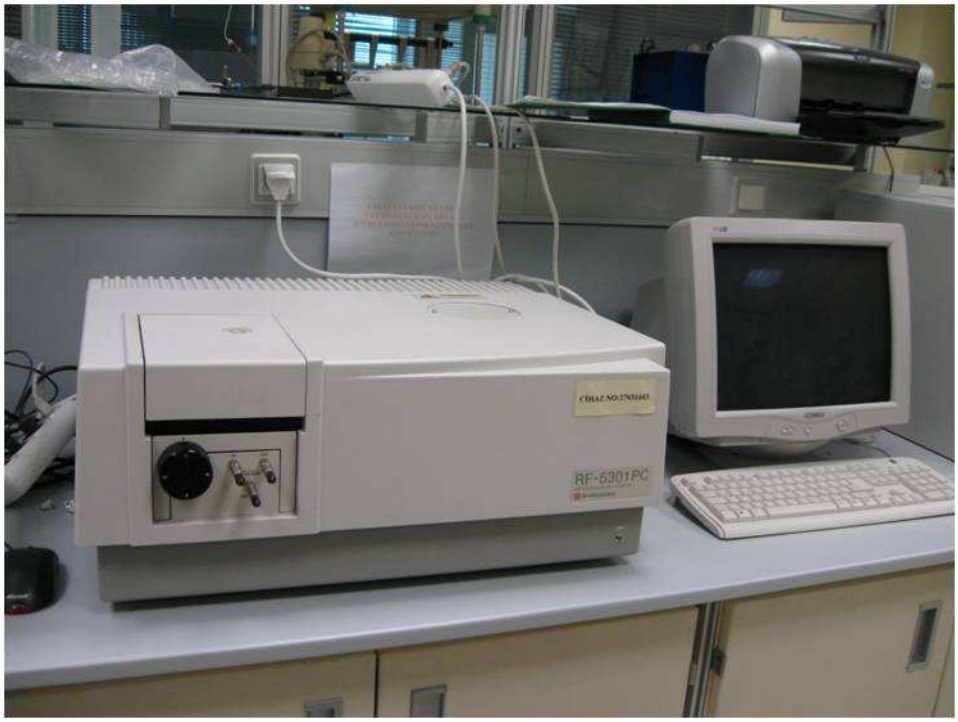

Figure 2.6 : Shimadzu RF-5301 PC spectrofluorophotometer.

Isoelectric point (pI) and molecular weight (MW) of the proteins was calculated by ExPasy ProtParam tool (Url-4).

2.1.13 Binding of GFPuv-HABP fusion constructs to hydroxyapatite

2.1.13.1 Cleaning HA powder

Synthetic HA powder (Sigma-Aldrich) was used for binding experiments. A 10-mg powder was suspended in 100 µL distilled water and a 900 µL of 1:1 methanol/acetone mixture. After vortexing, the suspension was sonicated for 20 minutes and then the procedure was repeated using isopropanol. Next, the powder was washed with phosphate/sodium carbonate (PC) buffer (55 mM KH_2PO_4, 45 mM Na_2CO_3, 200 mM NaCl pH 7.4) followed by drying in vacuum.

2.1.13.2 Incubation proteins with HA powder

Cleaned HA powder was incubated overnight with purified GFPuv, GFPuv-HABP1, GFPuv-HABP2, GFPuv-HABP1Met and GFPuv-HABP1Ala at 4 µM concentration in PC buffer containing 0.1% detergent (Tween 20 and 80, Merck) at room temperature and with constant rotation using a rotary mixer (Rotator STR4, Stuart Scientific) at 20 rpm for 4 hours.

2.1.13.3 Monitoring binding

After the incubation step, protein solutions with HA powder were centrifuged at 200xg for 3 min at room temperature. The pellets were then washed several times with PC buffer containing 0.1% detergent. After removing the supernatant, the GFPuv-bound HA samples were transferred to a microscope slide and examined under epifluorescence microscope (BX60, Olympus Corp. Japan).

2.1.14 Circular dichroism (CD) spectropolarimeter analysis of GFPuv-HABP constructs

The secondary structure analyses of the constructs were carried out using a Jasco J-810 circular dichroism (CD) spectropolarimeter (Jasco, Easton, MD, USA). The wavelength CD scans were recorded from 200-260 nm, and the scan parameters were set at 1 nm step size, 1 nm band width, 50 nm/min speed and 2 sec response time. The protein samples of 20 µM were prepared in PC buffer (pH 7), and their CD spectra were measured in the 1 mm path-length CD quartz cuvette (Starna Cells) at room temperature. For each spectrum, 3 scans were averaged after the background

subtraction of the buffer-alone sample. The mean residue molar ellipticity [θM] is expressed in deg * cm2dmol–1.

2.1.15 Quartz crystal microbalance analysis of GFPuv-HABP constructs

The quantitative binding of GFPuv, GFPuv-HABP1 and GFPuv-HABP2 on to HA substrate was carried out using a QCM-D (Quartz Crystal Microbalance with Dissipation Monitoring) system from KSV Instruments (KSV Instruments, Finland), equipped with a flow cell and a peristaltic pump (Figures 2.7 and 2.8).

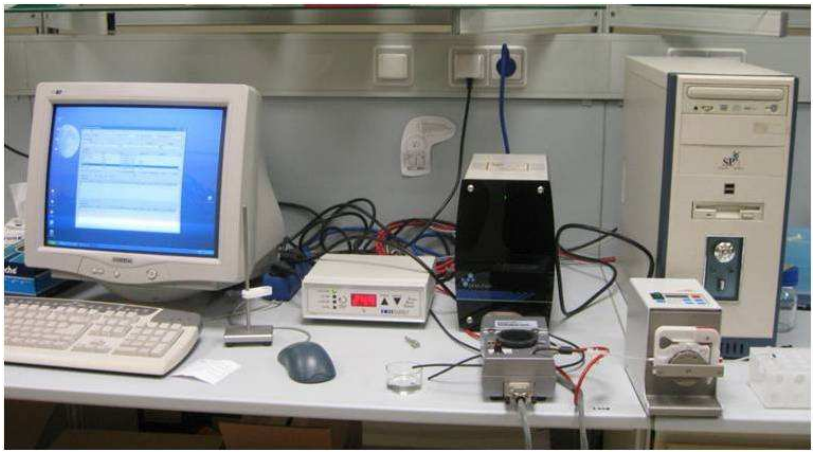

Figure 2.7 : The setup for QCM.

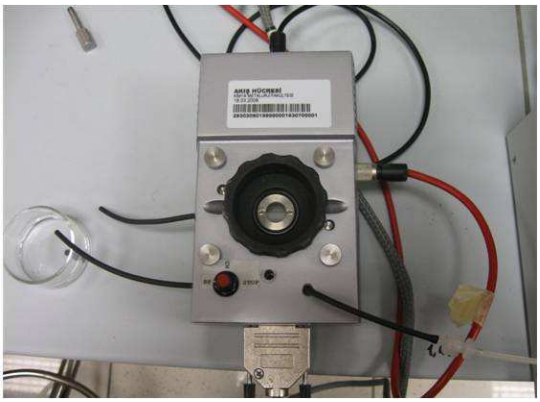

Figure 2.8 : Server-client architecture. The QCM flow cell, through which initially the buffer to clean the system, and then the tested sample solution at increasing concentration are channeled.

HA-coated QCM-D (Q-Sense, Switzerland) quartz crystals, cleaned using 96% (v/v) ethanol and deionized water were used. The cleaned crystals were mounted in QCM-D instrument and binding properties of the peptides were recorded as a function of time. The protein constructs were prepared in PC buffer at various concentrations of 300, 500, 1500 and 3000 nM. The protein solutions were introduced into the

chamber of QCM-D in a sequential order, following the baseline equilibration using PC buffer.

2.1.16 Labelling mineralized tissues

Teeth samples were kept in 70% ethanol. The specimens were sterilized by ultrasonicating in isopropyl alcohol several times to remove any organic remains or calculus from the tooth surface and expose the mineralized, native surface. Cylindrical pieces were cut from the acellular afibrillar cementum (AAFC), close to the cemento-enamel junction (Figure 2.9).

Cylindrical pieces incubated with protein samples were examined using a SEM. The cylindrical teeth samples were incubated with 1.4 μM GFPuv, GFPuv-HABP1 and GFPuv-HABP2-containing solutions. After incubation at room temperature for 2 h, samples were rinsed twice in wash buffer containing 0.1% detergent and once in 24 mM tris buffer (pH 7.4). Fluorescent microscopy with a Nikon Eclipse TE2000-U (Nikon, USA) microscope and the appropriate fluorescent filter (i.e., exciter 460-500, emitter 510-560, Chroma Technology Co., USA) was used.

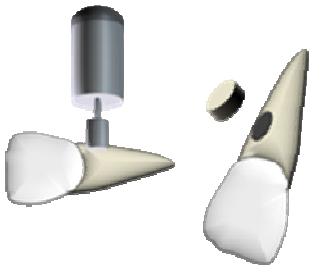

Figure 2.9 : Schematic description of the procedure for cutting cylindirical specimens from the root.

The average relative fluorescent intensities were measured real-time using Metamorph v7.5 image processing software (Molecular Devices, USA).

2.1.17 Time-wise monitoring of mineralization on surfaces

2.1.17.1 Preparation of calcium phosphate mineral covered glass slides

Mineral layers were formed according to an alkaline phosphatase (AP)-based mineralization model (Gungormus et al. 2008). This model involves enzymatic hydrolysis of an organic phosphate compound, namely β-Glycerophosphate (β-GP), to PO_4^{-3} by AP.

Mineralization solution was prepared using 24 mM Ca^{+2} ($CaCl_2$) and 14.4 mM β-GP in 25mM Tris-HCl buffer (pH 7.4). When PO_4^{-3} is released to the solution by the action of AP, Ca/P mineralized composition is produced. Following the mineralization reactions, calcium phosphate layers were formed on glass cover slides (Figure 2.10). Samples were examined by optical microscopy using a Nikon Eclipse TE2000-U (Nikon, USA) and scanning electron microscopy (SEM, JSM 7000F JEOL-) at different time intervals, including 0.5, 2, 8 and 24 hours. Upon completion of each time interval, the glass slides were taken out and the mineral covered areas on glass slides were determined using Metamorph v7.5 image processing software (Molecular Devices, USA).

Figure 2.10 : Glass coverslides on which calcium phosphate layers were formed following the mineralization reactions.

2.1.17.2 Incubation protein samples with mineral covered glass slides

Following determination of mineral covered areas, slides were incubated with 1.4 µM GFPuv and GFPuv-HABP1 (in 24 mM Tris-HCl buffer, pH 7.4) for 2 hours at room temperature. Then, the slides were rinsed twice in wash buffer containing 0.1% detergent (Tween 20 and 80) and once in Tris-HCl buffer (24 mM; pH: 7.4). Samples were monitored under fluorescent microscopy (Nikon Eclipse TE2000-U (Nikon, USA) with fluorescent filters (exciter 460-500, emitter 510-560, Chroma Technology Co., USA).

2.2 Construction, Expression and Analyses of MBP Tagged GFPuv Fusion Proteins

2.2.1 Oligonucleotide primers for GFPuv, GFPuv-AgBP2c and GFPuv-AuBP2c constructs

Primers for constructing GFPuv-AuBP (CGP-WALRRSIRRQSY-GPC) and GFPuv-AgBP (CGP-EQLGVRKELRGV-GPC) fusion proteins encoding expression vector were designed (Table 2.10).

Table 2.10: Oligonucleotide primers used in PCR reactions for GFPuv, GFPuv-AgBP2c and GFPuv-AuBP2c constructs.

Primer Name	Sequence
AuP1	5’ – CGAACGACGCAGAGCCCACGGACCGCAACCTCCA CCCGATTTGTAGAGCTCATCCATGCC – 3’
AuP2	5’- CGAACGACGCAGAGCCCACGG -3’
AuP3	5’- GCCAAGCTTTTAGCACGGACCATACGACTGACGAC GAATCGAACGACGCAGAGCCCA -3’
AuP4	5’- GCCAAGCTTTTAGCACGGACCATA -3’
PMGFP1	5’ - CGGGAATTCATGAGTAAAGGAGAAGAACTT - 3’
PMGFP2	5’- GCCAAGCTTTTATTTGTAGAGCTCATCCATGCC- 3’
AgP1	5’-ACGCACACCCAGCTGTTCCGGACCGCAACCTCCAC CCGATTTGTAGAGCTCATCCATGCC-3’
AgP2	5’-ACGCACACCCAGCTGTTCCGG-3’
AgP3	5’-GCCAAGCTTTTAGCACGGACCCACACCACGCAGTTCT TTACGCACACCCAGCTGTTC-3’
AgP4	5’-GCCAAGCTTTTAGCACGGACCCACACCACG-3’

2.2.2 Polymerase chain reaction for GFPuv, GFPuv-AgBP2c and GFPuv-AuBP2c DNA fragments

The vector pGFPuv used as a template in all polymerase chain reactions (PCR). The PCR experiments were performed using, Phusion High-fidelity DNA polymerase (NEB). This enzyme generates blunt ends in the amplification products. To obtain A-added fragments, Taq DNA polymerase (NEB) was added into the reaction before the final extension.

GFPuv encoding sequence was amplified using the forward PMGFP1 and the reverse PMGFP2 primers containing extra residues including a *EcoRI* or *HindIII* site at their

5’ ends, respectively. The DNA fragment encoding GFPuv-fused silver binding peptide AgBP2c (GFPuv-AgBP2c) and GFPuv-fused gold binder peptide AuBP2c (GFPuv-AuBP2c) were obtained in a four step PCR reactions.

The first PCR reaction was kept in 15 cycle and performed by using the forward primer PMGFP1 and the reverse primer AuP1 bearing the first part of gold binding peptide (AuBP2c) coding sequence (Table 2.10 and 2.11).

Table 2.11: Conditions for the first and third PCR steps for GFPuv-AuBP2c and GFPuv-AgBP2c constructs.

Temperature	Time	Cycle
98 ^{o}C	30 s	1
98 ^{o}C	10 s	15
50 ^{o}C	10 s	
72 ^{o}C	2 min	
72 ^{o}C	5 min	1

The second PCR reaction was kept in 30 cycle and performed by using the forward primer PMGFP1 and the reverse primer AuP2 and the first PCR product as a template (Table 2.12). The PCR product was purified by gel extraction and used as a template for the third PCR reaction. The third PCR reaction was kept in 15 cycle and performed by using the forward primer PMGFP1 and the reverse primer AuP3 bearing the second part of AuBP2c coding sequence with *HindIII* cleavage site (Table 2.11). The fourth PCR reaction was kept in 30 cycle and performed by using the forward primer PMGFP1 and the reverse primer AuP4 and the third PCR product as a template (Table 2.12).

Using the same PCR strategy described above, the DNA fragment encoding GFPuv fused silver binding peptide AgBP2c (GFPuv-AgBP2c) was obtained. PMGFP1, AgP1, AgP2, AgP3 and AgP4 primers were used with the same order.

Table 2.12: Conditions for the second and fourth PCR step for GFPuv-AuBP2c and GFPuv-AgBP2c constructs.

Temperature	Time	Cycle
98 ^{o}C	30 s	1
98 ^{o}C	10 s	30
54 ^{o}C	30 s	
72 ^{o}C	30 s	
72 ^{o}C	10 min	1

2.2.3 Cloning PCR products into TOPO TA cloning vector

2.2.3.1 Ligation and electroporation

Purified DNA fragments were cloned into TOPO TA cloning vector (pCR2.1-TOPO, Invitrogen (Figure2.11)).

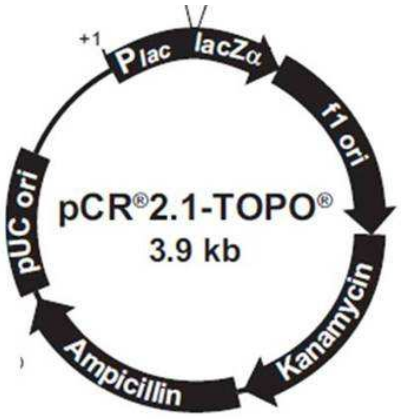

Figure 2.11 : Map of TOPO TA Cloning Vector (Url-5).

Table 2.13 describes the set up for TOPO TA cloning reaction. After mixing, the reaction was incubated for 15 minutes at room temperature.

Table 2.13: TOPO TA cloning setting up.

Reagent	Volume
PCR Product	3 µL
Diluted Salt Solution	1 µL
Water	1 µL
TOPO vector	1 µL
Total	**6 µL**

TOPO cloning constructs were transformed into *E. coli* TOP10 F' as decribed in Section 2.1.4.1. After electroporation and incubation cells were spread on pre-warmed selective X-gal/IPTG LB plate containing 100 µg/mL ampicillin.

2.2.3.2 Colony screening

An afficient TOPO TA cloning reaction produces several hundred blue or white colonies on the selective plate (Url-5). 10-20 white colonies were taken and cultured overnight in LB medium containing 100 µg/mL ampicillin. After isolation, plasmids were analyzed by restriction analyses using *EcoRI* and *HindIII* restriction enzymes as described section 2.1.5.2 (Fermentas).

2.2.4 Cloning into expression vector pMALc4x

2.2.4.1 Preparation insert and pMALc4x vector

pMALc4x expression vector (NEB) was also digested with the same restriction enzymes as described above. After gel electrophoresis, digested inserts (GFPuv, GFPuv-AgBP2c, GFPuv-AuBP2c) and pMALc4x vector were extracted from agarose gel.

2.2.4.2 Preparation competent E.coli ER2507 using rubidium chloride method

Overnight culture was subcultured at 1:100 in 100 mL of LB + 20 mM $MgSO_4$ and grown until OD_{600} reached 0.6. The culture was centrifuged at 5.000xg for 5 minutes at 4 ^{o}C. Cell pellet was resuspended 40 mL cold TFBI (30 mM KOAc, 100 mM RbCl, 10 mM $CaCl_2$, 50 mM $MnCl_2$, 15 % glycerol, pH 5.8) and incubated on ice for 5 minutes. After centrifugation at 5.000x for 5 minutes, the pellet was resuspended in 4 ml of TFB2 (10 mM MOPS, 75 mM $CaCl_2$, 10mM RbCl, 15% glycerol, pH 6.5) and incubated on ice 30 minutes. 80 µL aliquots of cells were prepared in 1.5 mL eppendorf tubes and frozen in liquid N_2 and stored at -80 °C.

2.2.4.3 Ligation and transformation

Quick ligation kit (NEB) was used for ligation. The components of ligation was combined acording to Table 2.14.

3 µL of reaction was used for each transformation. After thawing an aliquot of competent bacterial cells on ice, ligation reaction was added and the mixture was incubated 1 hour on ice.

Table 2.14: Reaction components for pMALc4x ligation.

Component	**Volume**
pMALc4x	3 µL
Insert	7 µL
2x Quick Ligation Reaction Buffer	10 µL
Quick T4 DNA Ligase	1 µL
Total	**21 µL**

Following a heat shock at 37 ^{o}C for 45 seconds, cells were incubated on ice for 2 minutes. 1 mL of LB was added and the cells incubated at 37 ^{o}C for 20 minutes. 100 µL of culture was spread on LB plate containing 100 µg/mL ampicillin. The LB plate was incubated at 37 °C over night.

2.2.4.4 Colony screenig

Colonies were analysed for the presence and orientation of the inserts using restriction and DNA sequence analyses.

2.2.5 Expression of MBP tagged GFPuv protein and GFPuv-AgBP2c, GFPuv-AuBP2c fusion proteins in E. coli ER2507 bacteria

1 liter of LB medium with 2 % glucose supplemented with 100 µg/mL ampicillin was inoculated with recombinant ER2507 *E. coli* bacteria harboring pMALc4x constructs. Each recombinant cell culture containing one of the pMALc4x constructs (pMALc4x-GFPuv, pMALc4x-GFPuv-AgBP2c, pMALc4x-GFPuv-AuBP2c) were grown at 37 °C until OD_{600} reached 0.5, after which IPTG was added to a final concentration of 0.3 mM. After induction, each culture incubated at 30 ^{o}C for 6 hours.

2.2.6 Purification of MBP tagged proteins

Following expression, cells were harvested by centrifugation at 4000xg for 20 minutes. The cell pellet was resuspended in 50 mL column buffer and frozen

overnight at -20 ^{o}C. Cells were then thawed in cold water and sonicated as described in 2.1.11.1.

After centrifugation at 9,000xg for 30 minutes, supernatant was saved and diluted at 1:5 with column buffer (20 mM Tris-HCl, 200 mM NaCl, 1mM EDTA). 10 ml amylose resin (NEB) was poured in a 2.5x10 cm colum. Column was washed with 8 column volumes of column buffer. Filtered supernatant sample was loaded to amylose column for the affinity chromatograpy (Figure 2.12) at a flow rate of 1 ml/minute.

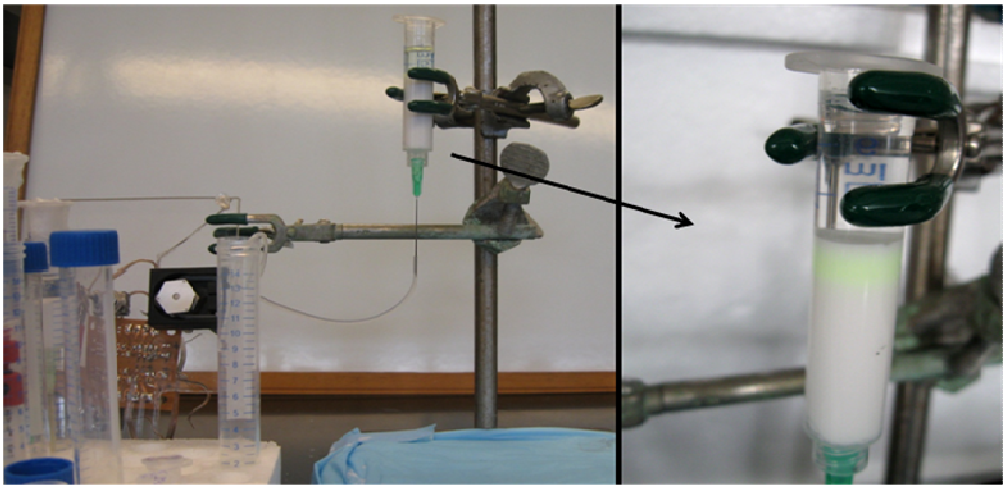

Figure 2.12 : Set up for affinity chromatography.

Following the washing of the column with 12 column volumes of column buffer, the protein of interest was eluted using column buffer with 10 mM maltose. Fractions were collected and concentrated by 10 kDa Amicon Ultra-15 protein centrifugal filter (Milipore, USA).

2.2.7 Cleavage of MBP tag

Purified MBP-GFPuv, MBP-GFPuv-AgBP2c and MBP-GFPuv-AuBP2c proteins were concentrated by Amicon Ultra-15 protein centrifugal filter to 1 mg/mL. Protein samples were transferred to buffer containing 20 mM Tris-HCl, 100 mM NaCl, 2 mM $CaCl_2$ (pH 8.0) by ultrafiltration using the same centrifugal filter tubes. 40 µL of 1mg/mL Factor Xa (NEB) was added to 2.5 ml fusion protein substrate. The reaction was incubated at 4 ^{o}C overnight and then at room temperature for 3 hours.

2.2.7.1 Removal of maltose by hydroxyapatite chromatography

2 g hydroxyapatite was swollen in 20 mM sodium phosphate, 200 mM NaCl (pH 7.2). Swollen hydroxyapatite was washed with the same buffer and poured into the column.

Each fusion protein cleavage mixture was loaded onto the column. Using 80 mL of the same buffer, the column was washed and maltose was washed away. Protein samples were eluted with 0.5 M Na phosphate (pH 7.2).

2.2.7.2 Analysis for the purified MBP-GFPuv, MBP-GFPuv-AgBP2c, MBP-GFPuv-AuBP2c, GFPuv, GFPuv-AgBP2c and GFPuv-AuBP2c proteins

Hydroxyapatite-eluted protein was loaded onto the amylose column as described 2.2.7.1. Protein samples in the flow-through should be free of MBP. Protein assay was performed by Bradford assay (Sigma) according to manifacturer's instruction. SDS-PAGE and spectrofluorophotometric analyses were done as desribed in 2.1.11.3 and 2.1.12, respectively.

2.2.8 Microcontact Printing of MBP-GFPuv and MBP-GFPuv-Metal Binding Peptides

The PDMS stamps were fabricated by molding a mixture of pre-polymer polydimethyl siloxane and curing agent with a ratio of 10:1 (w/w) (Sylgard 184, Dow Corning, USA) on the patterned silanized master. The stamps were then washed several times with ethanol, heptane, and last with ethanol, and dried with nitrogen. The patterned side of the PDMS stamp is incubated with MBP-GFP-AgBP, MBP-GFP-AuBP and MBP-GFP. After drying, the stamps were applied to silver and gold substrates. Then the stamps were removed from the substrates.

2.2.9 Self Assembly of Fusion Proteins on Silver Nanoparticle-arrayed Surface

Quartz binding peptide-PPP-Silver Binding Peptide (QBP-PPP-AgBP) was microcontact printed on the glass cover slides as described above. QBP-PPP-AgBP printed substrate was incubated with 80 nm and 20 nm AgNP. After 30 minutes incubation, the substrates were washed and dried under nitrogen. The silver nanoparticle arrays were observed under dark field microscopy. Silver patterned

surfaces were incubated with MBP-GFPuv-AgBP2c, GFPuv-AgBP2c, MBP-GFPuv and GFPuv.

2.2.10 Fluorescence Quenching/Enhancement by Metallic Nanoparticles

Fluorescent measurements were performed using TECAN Safire UV-vis spectrometer microplate reader (Figure 2.14). 384 well black clear flat bottom microplate (Corning) was used for the incubation and fluorescent measurements. 5 µL (10 µM) protein was incubated with gold nanoparticles with different total surface area in the 50 µl total reaction volume. After incubation, fluorescence intensity was measured at 394 nm excitation and 510 nm emission wavelengths.

Figure 2.13 : The spectrophotometer.

.

3. RESULTS AND DISCUSSION

3.1 Genetic Construction and Applications of Histidine Tagged GFPuv-HABP Fusion Proteins

In this study, fusion proteins encoding both the fluorescence activity of a GFP variant and hydroxyapatite-binding activity of phage display selected peptides have been engineered. Each fusion peptide was cloned into pQE1 expression vector encoding N-terminal Histidine tag.

In widely used phage display libraries (New England Biolab), 7 or 12 amino acid long peptides are displayed at the N-terminus of pIII coat protein. The displayed peptide sequences are separated from the pIII protein by short flexible SGGG linker (Brown et al., 2000; Tamerler et al., 2010) . In this study a flexible SGGG linker was used between GFP and HABPs (Figure 3.1).

There are many of studies in literature exploiting fluorescent protein fusions. In most of these studies it has been observed that fusion of GFP to the protein of interest does not alter the function of both GFP and the protein (Hoffman 2002; Zimmer 2002; Chudakov et al., 2005; Wiedenmann et al., 2009). In previous studies, it has been demonstrated that the single form or multiple repeat of inorganic binding peptides conserved their binding ability when they fused to functional proteins (Park et al., 2006; Kacar et al., 2009b). In this study it has been demonstrated that GFPuv-HABP1 construct conserved both fluorescence and HA binding activity.

GFPuv-HABP1 with multifunctional property, has been exploited for targeted labeling of mineralization on the synthetically mineralized surface and the naturally mineralized tissue.

3.1.1 Designing GFPuv-HABP fusion constructs

In order to generate GFPuv and GFPuv-HABP constructs, primers were designed according to amino acid sequence of HABPs, -SGGG linker and GFPuv. Multiple

cloning site of expression vector pQE1 has various restriction endonuclease cleavage sites including *PaeI* and *HindIII*.

GFPuv and GFPuv-HABP encoding sequences were amplified using a series of forward and reverse primers containing extra residues including a *PaeI* or *HindIII* site at their 5' ends respectively. As the constructs were cloned into pQE1 vector coding N-terminal His tag, in the final purified proteins, histidine tag was placed at the N terminal, while HABPs were located at the C- terminal (Figure 3.1).

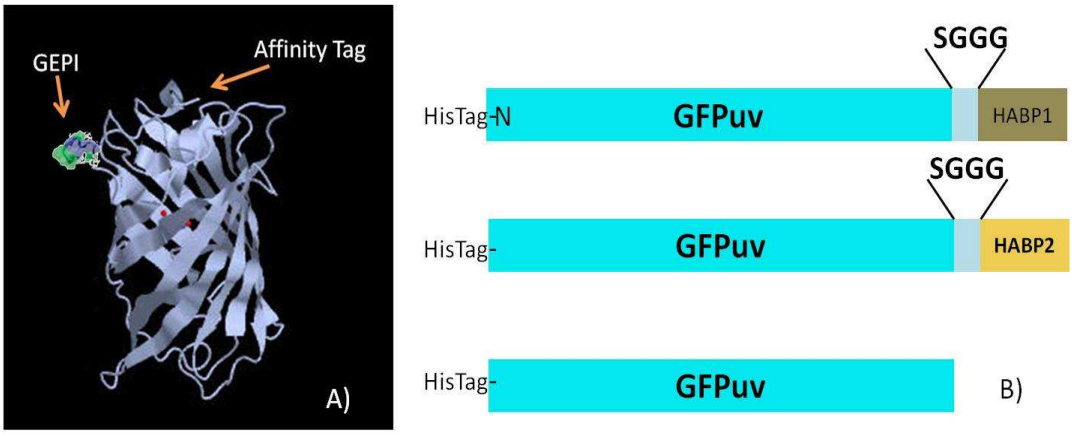

Figure 3.1 : Designing strategies of GFPuv-HABP fusion proteins. A. GFP-GEPI fusion. Modified from PDB ID: 1b9c. B. Schematic representation of the designing strategy.

3.1.2 Obtaining PCR products encoding GFPuv and GFPuv-HABP fusion proteins

The DNA fragment encoding GFPuv and GFPuv-HABPs were obtained by single and consecutive PCR reactions, respectively. Various conditions were applied for PCR to obtain the desired molecular weight. The GFPuv, GFPuv-HABP1/2 and GFPuv-HABPAla/Met PCR products were 735 bp, 774 bp and 768 bp respectively. PCR conditions were optimized for the fusion constructs. It was observed that when pfu polymerase was used, 50 ^{o}C was the optimum annealing temperature for the first step of PCR.

Using agarose gel electrophoresis, the molecular weight of GFPuv, GFPuv-HABP1, GFPuv-HABP2, GFPuv-HABP1Ala and GFPuv-HABP1Met encoding DNA fragments were verified (Figures 3.2, 3.3, 3.4 and 3.5).

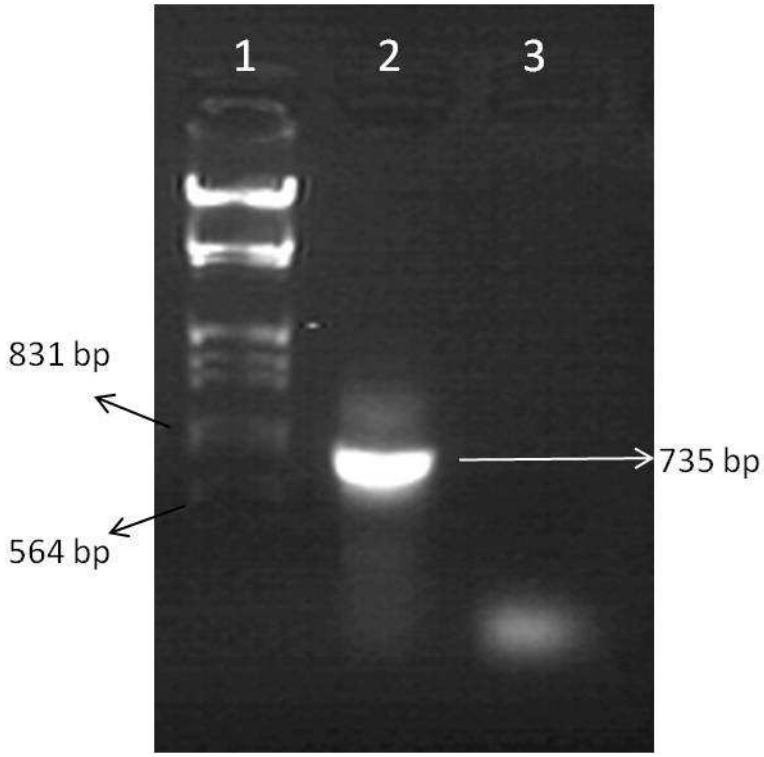

Figure 3.2 : Fragments amplified with pfu DNA polymerase; lane 1. Lambda DNA/EcoRI+HindIII Marker, 3 (Fermentas), lane 2. GFPuv encoding DNA fragment, lane 3. Control.

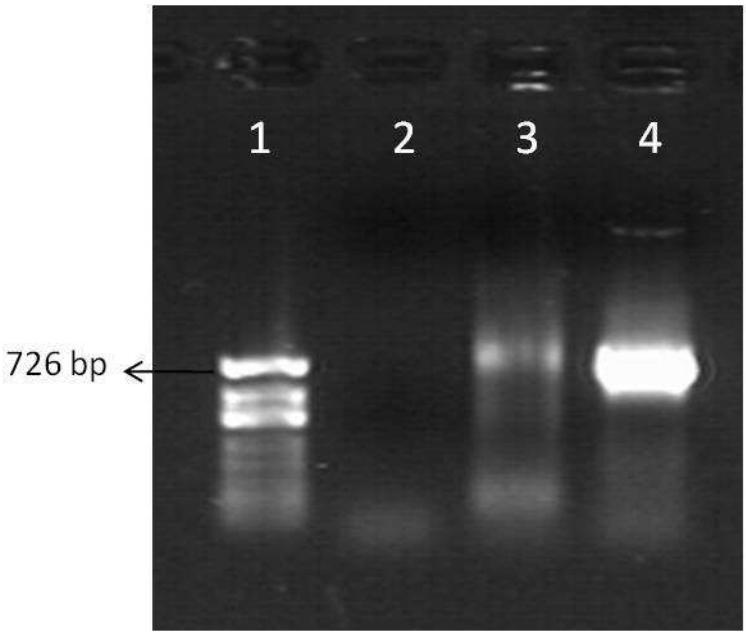

Figure 3.3 : Fragments amplified with pfu DNA polymerase; lane 1. φX174 DNA/HinfI Marker, 10 (Fermentas), lane 2. Control lane, 3. Hydroxyapatide binding peptide 1-GFPuv encoding DNA fragment, lane 4. GFPuv encoding fragment.

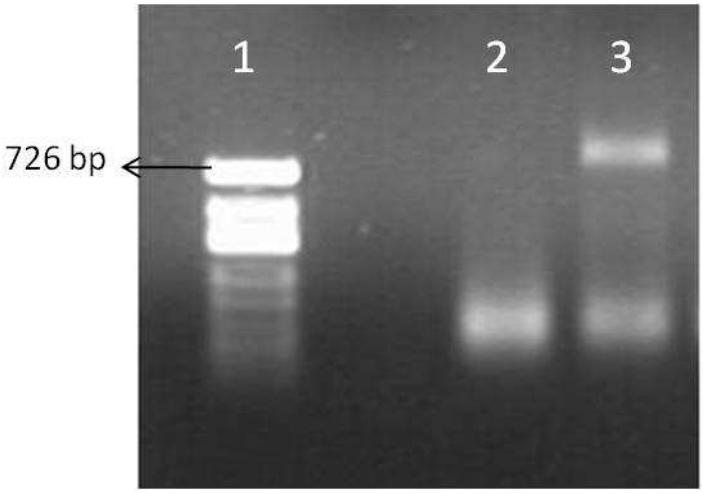

Figure 3.4 : Fragments amplified with pfu DNA polymerase; lane 1. φX174 DNA/HinfI Marker, 10 (Fermentas), lane 2. Control, lane 3. Hydroxyapatide binding peptide 2-GFPuv encoding DNA fragment.

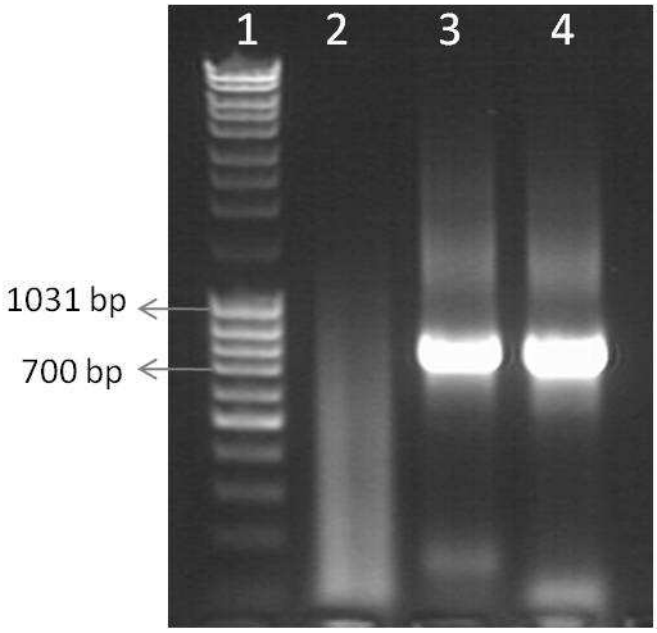

Figure 3.5 : Fragments amplified with Pfu DNA polymerase; lane 1. Mass Ruler DNA Ladder mix (Fermentas), lane 2. Control, lane 3. GFPuv-HABP1Ala (AGHHPLM), lane 4. GFPuv-HABP1Met (MLPHHGA) encoding DNA fragment.

3.1.3 Cloning the target DNA into pJET cloning vector

Using cloning vector, insert DNA can be carried and introduced into the bacteria. In this method, numerous copies of insert can be produced. After extraction of the PCR products from agarose gel, each purified DNA fragment was ligated into pJET cloning vector. After transformation of *E. coli* TOP10 F' cells with the ligation product, colonies were observed on agar plates containing ampicillin.

3.1.3.1 Positive selection for the transformant colonies

pJet cloning vector provides a positive selection strategy by containing the gene for a restriction endonuclease which is lethal for the *E.coli* strains used for cloning. Disrupting the lethal gene by the ligation reaction leads to amplification of only cells with recombinant plasmids (Url-2).

pJET vectors harboring GFPuv, GFPuv-HABP1, GFPuv-HABP2, GFPuv-HABP1Ala, GFPuv-HABP1Met inserts were isolated from selected colonies. These plasmids were digested with PaeI and HindIII to obtain the insert DNA fragments. Double digestion products were run in agarose gel (Figures 3.6, 3.7, 3.8 and 3.9).

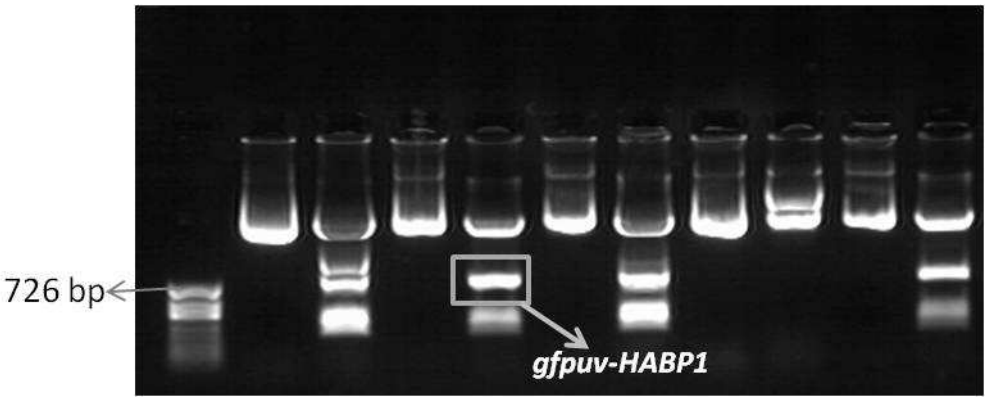

Figure 3.6 : Verification of cloning of gfpuv-HABP1 into pJET cloning vector. Undigested and double digested recombinant pJET plasmids harboring gfpuv-HABP1 were loaded into the gel sequentially.

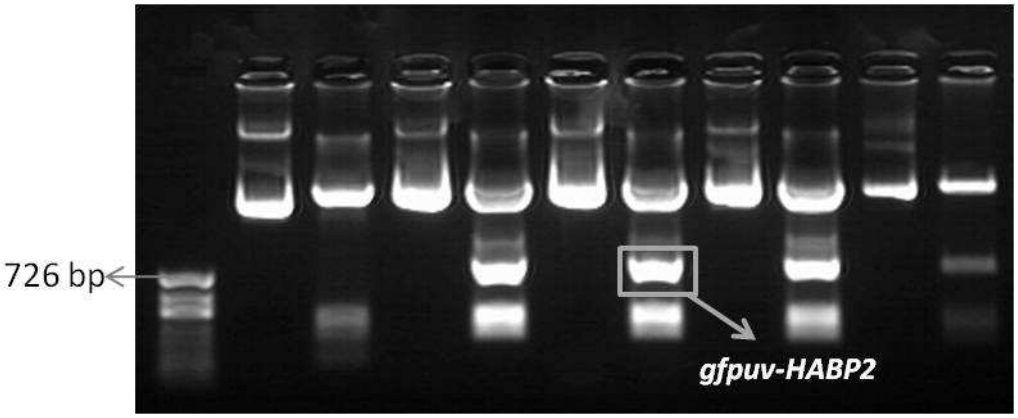

Figure 3.7 : Verification of cloning of gfpuv-HABP2 into pJET cloning vector. Undigested and double digested recombinant pJET plasmids harboring gfpuv-HABP2 were loaded into the gel sequentially.

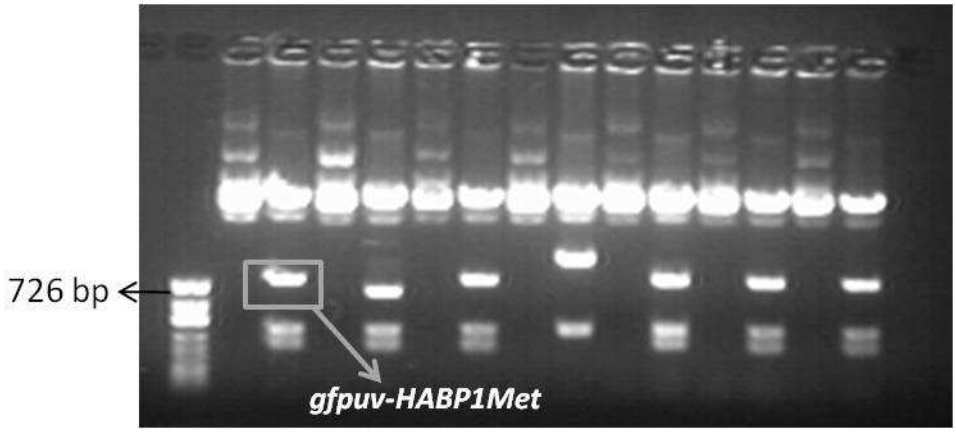

Figure 3.8 : Verification of cloning of gfpuv-HABP1Met into pJET cloning vector. Undigested and double digested recombinant pJET plasmids harboring gfpuv-HABP1Met were loaded into the gel sequentially.

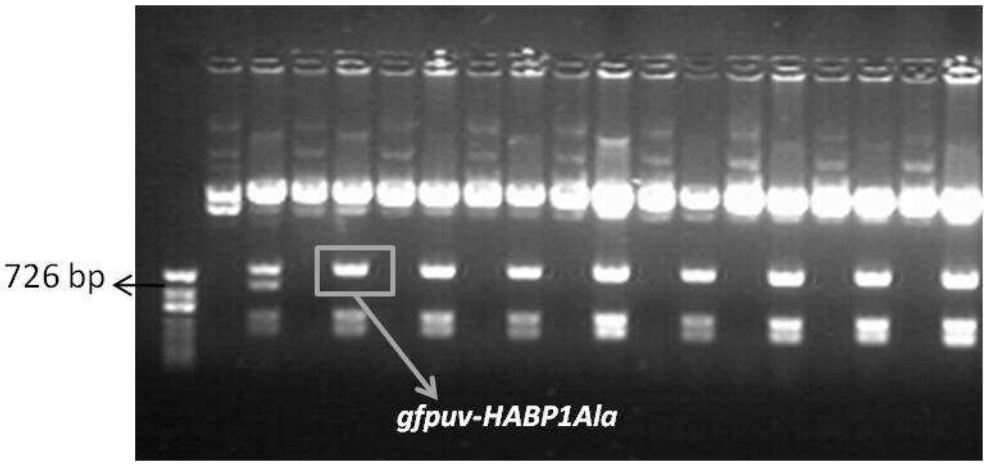

Figure 3.9 : Verification of cloning of gfpuv-HABP1Ala into pJET cloning vector. Undigested and double digested recombinant pJET plasmids harboring gfpuv-HABP1Ala were loaded into the gel sequentially.

Digested and undigested pJET vectors harboring GFPuv, GFPuv-HABP1, GFPuv-HABP2, GFPuv-HABP1Ala, GFPuv-HABP1Met inserts were run in an agarose gel and size of insert fragments were verified (Figures 3.6, 3.7, 3.8 and 3.9).

3.1.4 Generating histidine tagged GFPuv protein and GFPuv-HABP1, GFPuv-HABP2, GFPuv-HABP1Met, GFPuv-HABP1Ala fusion protein expressing bacteria

Recombinant *E. coli* Top10F' strains harboring 6His-GFPuv, 6His-GFPuv-HABP1, 6His-GFPuv-HABP2, 6His-GFPuv-HABP1Ala and 6His-GFPuv-HABP1Met expression constructs were obtained by cloning the each DNA fragment into pQE1 expression vector and transforming the bacteria with the constructs.

3.1.4.1 Cloning into expression vector pQE1

pQE1 vector having ColE1 origin of replication (Url-3) was exploited for high-level expression of His-tagged GFPuv and GFPuv-HABP proteins in E. coli. GFPuv and GFPuv-HABP encoding sticky ended DNA fragments were obtained by digesting the recombinant pJET plasmids. pQE1 vector was also linearized by the same restriction enzymes. Sticky ended insert fragments (*gfpuv, gfpuv-HABP1, gfpuv-HABP2, gfpuv-HABP1Ala, gfpuv-HABP1Met*) and pQE1 vector were run into agarose gel. After gel extraction, all fragments were again run into the gel and purification of the DNA fragments were verified. Purified gfpuv-HABP1 DNA fragment is shown in Figure 3.10.

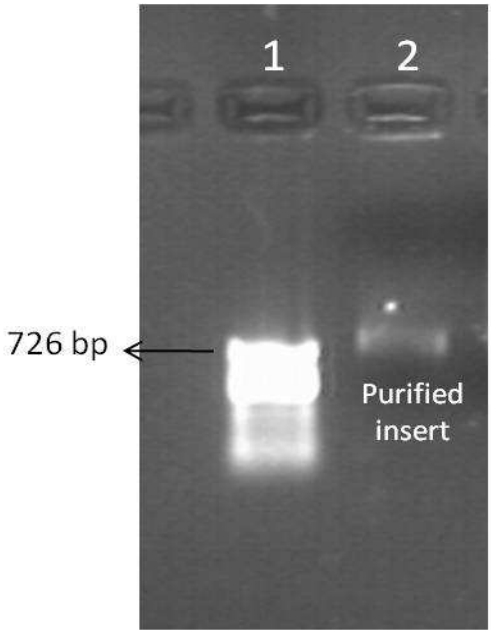

Figure 3.10 : Purifired gfpuv-HABP1 fragment. After gel extraction, insert fragments were run into 1% agarose gel and purification of the DNA fragments was verified.

Following the ligation reactions, *E. coli* TOP10 F' electrocompetent cells were transformed with each ligation product. Recombinant colonies were selected on ampicillin including LB plates. For each construct, more than 50 colonies were observed on the plate after overnight incubation.

3.1.4.2 Colony Screening after transformation

The resulting transformant colonies were picked up and replicated. Bacterial cultures inoculated with the selected colonies were used for plasmid isolation. Insertion of gfpuv, gfpuv-HABP1, gfpuv-HABP2, gfpuv-HABP1Ala, gfpuv-HABP1Met

fragments into PQE1 was verified by digestion of purified plasmids with *PaeI* and *HindIII*. Insertion of the insert fragments into PQE1 expression vector is indicated by Figures 3.11, 3.12, 3.13.

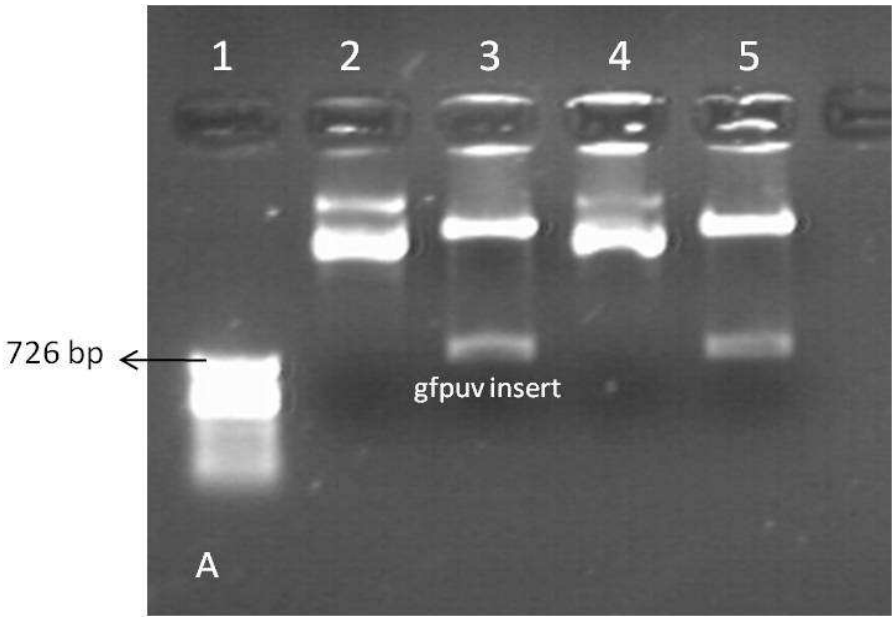

Figure 3.11 : Verification of cloning of gfpuv into pQE1 expression vector. Undigested and double digested recombinant pQE1 plasmids harboring gfpuv were loaded into the gel sequentially.

After insert verification, the sequences of pQE1 constructs harboring the insert fragments were confirmed by DNA sequence analyses. It has been demonstrated that the pQE1GFPuv and pQE1GFPuv-HABP constructs do not carry any mutation.

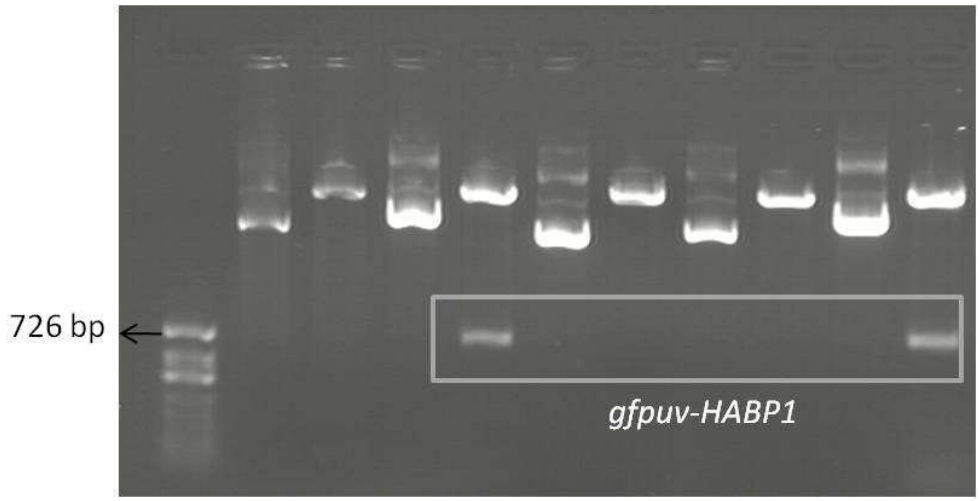

Figure 3.12 : Verification of cloning of gfpuv-HABP1 into pQE1 expression vector. Undigested and double digested recombinant pQE1 plasmids harboring gfpuv-HABP1 were loaded into the gel sequentially.

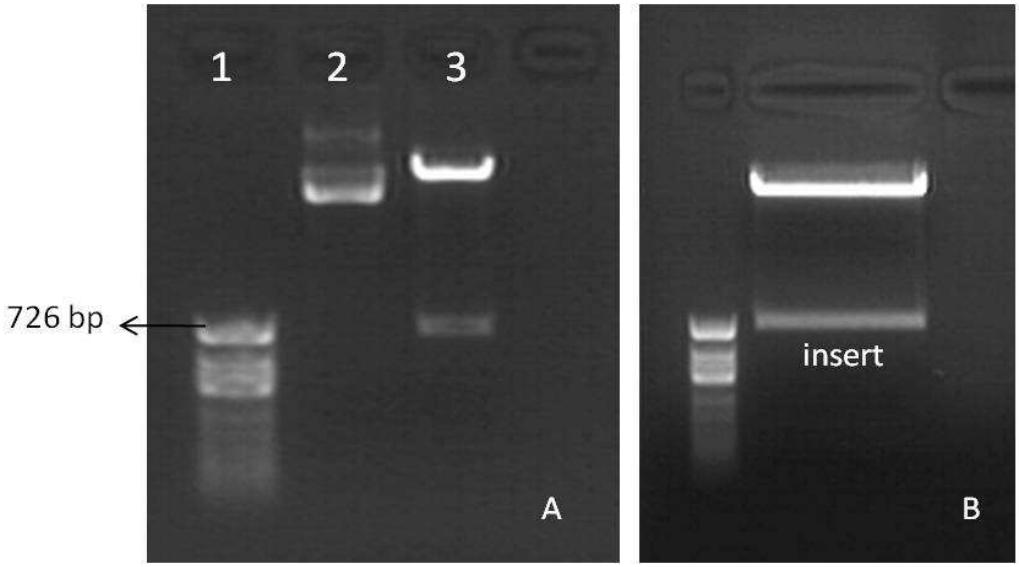

Figure 3.13 : Verification of cloning of gfpuv-HABP2 (A) and gfpuv-HABP1Ala (B) into pQE1 expression vector.

Transformant colonies were also monitored under UV light. After transformation, transformant colonies were picked up by sterile toothpick by touching the colonies. After lightly dragging the toothpick to plate surface, replica plates were incubated overnight.

For each construct, one of the replica plates contained IPTG for inducing recombinant protein production. IPTG containing replica plates were examined under UV light and gfp based fusion protein expressing bacterial colonies were monitored (Figure 3.14).

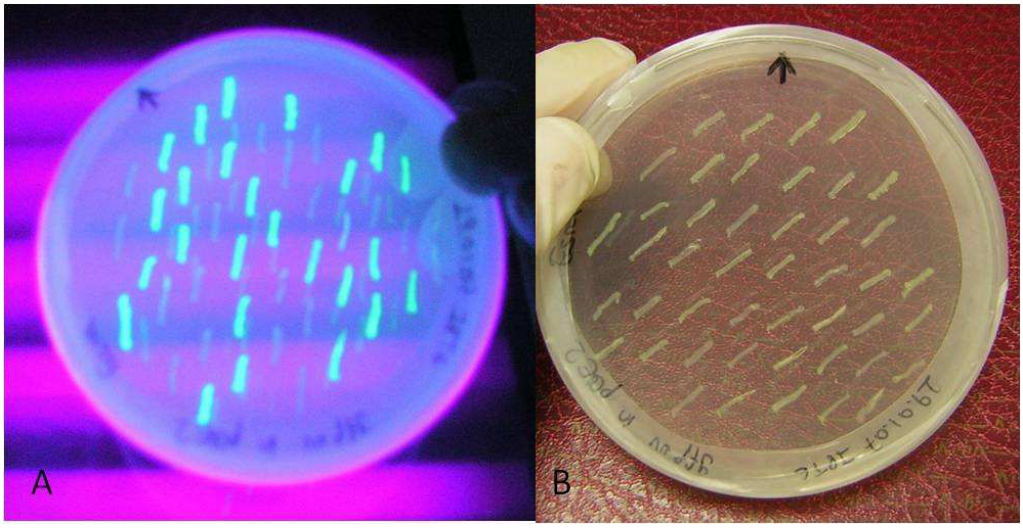

Figure 3.14 : After transformation, transformant colonies were picked up. IPTG containing replica plates were examined under UV light (A) and gfp based fusion protein expressing bacterial colonies were monitored. B) Image of replica plate under visible light.

3.1.5 Production and Purification of The Recombinant Histidine Tagged Proteins

6His-GFPuv, 6His-GFPuv-HABP1, 6His-GFPuv-HABP2, 6His-GFPuv-HABP1Ala and 6His-GFPuv-HABP1Met fusion proteins were expressed in *E. coli* TOP10 F´ strains. Colonies were grown in ampicillin containing LB medium and were induced with IPTG for overexpression of the his-tagged proteins. After cell lysing, overexpressed proteins were purified using Ni-NTA resin. The expression level, purity and molecular weights of fusion proteins were analyzed by SDS-PAGE (Figures 3.15, 3.16 and 3.17).

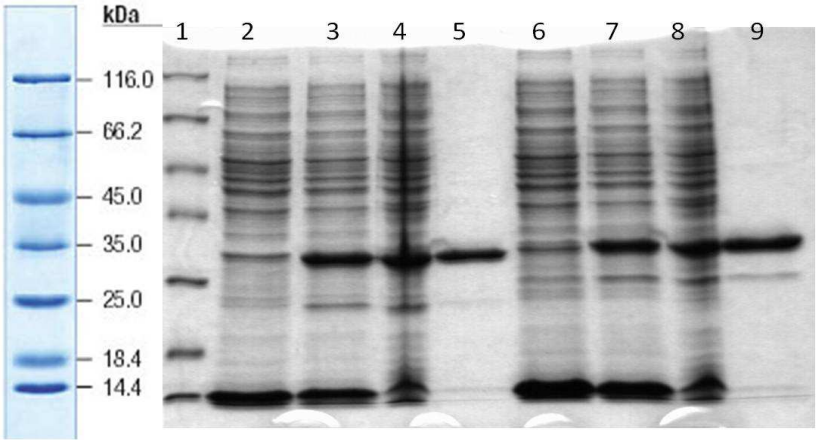

Figure 3.15 : SDS-PAGE analysis of the protein samples extracted from GFPuv (Lanes 2-5) and GFPuv-HABP1 (Lanes 6-9) expressing E. coli TOP10 F'. Lane 1- molecular weight marker, lanes 2 and 6 - total protein, lanes 3 and 7 - supernatant of the cell extract (soluble proteins), lanes 4 and 8 – pellet of the cell extract, lanes 5 and 9 - purified GFPuv and GFPuv-HABP1 proteins.

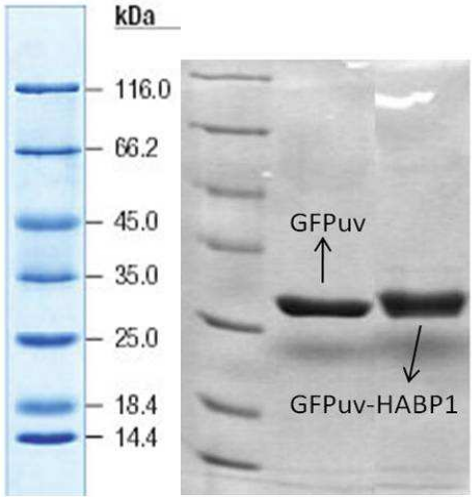

Figure 3.16 : SDS-PAGE analysis of purified GFPuv and GFPuv-HABP1 proteins.

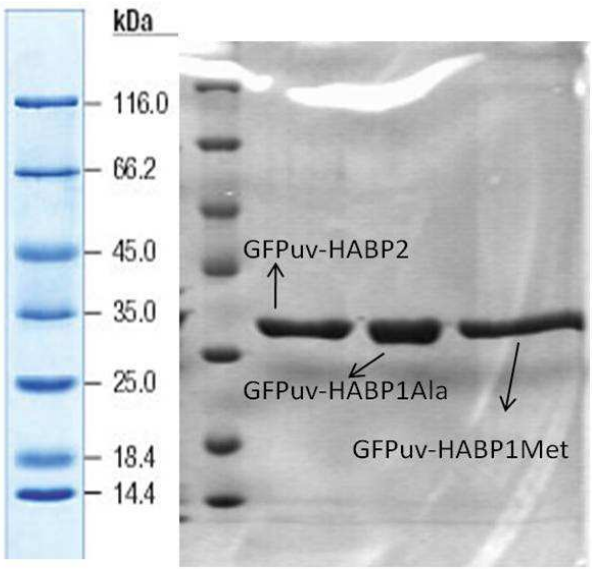

Figure 3.17 : SDS-PAGE analysis of purified GFPuv-HABP2, GFPuv-HABP1Ala, GFPuv-HABP1Met proteins.

The physicochemical properties of the his-tagged proteins are listed on Table 3.1. The protein bands of GFPuvHABP1, GFPuvHABP2, GFPuv-HABP1Ala, GFPuv-HABP1Met and GFPuv were approximately at 28 kDa, compared to theoretical molecular weights (Table 3.1).

Table 3.1: Reaction components for pMALc4x ligation. Physicochemical properties of the MBP-tagged proteins.

Protein	Number of amino acids	pI	MW (kDa)
6His-GFPuv	250	6.26	28,327
6His-GFPuv-HABP1	263	6.33	29.536
6His-GFPuv-HABP2	263	6.26	29.478
6His-GFPuv-HABP1Ala	261	6.33	29.329
6His-GFPuv-HABP1Met	261	6 .33	29.329

3.1.6 Molecular and structural characterization of GFPuv and GFPuv-HABP proteins

3.1.6.1 Fluorescence Properties of the GFPuv and GFPuv-HABP Proteins

Fluorescence properties of the fusion proteins were first examined under UV light. It has been observed that purified his-tagged GFPuv based proteins have fluorescence under UV light (Figure 3.18).

Excitation and emission properties of the proteins were analyzed by fluorescence spectroscopy. It has been demonstrated GFPuv-HABP fusion proteins have equivalent excitation (394 nm) and emission (510 nm) at the same wavelengths with similar intensities (Figure 3.19) as compared to that of GFPuv alone. This implies that fluorescence properties of GFPuv were protected upon the insertion of combinatorially selected peptide sequences.

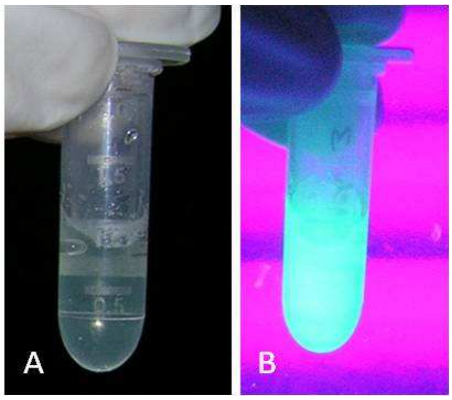

Figure 3.18 : Images of purified GFPuv-HABP1 protein under visible (A) and UV light (B).

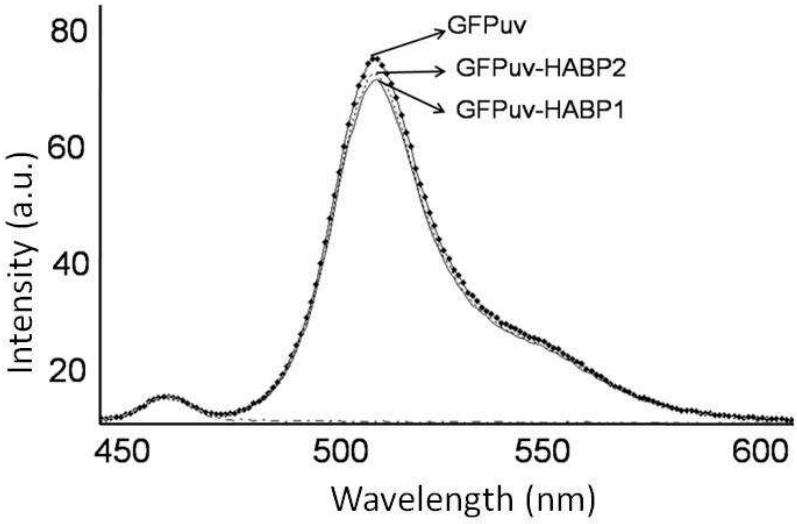

Figure 3.19 : Emission spectra for GFPuv, GFPuv-HABP1 and GFPuv-HABP2 proteins.

3.1.6.2 Binding of fusion proteins to HA surface

The binding properties of GFPuv-HABP1, GFPuv-HABP2, GFPuv-HABP1Ala and GFPuv-HABP1Met proteins to HA surface were examined. GFPuv protein was used as negative control. Synthetic HA powder was incubated with the purified proteins. After washing steps, HA samples were examined with fluorescence microscopy. The construct with the strong binder sequence, i.e., GFPuv-HABP1 fusion, bound to the

HA particles with higher affinity than those of GFPuv-HABP2, GFPuv-HABP1Ala, GFPuv-HABP1Met and GFPuv (Figures 3.20 and 3.21).

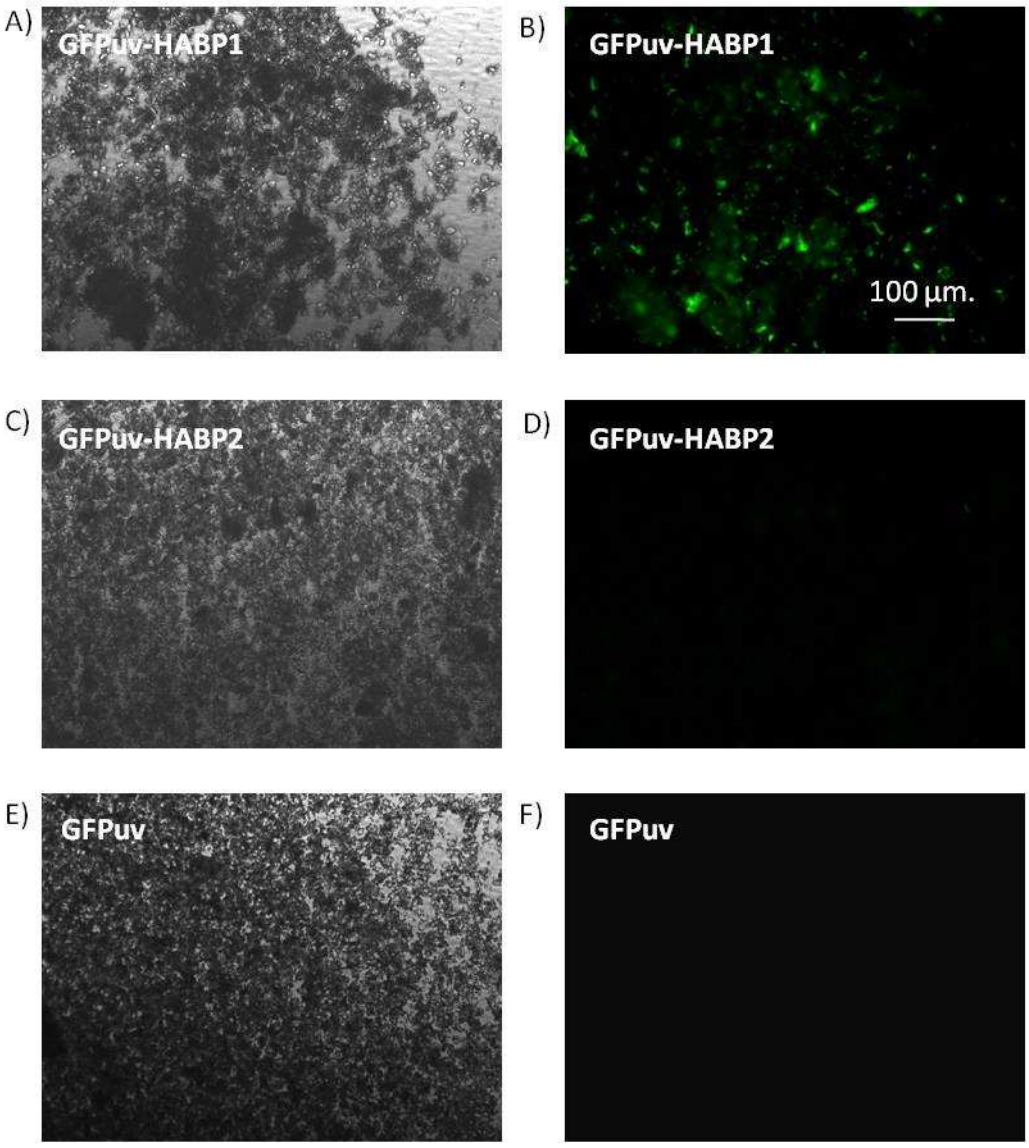

Figure 3.20 : Qualitative binding characterization of GFPuv, GFPuv-HABP1 and GFPuv-HABP2 proteins on HA powders. A, C, E the bright field images and, B, D, F the fluorescence images of the bound proteins, respectively.

The effect of inorganic binding peptide molecular architecture on peptide binding has been assessed in previous studies. In these studies, the inorganic binding peptides selected from constraint peptide libraries were used (Choe et al., 2007; Seker et al., 2007; Hnilova et al., 2008).

It has been indicated that when the inorganic binding peptide retains its molecular conformation in both cyclic and linear forms, it also preserves similar adsorption

behavior on the surfaces. On the other hand, when the molecular structure of the respective sequence in the linear forms differs from their cyclic form, a decrease in the solid-binding affinities is observed.

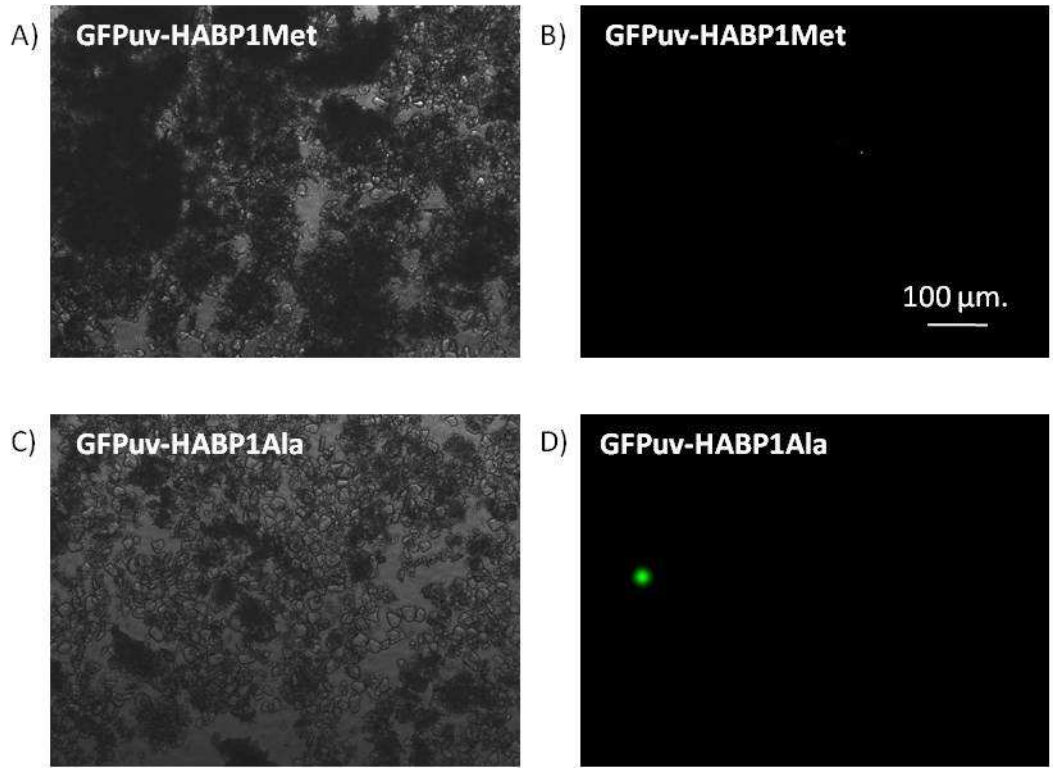

Figure 3.21 : Qualitative binding characterization of GFPuv-HABP1Ala and GFPuv-HABP1Met on HA powders. A, C the bright field images and B, D fluorescence images.

In this study, the effect of inorganic binding peptide fused GFPuv protein molecular structure on its binding to inorganic surface was also demonstrated. While the fusion construct with the constraint strong binder sequence, i.e., GFPuv-HABP1, bound to the HA with high affinity, GFPuv-HABP protein with the linear strong binder sequence did not bind to HA surface.

Both directions of the sequence, i.e., -N to- C or -C to -N (MLPHHGA or AGHHPLM) were assessed and determined that both constructs with linear strong binder HABP did not bind to HA powder.

3.1.6.3 Quantitative binding characterization of the GFPuv and GFPuv-HABP proteins

Quantitative binding characterization of the constructs, GFPuv, GFPuv-HABP1 and GFPuv-HABP2 was tested using QCM-D adsorption studies, carried out real time and recorded as a function of time. Each step on the sensograms represents the

addition of a higher concentration, as the plateaus represent the buffer rinse between the equilibrium conditions reached after addition of each concentration. The higher amount of protein deposited on the HA-coated QCM-D crystal results in a higher frequency shift. The frequency shift was detected at a very low level for GFPuv protein. This indicated that the GFPuv did not bind to HA surface. High level frequency shift resulted from the binding of the GFPuv-HABP1 on HA surface. GFPuv-HABP2 with a weak binder sequence resulted in a limited degree of binding (Figures 3.22 and 3.23).

QCM-D data was utilized to calculate KD (desorption equilibrium constant) of the GFPuv-HABP1 and GFPuv-HABP2 fusion proteins. Simple Langmuir interaction model was used to describe the behavior of molecular adsorption. The frequency change is related to the adsorbed protein, i.e., $\Delta f=(f_{max}\ x\ C)\ /\ (K_D+C)$, where Δf represents the change in the frequency of the QCM-D at any given protein concentration and C is the corresponding protein concentration. To fit the Langmuir model to the experimental data, i.e., frequency shift versus protein concentration, the least-squared curve fitting was used, and from these, the f_{max} and K_D values were extracted. The equilibrium binding constant of the GFPuv-HABP1 construct (6.6+0.3 mol) was almost 70 times lower than that of the GFPuv-HABP2 (429+23 mol). These data indicated that GFPuv-HABP1 had a higher affinity to the HA substrate.

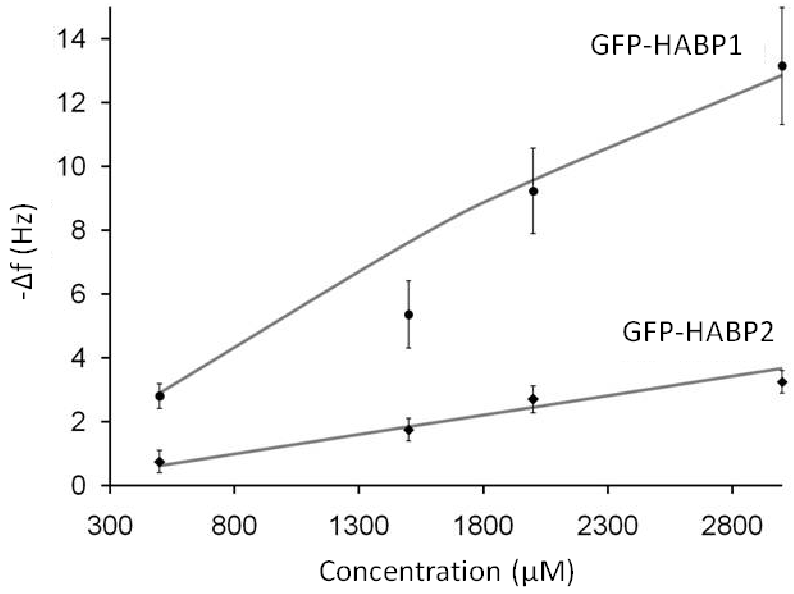

Figure 3.22 : QCM-D signal change during the adsorption of GFP-HABP1 and GFP-HABP2 as a function of protein concentration.

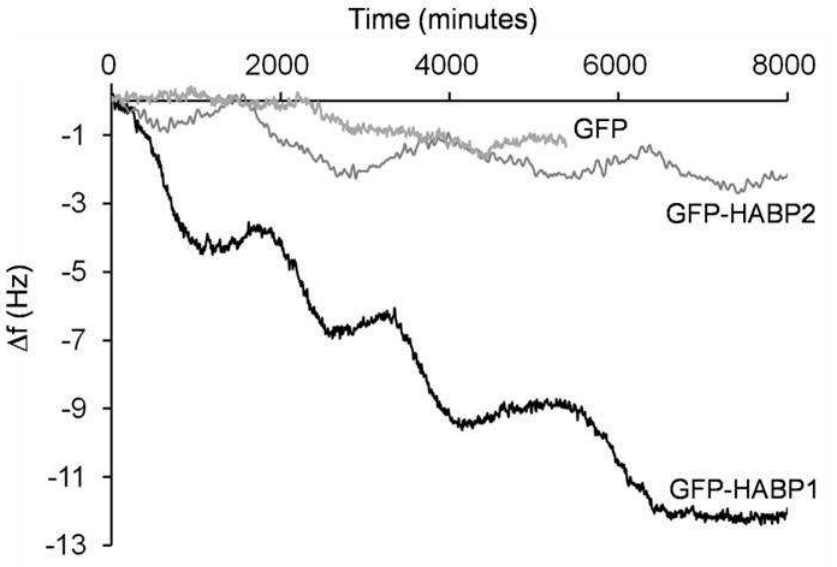

Figure 3.23 : Overall QCM-D sensograms for the adsorption of GFPuv-HABP1, GFPuv-HABP2 and GFPuv on crystalline hydroxyapatite surfaces.

3.1.6.4 Secondary structure of the proteins

The CD spectra performed using a Jasco J-810 circular dichroism (CD) spectropolarimeter (Jasco, Easton, MD, USA) correspond to the dominating β-sheet structure in all cases resulting from the presence of the β-barrel core in the GFPuv (Figure 3.24).

A change was observed in the amount of molar ellipticity possibly revealing a gain in GFPuv-HABP2, and a loss in GFPuv-HABP1, of protein structure. On the other hand, the variation in the molar ellipticity values did not correlate with the changes in fluorescence intensities of these constructs. GFPuv-HABP2 has almost doubled its molar ellipticity value compared to that of GFPuv, and the spatial orientation of the peptide might have caused a slight decrease in the GFPuv intensity (Figure 3.19).

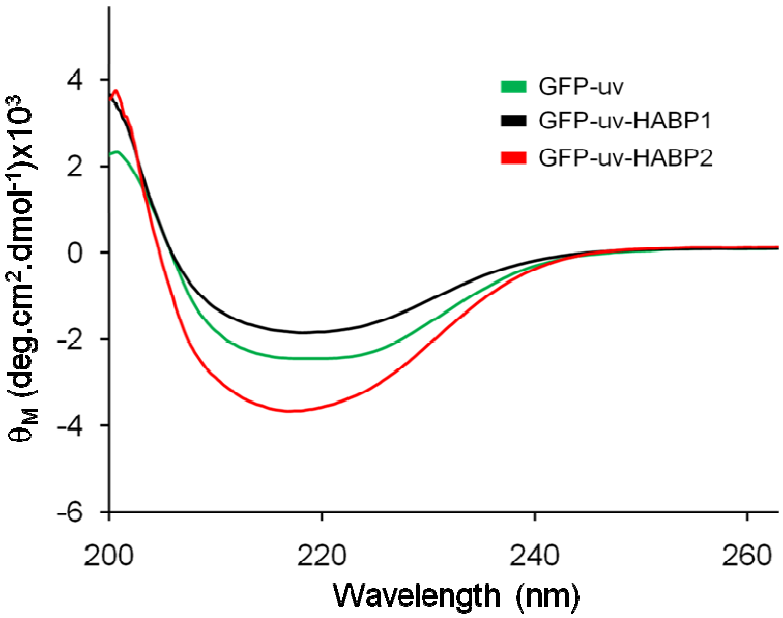

Figure 3.24 : Elements of a neuron cell, adapted from Cetin (2003). Secondary structure analysis of GFPuv-HABP1, GFPuv-HABP2 and GFPuv proteins using CD, far-UW wavelength scan.

3.1.7 Labeling synthetic and natural minerals

3.1.7.1 Monitoring mineralization

Time-wise mineralization was monitored by GFPuv-HABP1. HA crystals were formed on glass slides using an alkaline phosphate-based mineralization model (Gungormus et al., 2008). Using optical microscopy, it has been observed the amount of mineral on the glass slides increased linearly over time.

The fluorescence imaging experiments of the glass slides labeled with GFPuv-HABP1 resulted in an increase in the fluorescence intensity with the increasing mineral amount. However, the glass slides incubated with GFPuv exhibited no significant increase in fluorescence intensity as the amount of mineral was increased. Without HABP1 fusion partner, GFPuv was demonstrated to lack the mineral-binding capability. As GFPuv was not able to specifically bind to the mineral surface, the non-specifically bound GFPuv was washed away from the surface upon the washing step. On the other hand, GFPuv-HABP1 fusion proteins with the mineral binding domain, facilitated a robust attachment of GFPuv onto HA surface and prevented resorption upon washing steps (Figure 3.25).

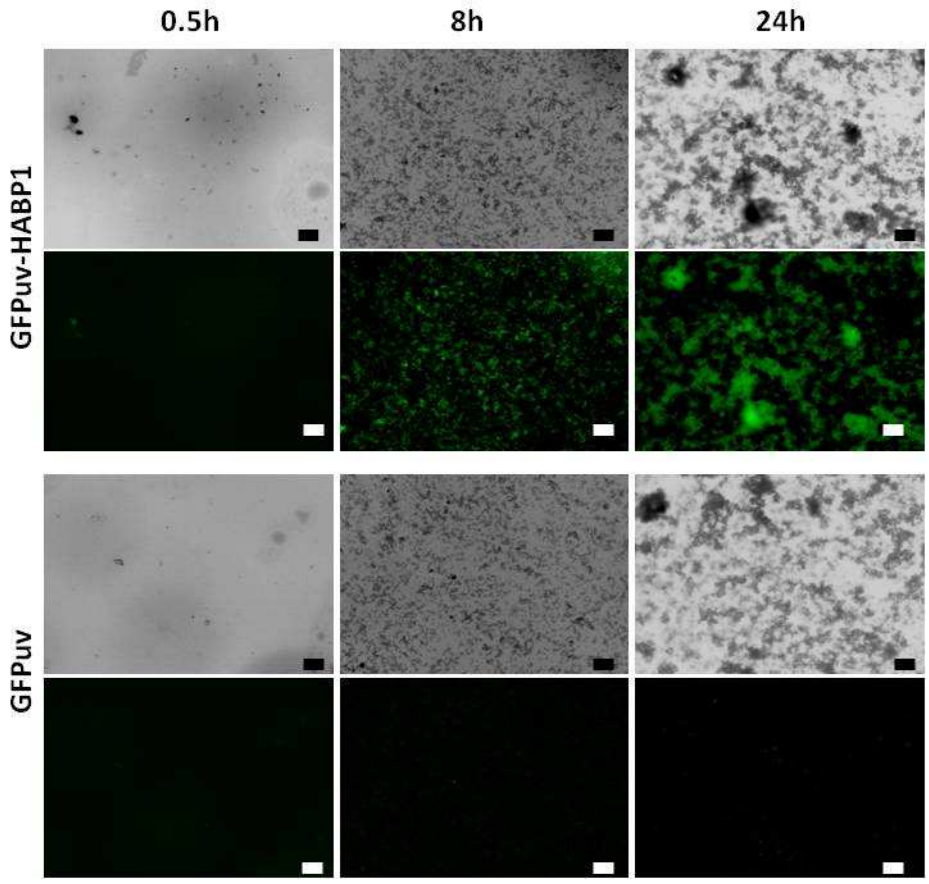

Figure 3.25 : Time-wise monitoring of mineralization. Increase in mineral coverage and the corresponding fluorescence microscopy images of the slides incubated with GFPuv and GFPuv-HABP1. Size bars correspond to 10 µm.

The fluorescence microscopy measurements indicate a linear increase in intensity vs. the amount of mineral. All of the time-wise monitoring results show that the GFPuv-HABP1 fusion protein has a potential utility for rapid and accurate monitoring of mineralization of HA.

3.1.7.2 Labelling the biomineralized tissue

The acellular afibrillar cementum, produced by cementoblasts, consists of a mineralized matrix, lacking collagen fibers and cementocytes. The binding ability of the GFPuv-HABP constructs on biomineralized samples was tested on human acellular afibrillar cementum. Cylindrical pieces cut from the acellular afibrillar cementum, close to the cemento-enamel junction were incubated with GFPuv, GFPuv-HABP1 and GFPuv-HABP2. Under the fluorescence microscope, samples incubated with neither GFPuv nor GFPuv-HABP2 displayed any contrast on teeth surfaces, while fluorescence contrast was observed in fluorescence imaging

experiments of the samples incubated with GFPuv-HABP1 (Figure 3.26). All of these data demonstrated that the GFPuv-HABP1 construct can recognize biologically mineralized tissues as well as synthetically formed HA. Fluorescence intensity measurements indicated that GFPuv-HABP1 fusion protein, containing the strong binder sequence, fluoresces greater than 6 fold on acellular afibrillar cementum samples, compared to those containing either GFPuv or GFPuv-HABP2 (Figure 3.27).

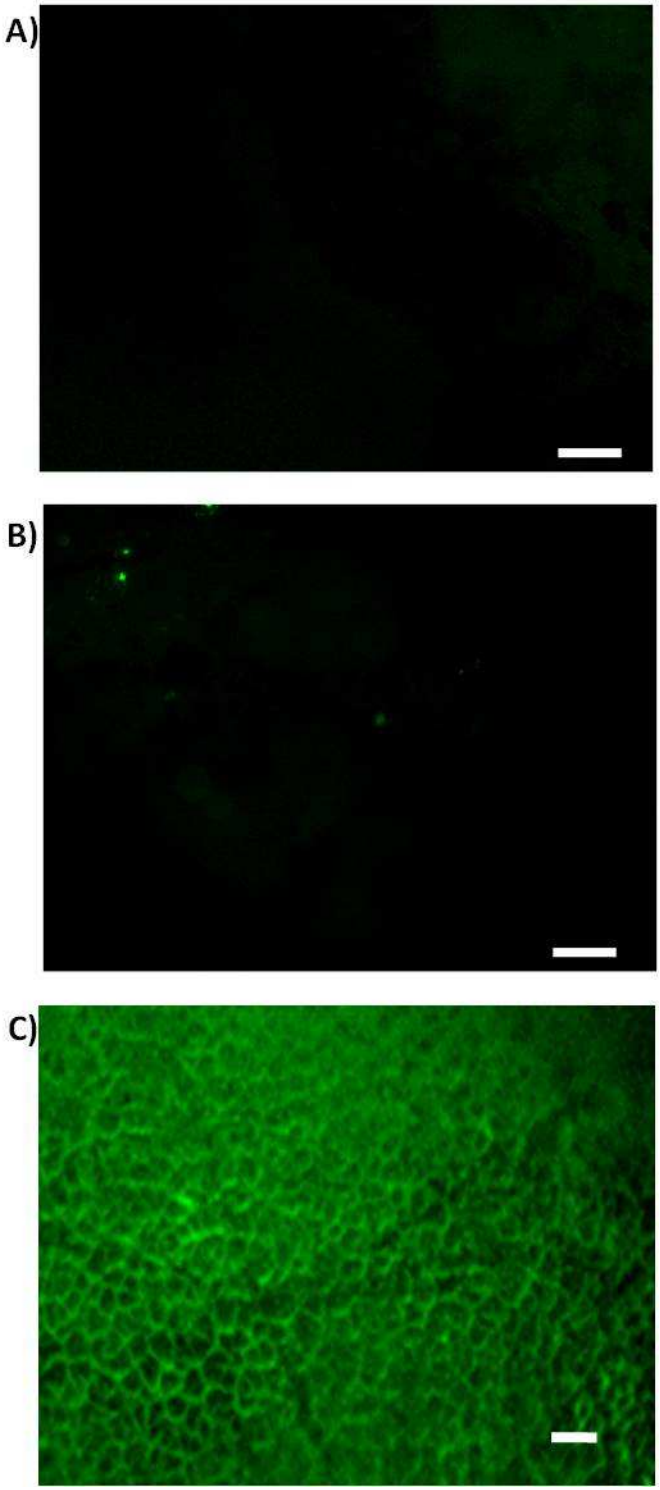

Figure 3.26 : Binding of (A) GFPuv, (B) GFPuv-HABP2 and (C) GFPuv-HABP1 on acellular afibrillar cementum samples. Size bars correspond to 100 µm.

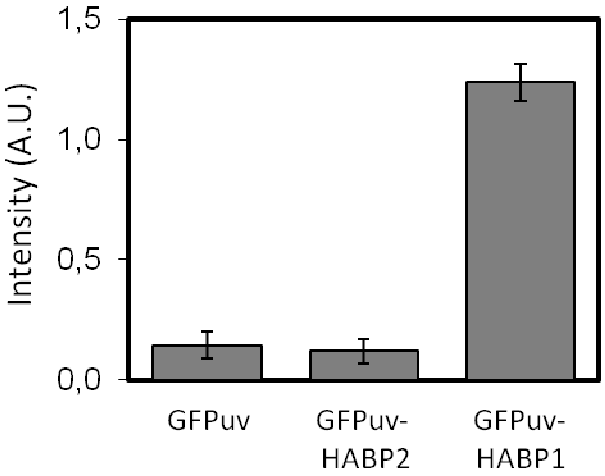

Figure 3.27 : Average fluorescence intensities obtained from the acellular afibrillar cementum samples labeled with GFPuv, GFPuv-HABP2 and GFPuv-HABP1. The values are normalized to the negative control with no protein incubation.

3.2 Genetic Construction and Applications of MBP Tagged GFPuv and GFPuv-Metal Binding Peptide Fusion Proteins

In this part of the study, fusion proteins encoding GFPuv fluorescent protein and metal binding peptides selected by cell surface display have been engineered. It has been demonstrated the utility of gold-binging peptide AuBP2c and silver-binding peptide AgBP2c genetically fused to fluorescent protein GFPuv for site-specific immobilization of GFPuv protein onto gold and silver solid supports. Each fusion peptide was cloned into pMALc4x expression vector encoding N-terminal MBP tag. In pMALc4x expression system, the cloned gene is inserted down-stream from the malE gene of E. coli, which encodes maltose-binding protein (MBP), resulting in the expression of an MBP fusion protein (Maina et al., 1988, Url-6). The MBP expressed from pMALc4x has been engineered for tighter binding to amylose. pMAL expression system provides one-step purification of the fusion proteins using MBP's affinity for maltose (Url-6).

Combinatorially selected AuBP2c and AgBP2c peptides were fused to C-terminus of the GFPuv protein and the fusion peptide encoding sequence was cloned into MBP expressing vector pMALc4x. As a negative control, GFPuv was also cloned into the pMALc4x. Final engineered constructs were named as pMALc4x-GFPuv, pMALc4x-GFPuv-AuBP2c and pMALc4x-GFPuv-AgBP2c.

3.2.1 Designing GFPuv-metal binding peptide constructs

In order to generate GFPuv, GFPuv-AuBP2c, and GFPuv-AgBP2c constructs, primers were designed according to amino acid sequence of AuBP2c (CGP-WALRRSIRRQSY-GPC), AgBP2c (CGP-EQLGVRKELRGV-GPC), -SGGG linker and GFPuv. Multiple cloning site of pMALc4x has various restriction endonuclease cleavage sites including *EcoRI* and *HindIII*. GFPuv, GFPuv-AuBP2c and GFPuv-AgBP2c encoding sequences were amplified using a series of forward and reverse primers containing extra residues including a *EcoRI* or *HindIII* site at their 5' ends, respectively. As the pMALc4x expression vector encodes N-terminal MBP tag, in the final purified proteins, MBP tag was placed at the N- terminal, while in the AgBP2c and AuBP2c, it was located at the C- terminal.

3.2.2 Obtaining PCR products encoding GFPuv and GFPuv-metal binding peptide fusion proteins

The DNA fragment encoding GFPuv, GFPuv-AgBP2c and GFPuv-AuBP2c were obtained by single and consecutive PCR reactions, respectively. The GFPuv, GFPuv-AgBP2c/AuBP2c PCR products should be approximately 730 bp, and 790 bp respectively. In the previous GFPuv-HABPs constructs pfu polymerase has been used. However, when sequence analyses were done at the end of the cloning, it has been observed that there were some point mutations in some of the constructs. Therefore, all the cloning steps were repeated to obtain the constructs without any mutation. Instead of pfu, Phusion High-fidelity DNA polymerase (NEB) was used to avoid mutation and prevent wasting time. For the first step PCR using Phusion High-fidelity DNA polymerase (NEB), the annealing temperature for the fusion constructs was optimized at 50°C for 10 seconds. O'RangeRuler 50 bp DNA ladder (Appendix A1, Fermentas) was loaded into the agarose gel as a DNA marker.

After agarose gel electrophoresis, the molecular weight of GFPuv, GFPuv-AgBP2c and GFPuv-AuBP2c encoding DNA fragments were verified (Figures 3.28, 3.29, and 3.30).

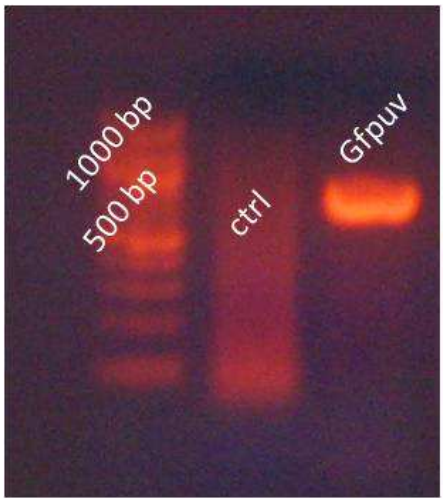

Figure 3.28 : Agarose gel image of GFPuv encoding DNA fragment amplified with Phusion High-fidelity DNA polymerase (NEB).

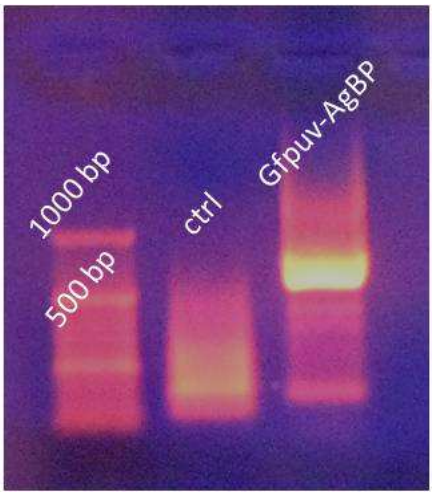

Figure 3.29 : Agarose gel image of GFPuv-AgBP2c encoding DNA fragment amplified with Phusion High-fidelity DNA polymerase (NEB).

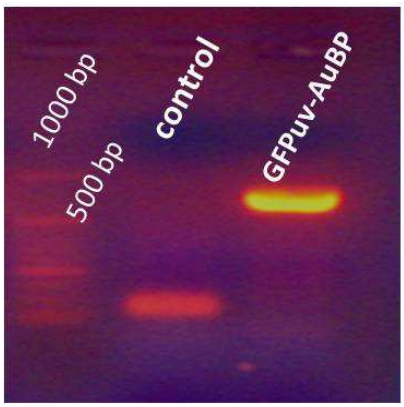

Figure 3.30 : Agarose gel image of GFPuv-AuBP2c encoding DNA fragment amplified with Phusion High-fidelity DNA polymerase (NEB).

3.2.3 Cloning the target DNA into TOPO TA cloning vector

Following the extraction of the PCR products from agarose gel, each purified DNA fragment was ligated into TOPO TA pCR2.1 TOPO (Invitrogen) cloning vector. pCR2.1 TOPO cloning vector has a single 3´ deoxythymidine (T) overhang for TA cloning. Taq polymerase adds a single deoxyadenosine (A) to the 3´ ends of PCR products through its nontemplate-dependent terminal transferase activity. Phusion High-fidelity DNA polymerase (NEB) was used to obtain GFPuv, GFPuv-AgBP2c and GFPuv-AuBP2c encoding DNA fragments. At the final extention step of the each PCR, taq polymerase was added to the reaction to obtain PCR products with a single deoxyadenosine (A) to the 3´ ends.

After transformation of *E. coli* TOP10 F' cells with the ligation product, colonies were observed on agar plates containing X-gal, IPTG and ampicillin. TOP10 F' cells overexpress the Lac repressor (lacIq gene). IPTG was added to plates to obtain expression from the lac promoter in parallel with blue-white screening. Following transformation, blue and white colonies were observed on the agar plate (Figure 3.31).

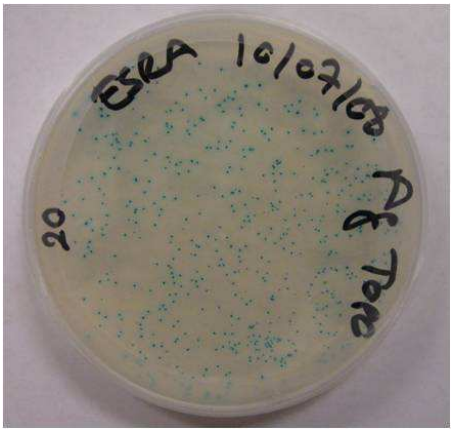

Figure 3.31 : X-Gal, IPTG and ampicillin containing agar plate showing the blue-white screening result for the TA cloning of GFPuv-AgBP2c encoding DNA fragment.

3.2.3.1 Restriction endonuclease analysis

White colonies were selected and pCP2.1 TOPO vectors harboring GFPuv, GFPuv-AgBP2c and GFPuv-AuBP2c inserts were isolated from selected colonies. These plasmids were digested with *EcoRI* and *HindIII* to obtain the insert DNA fragments. Double digestion products were run in agarose gel (Figure 3.32).

Cloning of *gfpuv, gfpuv-AgBP2c* and *gfpuv-AuBP2c* fusion fragments was verified. The insert fragments obtained after the restriction digestion reaction were pufied for further cloning.

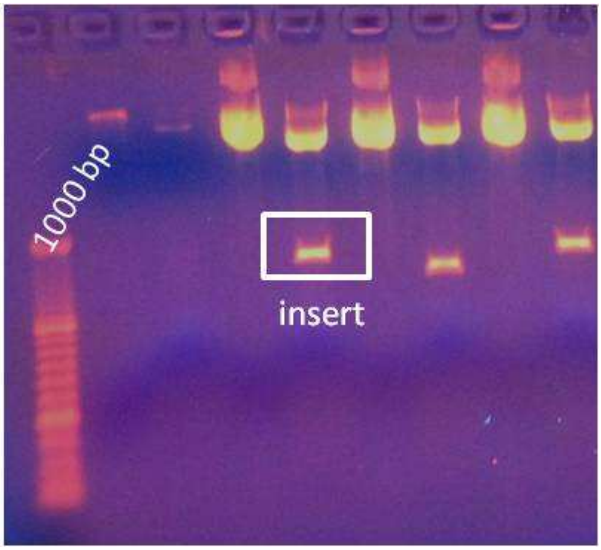

Figure 3.32 : Verification of cloning of *gfpuv-AgBP2c* into TOPO TA cloning vector. Undigested and double digested recombinant TOPO plasmids harboring *gfpuv-AgBP2c* were loaded into the gel sequentially.

3.2.4 Generating MBP tagged GFPuv protein and GFPuv-metal binding peptides fusion protein expressing bacteria

Recombinant *E. coli* ER2507 strains expressing MBP-GFPuv, MBP-GFPuv-AgBP2c and MBP-GFPuv-AuBP2c were obtained by cloning each DNA fragment into pMALc4x expression vector and transforming the ER2507 bacteria with the constructs.

3.2.4.1 Cloning into pMALc4x expression vector

The pMALcx vector express the malE gene fused to the lacZα gene. Fusion protein encoding DNA fragment were inserted into restriction sites between malE and lacZα. In pMAL vectors, insertion inactivates the β-galactosidase α-fragment activity of the malE-lacZα fusion, resulting in a blue to white color change on Xgal plates when the construction is transformed into an α-complementing host (Url-6).

In this study, the pMALC4x-GFP-GEPI fusion constructs were transformed into ER2507 host which have F- ara-14 leuB6 fhuA2 Δ(argF-lac)U169 lacY1 glnV44 galK2 rpsL20 xyl-5 mtl-5 Δ(malB) zjc::Tn5(KanR) Δ(mcrC-mrr) genotype. The

malE gene is included in the malB deletion. Therefore, ER2507 strain does not produce any MBP from the chromosome. It also does not have the lacZΔM15 allele, so it cannot be used for blue-to-white screening on X-gal plate (NEB pMAL protein purification and expression system, instruction manual). Cloning of gfpuv, gfpuv-AgBP2c and gfpuv-AuBP2c fusion fragments into expression vector pMALc4x was verified by both restriction and sequence analyses.

3.2.5 Production and purification of MBP tagged proteins under native conditions

pMALc4x vector carries the lacIq gene, which codes for the Lac repressor. This keeps expression from "tac" promoter low in the absence of IPTG induction. Expression conditions were optimized for pMALc4x-GFPuv, pMALc4x-GFPuv-AgBP2c and pMALc4x-AuBP2c constructs.

It was observed that incubation of the culture at 30 ^{o}C for 6 hours after induction is ideal for expression of the multifunctional proteins. Following the expression, each *E. coli* ER2507 culture expressing the multifunctional proteins were examined under UV light (Figure 3.33).

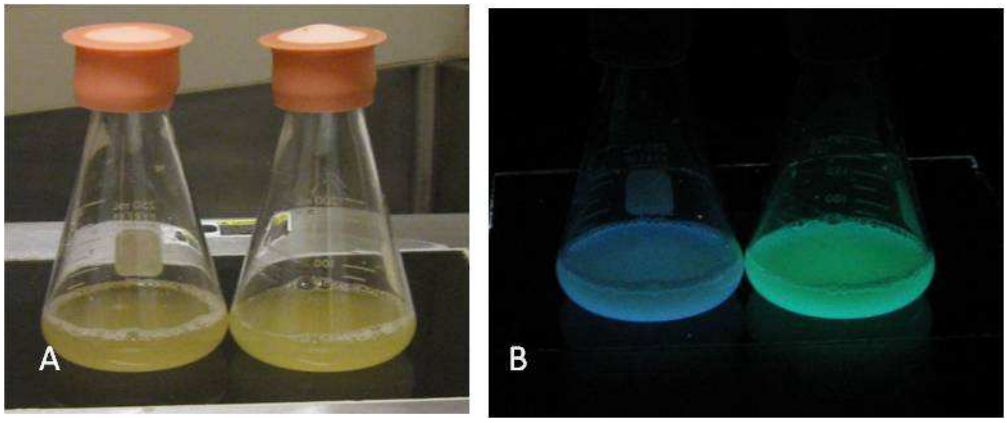

Figure 3.33 : E. coli ER2507 bacterial culture expressing MBP tagged GFP based fusion protein (right) and negative control E. coli ER2507 (left) under visible (A) and UV (B) light.

The cloned genes were inserted into pMALc4x vector downstream from the MBP encoding malE gene. Hence, the fusion proteins were expressed with MBP tag. MBP-GFPuv, MBP-GFPuv-AgBP2c and MBP-GFPuv-AuBP2c proteins were purified by affinity purification specific for MBP tag (Figure 3.34).

The pMALc4x vector contains the sequence coding for the recognition site of apecific protease, i.e. Factor Xa, located just 5´ to the polylinker insertion sites. This recognition site allows MBP to be cleaved from the protein of interest after purification (Nagai and Thogersen 1987). Factor Xa cleaves after its four amino acid recognition sequence. This provides the attachment of few or no vector-derived residues to the cloned protein, depending on the site used for cloning (Url-6). In this study, *EcoRI* site was used for the cloning, so a few vector-derived residues were attached to the GFP-fusion protein.

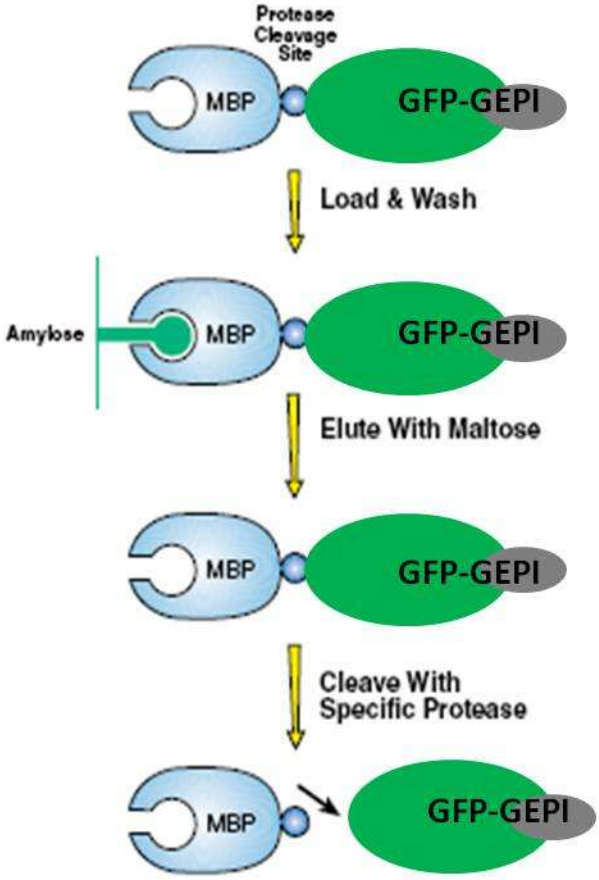

Figure 3.34 : GFP-GEPI (AuBP2c or AgBP2c) fusion proteins were expressed with MBP tag. Fusion proteins were purified by affinity purification specific for MBP tag (Adapted from Url-7).

Following expression, purification and Factor Xa cleavage, the purity and molecular weights of fusion proteins were analyzed by SDS-PAGE (Figures 3.35 and 3.36). A single, purified band was observed for each protein of interest.

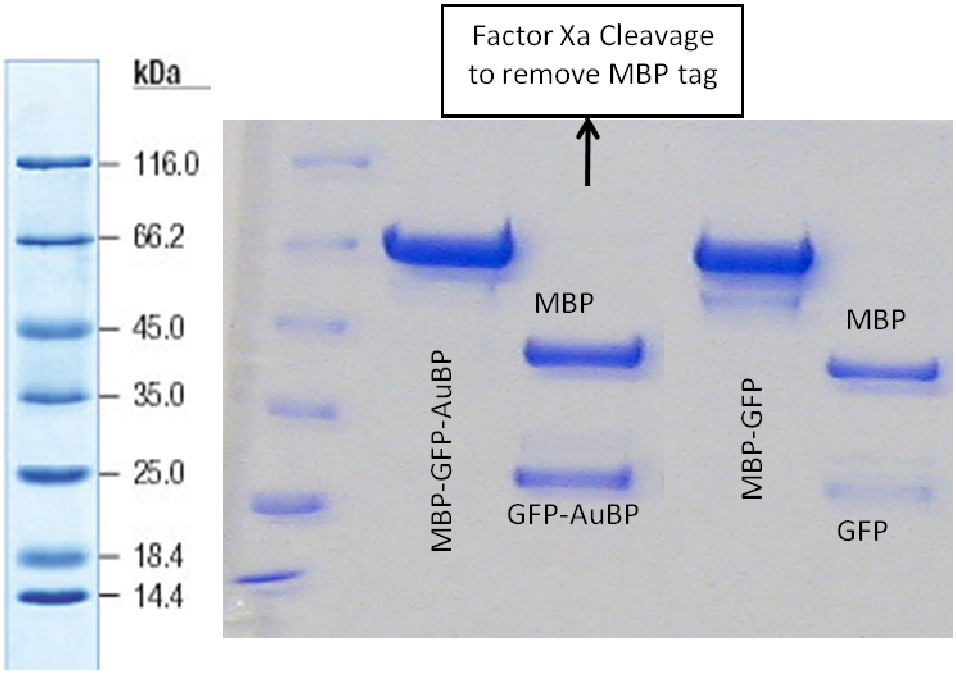

Figure 3.35 : SDS-PAGE analysis of purified, cleaved and uncleaved MBP-GFPuv-AgBP and MBP-GFPuv proteins.

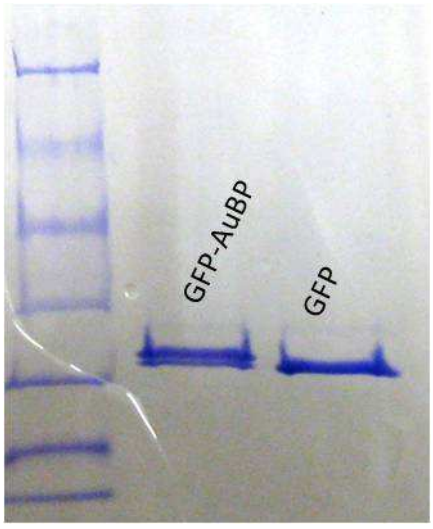

Figure 3.36 : SDS-PAGE analysis of purified GFPuv-AuBP and GFPuv proteins. Following purification of MBP-GFPuv-AuBP and MBP-GFPuv fusion proteins, MBP tags were cleaved by Factor Xa and than removed by subsequent chromatography steps.

The physicochemical properties of the purified proteins are listed on Table 3.2. While the protein bands of MBP-GFPuv, MBP-GFPuv-AgBP2c and MBP-GFPuv-AuBP2c were approximately at 70 kDa, GFPuv, GFPuv-AgBP2c and GFPuv-AuBP2c were at 30 kDa compared to theoretical molecular weights (Table 3.2) .

Table 3.2: Physicochemical properties of proteins expressing from pMALc4x.

Protein	Number of amino acids	pI	MW (kDa)
MBP-GFPuv	629	5.33	69.764
MBP-GFPuv-AgBP2c	651	5.39	71.903
MBP-GFPuv-AuBP2c	651	5.55	72.111
GFPuv	242	5.68	27.272
GFPuv-AgBP2c	264	5.82	29.411
GFPuv-AuBP2c	264	6.22	29.619

3.2.6 Fluorescence properties of purified MBP-GFPuv, MBP-GFPuv-metal binding peptide proteins

Excitation and emission properties of the purified proteins were analyzed by fluorescence. It has been demonstrated MBP tagged GFPuv-fusion proteins have equivalent excitation (394 nm) and emission (510 nm) at the same wavelengths with similar intensities (Figure 3.37) as compared to that of GFPuv alone. This implies that fluorescence properties of GFPuv were protected upon the insertion of GEPIs and fusion of MBP tag.

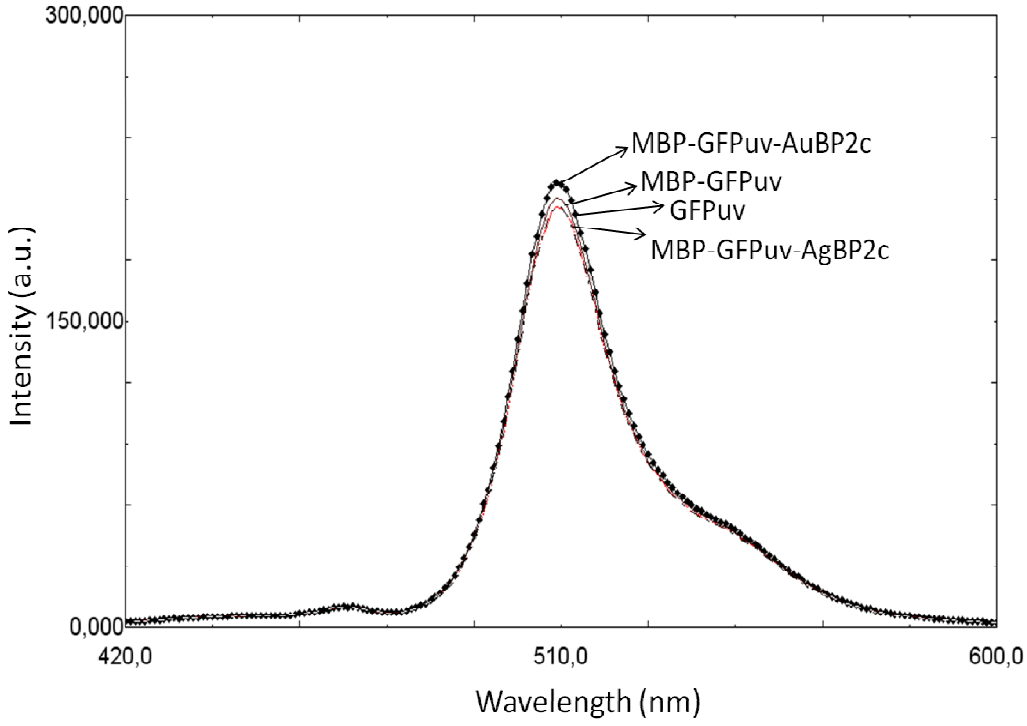

Figure 3.37 : Emission spectra for GFPuv, MBP-GFPuv, MBP-GFPuv-AuBP2c and MBP-GFPuv-AgBp2c proteins.

3.2.7 Micropatterning of fluorescence fusion constructs

Microcontact printing, one of the soft-lithography techniques, is an efficient technique for micropatterning of biomolecules (Ruiz and Chen 2007). Microcontact printing has been used by different groups to pattern biological materials, such as proteins (Bernard et al., 1998; Kacar et al., 2009a), DNA molecules (Lange et al., 2004) and cells (Mrksich et al., 1997).

The multifunctionality of the constructs created in this part of the study, was evaluated for fluorescence and noble metal binding characteristics using microcontact printing technique. The control experiments were carried out using MBP-GFPuv protein.

Protein patterns were fabricated by taking advantage of the binding affinities of gold and silver binding peptide sequences of multifunctional MBP-GFPuv-AuBP2c and MBP-GFPuv-AgBP2c proteins. Using a soft lithography technique, is has been demonstrated that GEPI amino acid sequences of the MBP-GFPuv-GEPI fusion proteins can control the interaction of the multifunctional proteins with the noble metal surface.

In the experiments for microcontact printing of protein samples on the inorganic surface, a fluorescence labeling procedure, like immune-staining process, is applied to visualized immobilized proteins on the surface by fluorescence microscope. In this study, using GFPuv fluorescence protein as a fusion partner for the multifunctional protein eliminated the fluorescence labeling step.

MBP-GFPuv-AgBP2c, MBP-GFPuv-AuBP2c and MBP-GFPuv protein samples were patterned at 2 µM, 4 µM and 8µM concentrations

3.2.7.1 Microcontact printing of MBP-GFPuv-AgBP2c on silver substrate

Protein patterned surfaces were prepared by directed stamping of MBP-GFPuv-AgBP2c proteins to flat silver surface. The stamping procedure for microcontact printing of the MBP tagged fusion protein on silver surface is schematically represented in Figure 3.38.

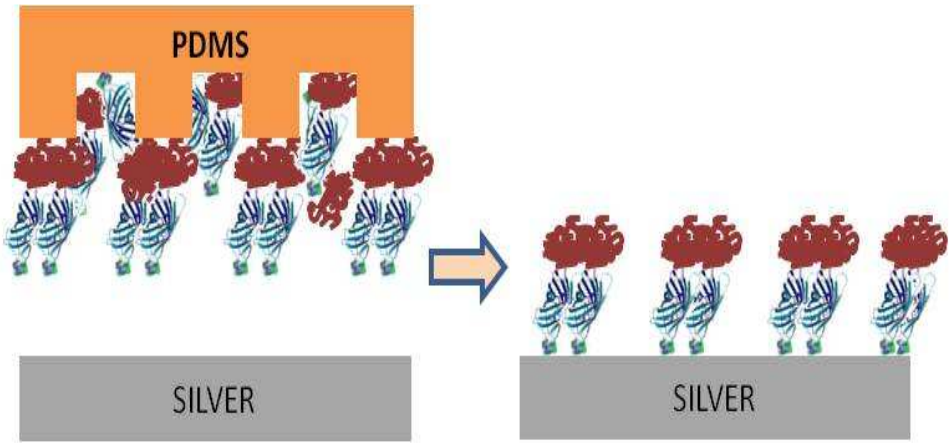

Figure 3.38 : Schematics of micro-contact printing of MBP-GFPuv-AgBP2c fusion protein on flat silver surface.

It has been observed that for each protein concentration, fluorescence contrast is significantly higher in the case of MBP-GFPuv-AgBP2 compared with MBP-GFPuv alone (Figures 3.39, 3.40 and 3.41).

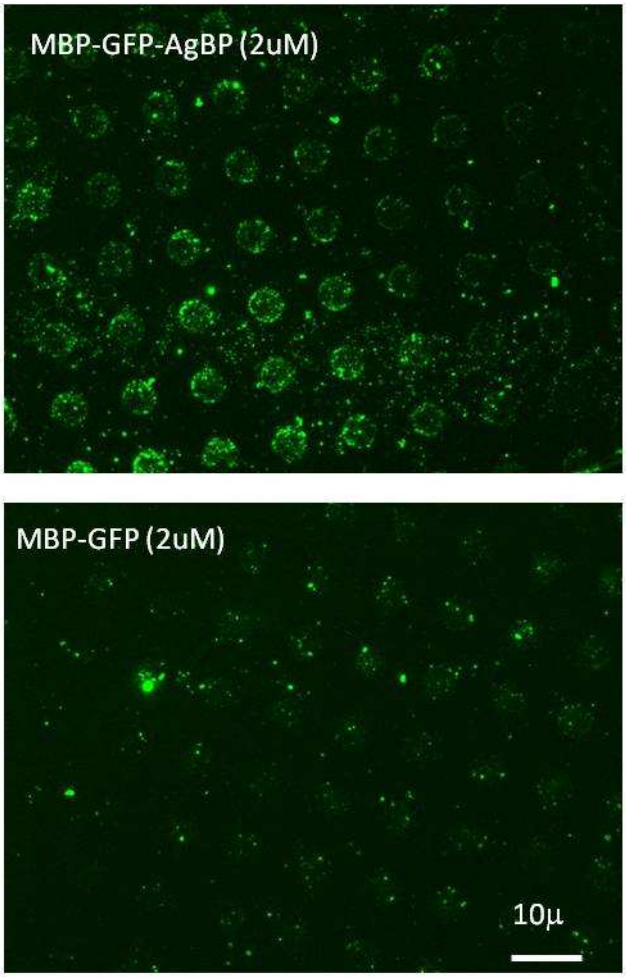

Figure 3.39 : FM images of patterning of 2 μM MBP-GFPuv-AgBP2c protein on flat silver surface via PDMS stamping. MBP-GFPuv, lacking the AgBP2c peptide, was used as a control.

It has also been observed that the higher concentration of the MBP-GFPuv-AgBP2c multifunctional proteins led the higher fluorescence intensity (Figures 3.39, 3.40 and 3.41). This indicates that there is a correlation between the concentration of the multifunctional protein and the amount of the protein immobilized on the surface.

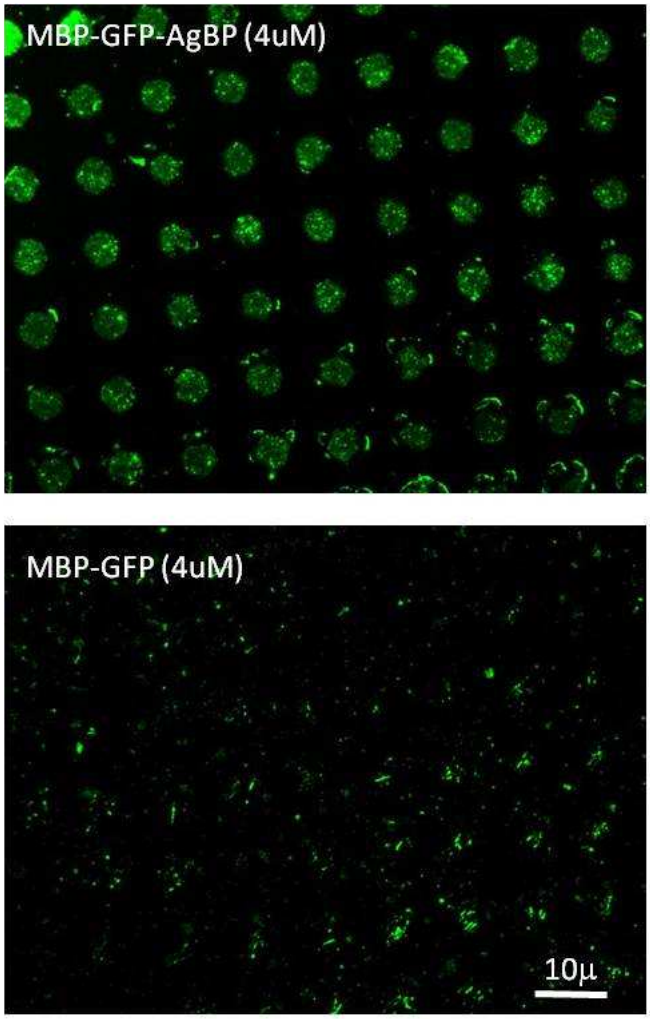

Figure 3.40 : FM images of patterning of 4 µM MBP-GFPuv-AgBP2c protein on flat silver surface via PDMS stamping. MBP-GFPuv, lacking the AgBP2c peptide, was used as a control.

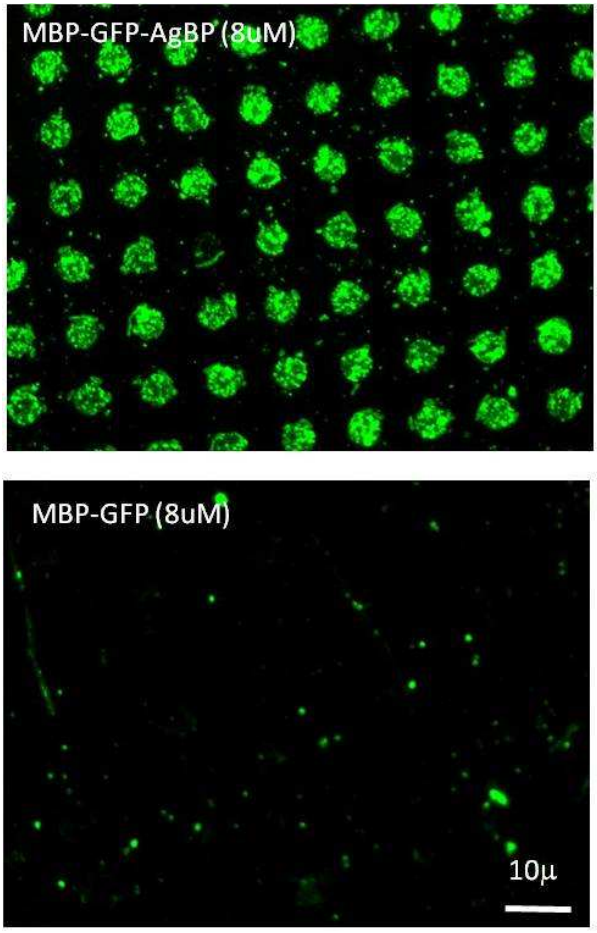

Figure 3.41 : FM images of patterning of 8 µM MBP-GFPuv-AgBP2c protein on flat silver surface via PDMS stamping. MBP-GFPuv, lacking the AgBP2c peptide, was used as a control.

3.2.7.2 Microcontact printing of MBP-GFPuv-AuBP2c on gold substrate

Protein patterns were prepared by directed stamping of MBP-GFPuv-AuBP2c proteins on flat gold surface. The stamping procedure for microcontact printing of MBP-GFPuv-AuBP2c on gold surface is schematically represented in Figure 3.42.

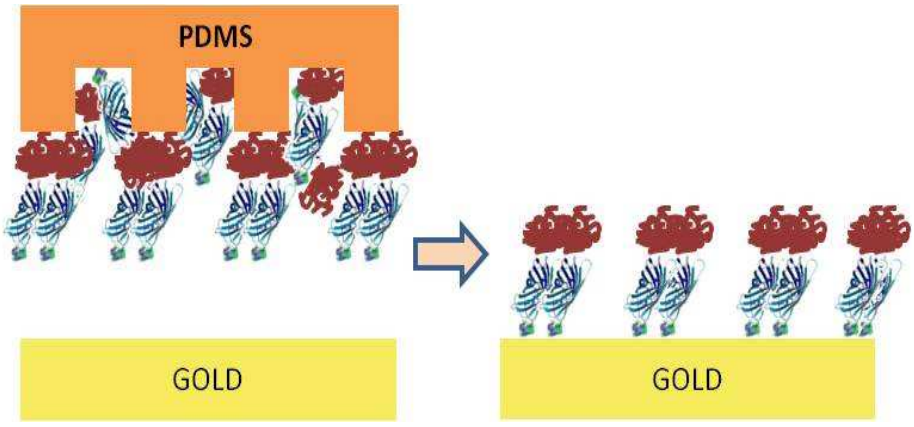

Figure 3.42 : Schematics of micro-contact printing of MBP-GFPuv-AuBP2c fusion protein on flat gold surface.

The fluorescence microscopy results have shown that for each protein concentration, fluorescence contrast is significantly higher in the case of MBP-GFPuv-AuBP2 compared to MBP-GFPuv alone (Figures 3.43, 3.44 and 3.45).The increasing concentration of the MBP-GFPuv-AuBP2c multifunctional proteins yielded increasing fluorescence intensity (Figures 3.43, 3.44 and 3.45). This data reveals that there is a correlation between the concentration of the multifunctional protein and the amount of the protein immobilized on the surface.

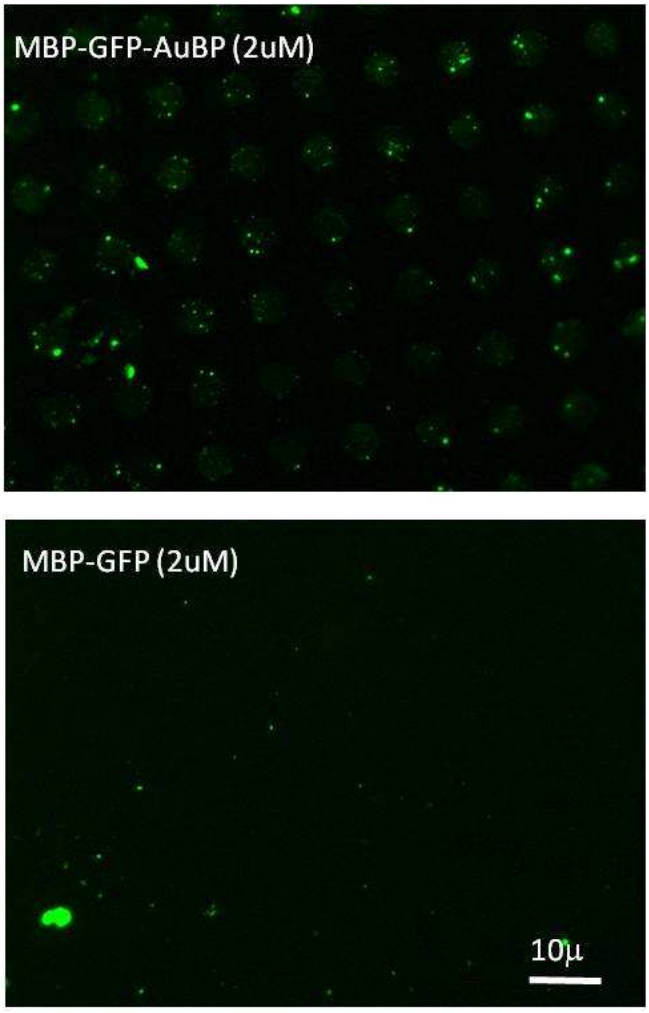

Figure 3.43 : FM images of patterning of 2 μM MBP-GFPuv-AuBP2c protein on flat gold surface via PDMS stamping. MBP-GFPuv, lacking the AuBP2c peptide, was used as a control.

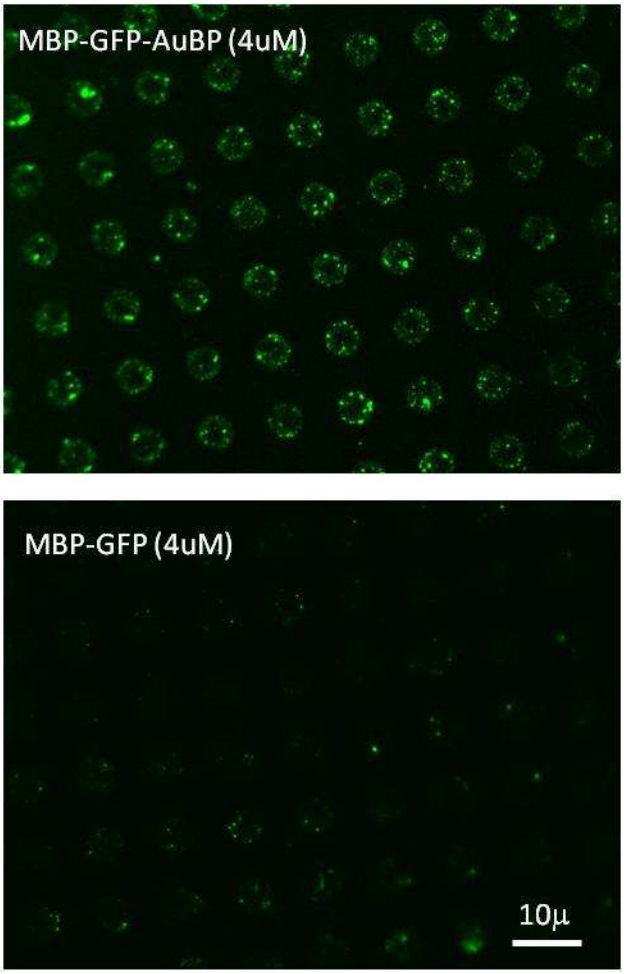

Figure 3.44 : FM images of patterning of 4 µM MBP-GFPuv-AuBP2c protein on flat gold surface via PDMS stamping. MBP-GFPuv, lacking the AuBP2c peptide, was used as a control.

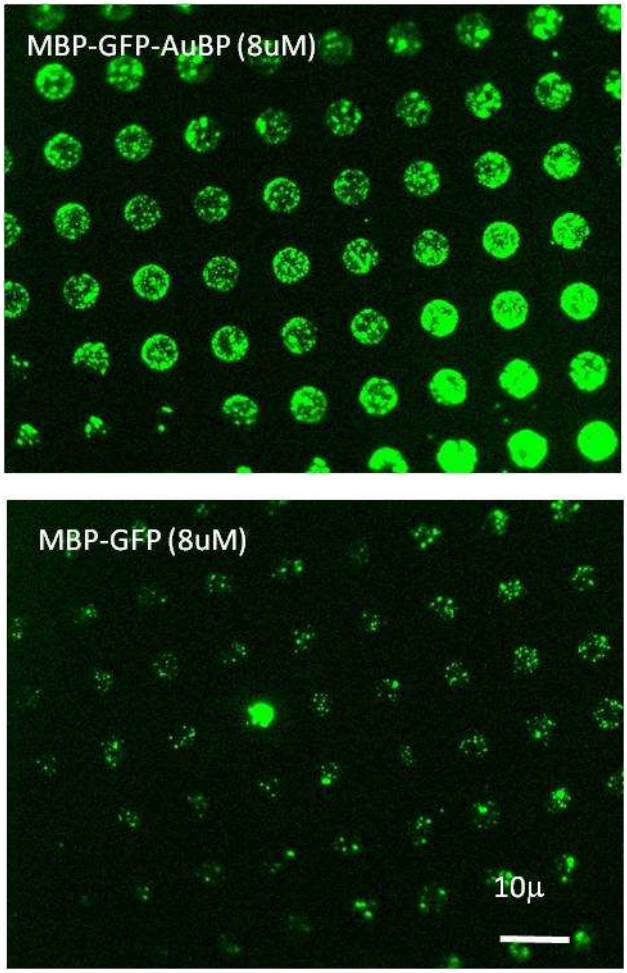

Figure 3.45 : FM images of patterning of 8 µM MBP-GFPuv-AuBP2c protein on flat gold surface via PDMS stamping. MBP-GFPuv, lacking the AuBP2c peptide, was used as a control.

3.2.8 Self-assembly of GFPuv-GEPI fusion proteins on nanoparticle-arrayed surface

Following molecular construction, expression, purification and removal of MBP steps, GFPuv-AgBP2c and MBP-GFPuv-AgBP2c fusion proteins were immobilized on silver nanoparticle arrayed surfaces. Oriented immobilization of GFPuv-AgBP2c and MBP-GFP-GEPI fusion proteins on a noble metal surface was achieved. The control experiments were carried out using GFPuv and MBP-GFPuv proteins. Bifunctional AgBP-QBP peptide has been used as linker for the attachment of nanoparticles onto glass surface. GFPuv-AgBP2c and MBP-GFPuv-AgBP2c fusion proteins were immobilized on these patterned surfaces. The experimental procedure for immobilization of the GFPuv based fusion proteins on silver nanoparticle patterned surface is schematically represented in Figure 3.46.

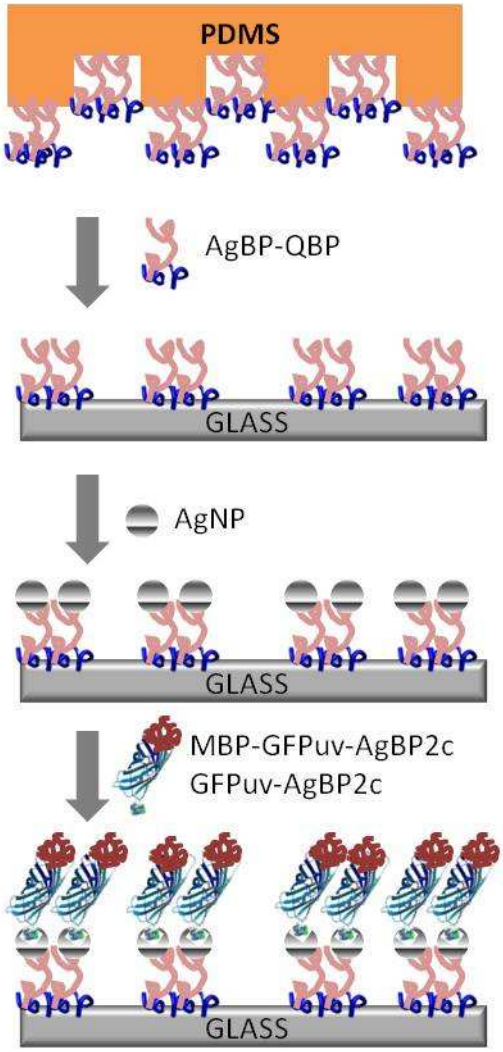

Figure 3.46 : The procedure for self assembly of MBP-GFPuv-AgBP2c and GFPuv-AgBP2c fusion proteins on silver nanoparticle patterned surface.

The multifunctionality of MBP-GFPuv-AgBP2c and GFPuv-AgBP2c were evaluated for fluorescence and silver binding characteristics using self assembly experiments. GEPI mediated self immobilization of functional proteins was applied to generate heterofunctional protein arrays.

QBP-AgBP printed substrates were incubated with 80 nm and 20 nm AgNP. The micropatterns formed through microcontact printing of QBP-AgBP followed by silver nanoparticle assembly used as negative control. Surface, patterned with 80 nm silver nanoparticle was incubated with MBP-GFPuv-AgBP2c and MBP-GFPuv. Fluorescence microscopy was used for demonstrating the specific binding and multifunctionality of MBP-GFPuv-AgBP2c. It has been observed that only the

pattern incubated with MBP-GFP-AgBP fusion protein exhibits high contrast (Figure 3.47).

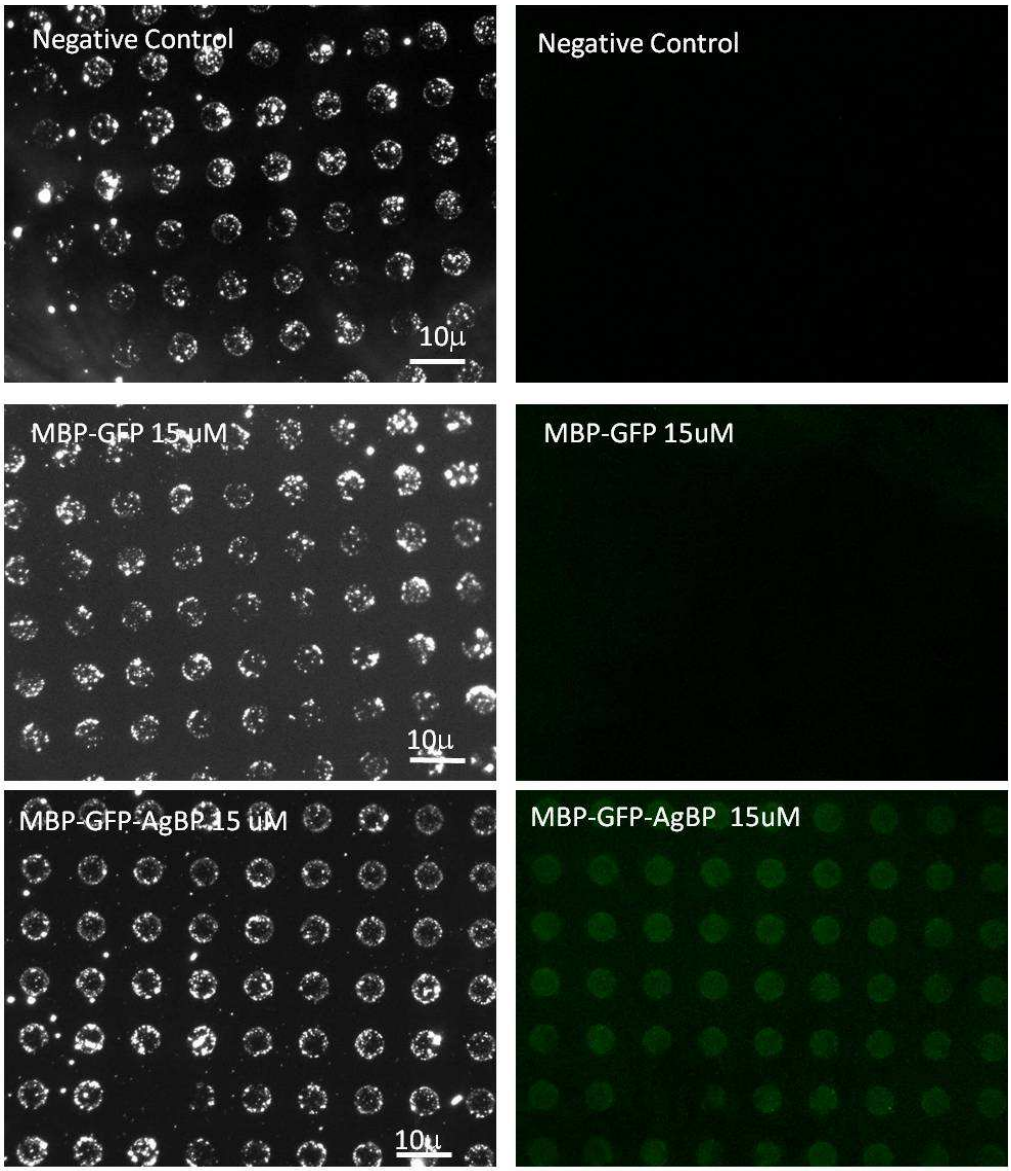

Figure 3.47 : Dark field and fluorescence images of the micropattern formed through PDMS stamping of QBP-AgBP followed by 80 nm silver nanoparticle assembly (negative control) and the micropatterns incubated with 15 µM MBP-GFPuv and MBP-GFPuv-AgBP2c proteins.

The procedure was repeated using 20 nm silver particle to test specific binding of GFPuv-AgBP2c. Surface patterned with 20 nm silver nanoparticle was incubated with GFPuv-AgBP2c and GFPuv proteins. Using fluorescence microscopy, specific binding and bifunctionality of GFPuv-AgBP2c were demonstrated. It has been observed that only the pattern incubated with GFP-AgBP bifunctional protein exhibits high contrast (Figure 3.48). Immobilization data have shown that GFPuv-

AgBP2cs have significantly higher binding affinity to silver compared to control GFPuv protein as a result of specific binding. The results have also shown that the immobilization of the GFP base fusion protein is material specific. Engineered proteins were immobilized onto silver nanopatterned surface; however, they did not bind to glass surface.

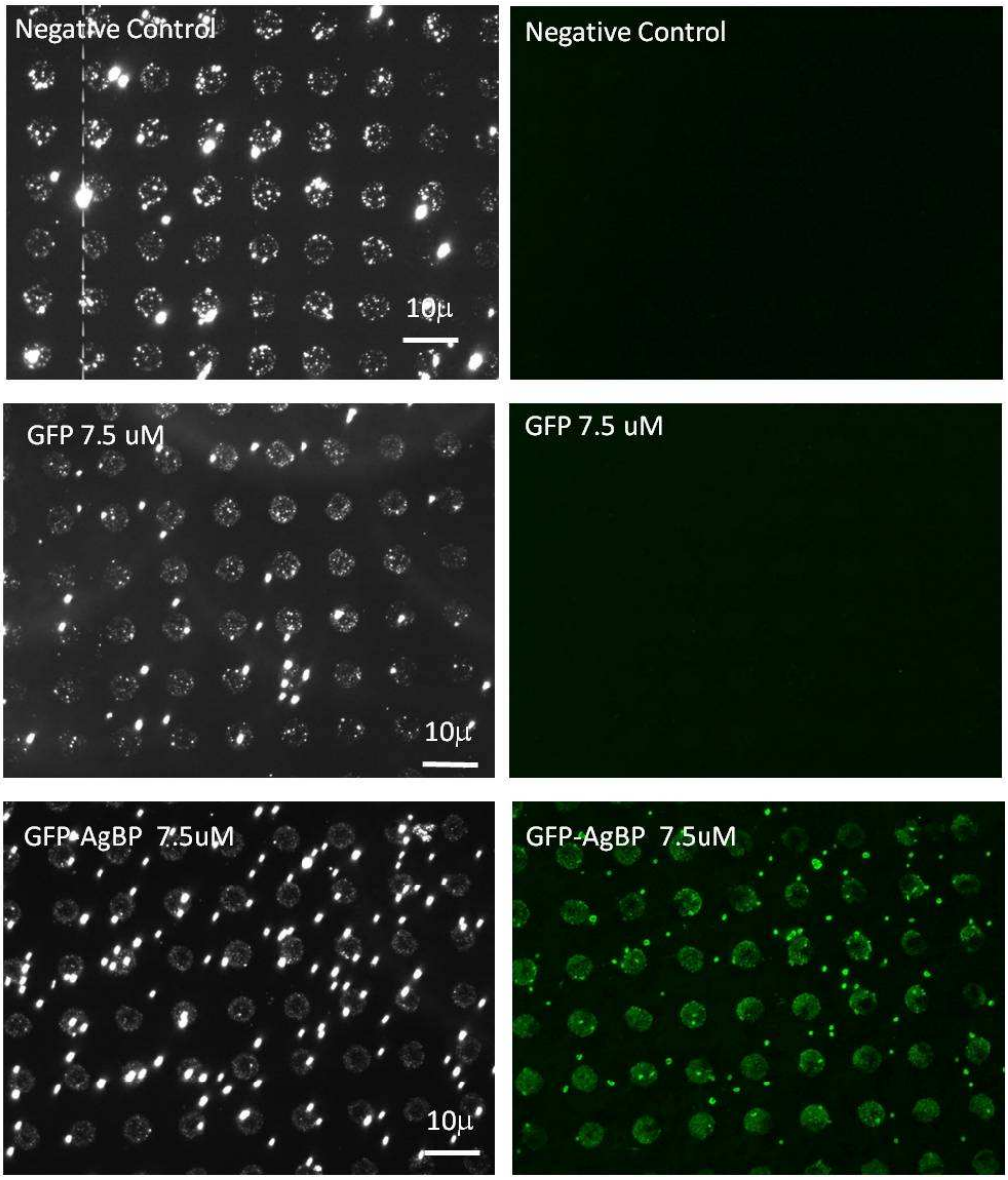

Figure 3.48 : Dark field and fluorescence images of the micropattern formed through PDMS stamping of QBP-AgBP followed by 20 nm silver nanoparticle assembly (negative control) and the micropatterns incubated with 7.5 µM GFPuv and GFPuv-AgBP2c proteins.

3.2.9 Analysis of fluorescence quenching/enhancement assays on fusion protein bound NPs

The multifunctionality of the GFPuv-GEPI fusion proteins was evaluated for fluorescence and noble metal binding characteristics also using fluorescence spectrophotometric measurements.

Although the exact mechanism for the quenching by NPs has not been exhibited yet (Algar et al., 2009), some research groups have suggested that the efficiency of quenching by gold nanoparticles depends on the size and shape of the nanoparticle, distance from the fluorophore, spectral overlap and dipole orientation (Dulkeith et al., 2002; Dulkeith et al., 2005; Algar et al., 2009).

The affinity of the bifunctional GFPuv-GEPI fusion proteins for colloidal noble metal nanoparticles was tested by quenching analyses using different sizes of nanoparticles. The correlation between the binding of bifunctional proteins to nanoparticles and quenching efficiency was evaluated. The samples were measured in microtiter plate through a fluorescence spectrophotometer at room temperature.

3.2.9.1 Fluorescence quenching/enhancement by gold nanoparticles

Fluorescence quenching due to the binding GFPuv-AuBP fusion protein to gold was tested on 2 nm, 5nm and 15 nm gold nanoparticles. The citrate-capped AuNPs (Ted Pella) and GFPuv-AuBP2 protein samples were mixed at different ratios and incubated for two hours. As the gold NP surface area for each NP size was increased, the higher quenching of GFPuv fluorescence was observed (Figures 3.49, 3.50 and 3.51).

In experiments using 15nm and 2nm gold NP, it has been observed that the GFPuv and GFPuv-AuBP displayed similar quenching characteristics with a decrease in fluorescence (Figures 3.49, 3.51). On the other hand, at 5 nm gold NP size, a difference in level of fluorescence quenching between GFPuv-AuBP and GFPuv is observed (Figure 3.50).

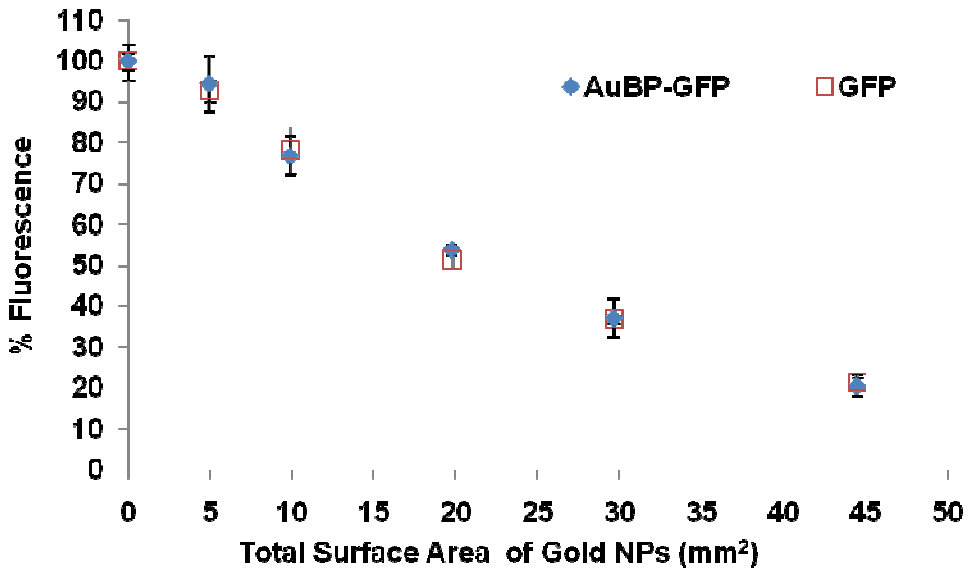

Figure 3.49 : Fluorescence quenching/enhancement assay on GFPuv and GFPuv-AuBP2c proteins bound to 15 nm AuNP.

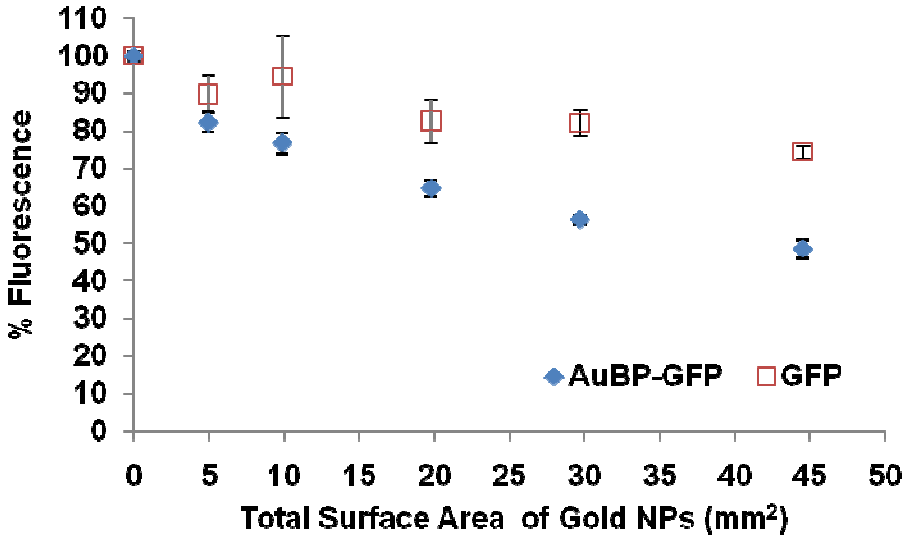

Figure 3.50 : Fluorescence quenching/enhancement assay on GFPuv and GFPuv-AuBP2c proteins bound to 5 nm AuNP.

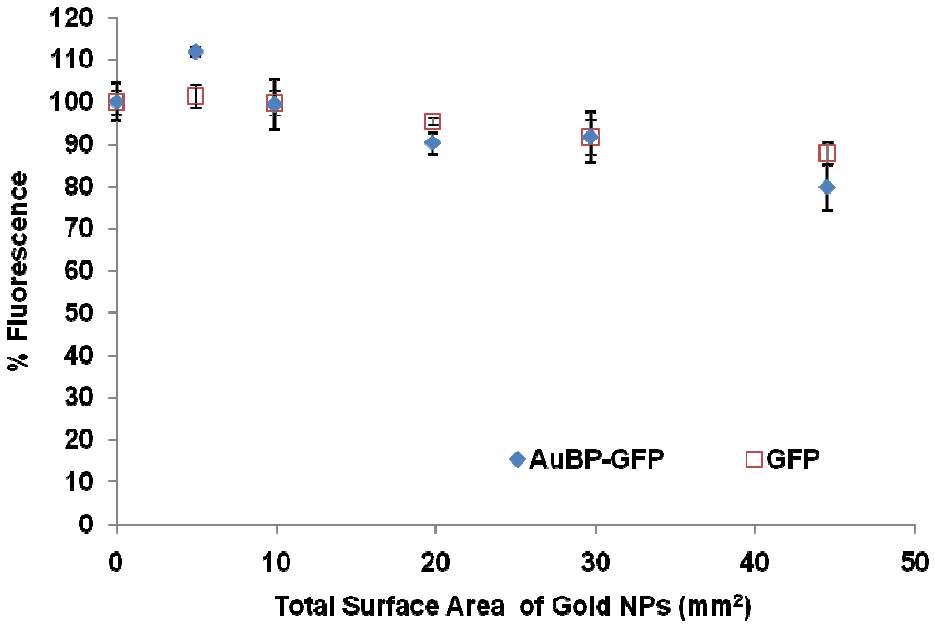

Figure 3.51 : Fluorescence quenching/enhancement assay on GFPuv and GFPuv-AuBP2c proteins bound to 2 nm AuNP.

Lapienc et al. (2010), have demonstrated that fluorescence of the fluorescence protein is quenched by 25 nm gold NP. Quenching is the decrease in the intensity of the fluorescence by a variety of mechanisms. In many fluorescence molecules the intensity primarily depends on the alterations in the efficiency of photon emission (Crowley et al., 1993). In addition, the intensity changes can be a result of changes in the absorbance that depends on pH, environment or other effects (Mercola et al., 1972; Adkins et al., 1983). In this study, when NP is added to solution, GFPuv lacking the AuBP2c can be quenched by energy transfer. On the other hand, binding of AuBP2c part of fluorescence fusion protein can cause quenching by a different mechanism.

Here, it can be suggested that specific binding of GFPuv-AuBP2c bifunctional protein to AuNPs may depend on physical characteristics of the NPs.

3.2.9.2 Fluorescence quenching/enhancement by silver nanoparticles

Binding of GFPuv-AgBP2c fusion protein to silver was demonstrated on 20 nm and 80 nm silver nanoparticles. Quenching of fluorescence with binding of the protein to nanoparticles was evaluated as described in section 3.2.9.1.

In the experiments with 20 nm silver NP, GFPuv and GFPuv-AuBP displayed similar quenching characteristics (Figure 3.52). On the other hand, at 80 nm silver NP size, a

difference in level of fluorescence quenching between GFPuv-AgBP and GFPuv. GFPuv-AgBP2c displayed a higher quenching ratio than that of GFPuv alone (Figure 3.53).

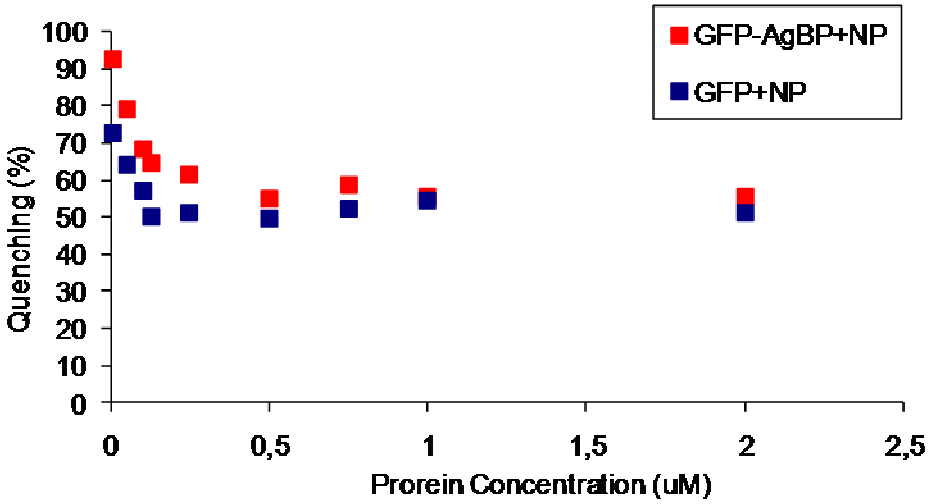

Figure 3.52 : Fluorescence quenching/enhancement assay on GFPuv and GFPuv-AgBP2c proteins bound to 20 nm AgNP.

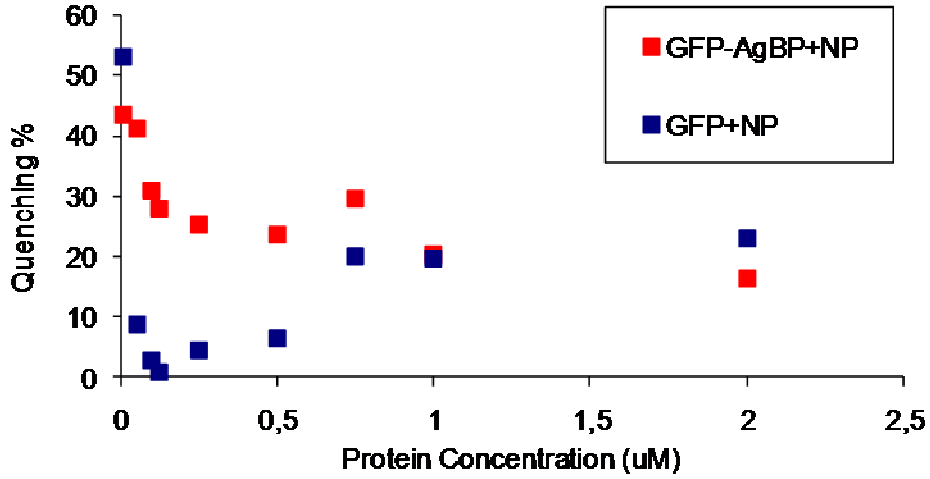

Figure 3.53 : Fluorescence quenching/enhancement assay on GFPuv and GFPuv-AgBP2c proteins bound to 80 nm AgNP.

As discussed in section 3.2.9.2, specific binding of GFPuv-AgBP2c bifunctional protein to AgNPs may depend on the physical characteristics of NPs and a different mechanism can affect the quenching of GFPuv and GFPuv-AgBP2c proteins.

4. CONCLUSION

Molecular Biomimetics offers biological routes for the utilization of materials assembly and fabrication starting at the molecular scale. The proof of concept studies towards understanding the fundamentals and initiating the applications in bio-nanotechnology are exponentially increasing over the years through the solid integration of molecular biology and materials sciences. Based on these studies, one can imagine that realization of truly green technologies is not very far away. In the scope of the thesis, the multifunctional protein based molecular constructs were designed for different applications varying from tissue engineering to controlling quecheing/enhancement properteis of metalic nanotructures.

Inorganic binding peptides that were selected using combinatorial techniques became an important component of the majority of the bionanotechnological studies. Our group (Sarikaya and Tamerler) has been one of the first groups involved in the selection and re-engineering of peptides recognizing solid materials and using this property to fabrication of novel practical systems.

In this study, heterofunctional fusion proteins were successfully produced through genetic conjugation of combinatorially selected solid binding peptides (HA binding peptide, silver binding peptide, gold binding peptide) to green fluorescent protein as multifunctional molecular probes for various applications such as monitoring inorganics formation, and assembly of nanoparticles. Using recombinant protein cloning and expression, and then purification techniques, GFP-GEPI based molecular constructs were produced. Heterofunctional fusion proteins were obtained in soluble form without any loss in original activities. Here, GEPIs are shown as effective fusion partners to link the inorganic recognition and binding property through controlling the biological and material interface without affecting the activity of the fusion partner.

In biomedical application, tracking of HA formation can be achived by several methods, and it is very important. There have been various efforts on HA labelling, including synthesizing HA particles doped with fluorescent ions (de Araujo et al.,

2007; Yang et al., 2008), synthesizing HA-quantum dot composites (Guo et al., 2008; Hsieh et al., 2009). As an alternative and also more importantly as a targted method, here we develop HA labelling with biological fluorescence molecule. GFPuv-HABP1 fusion protein is the first molecule which can be used to functionalize HA surfaces for biomedical and biotechnological applications. GFPuv-HABP1 bifunctional protein can be used as an efficient reporter to detect calcium phosphate mineral structures and as a real time agent for monitoring biomineralization processes.

The structural studies of the engineered GFPuv-HABP proteins revealed that there is some degree of structural rearrangement following the insertion of the HABPs compared to the GFPuv alone. On the other hand, the GFPuv fluorescence of the fusion proteins was not result in significant changes. The QCM-D data indicated that GFPuv-HABP1 had granted the ability to bind to biomineral surfaces specifically. We also demonstrated the versatility of the GFPuv-HABP1 heterofunctional protein by carrying out time-wise monitoring of mineralization as well as visualization of mineralized tissues.

Site-specific protein immobilization is required for the fabrication of efficient biotechnological tools such as enzymatic assays, protein chips, biosensors and microarrays (Bailey et al., 2007; Rusmini et al., 2007; Jung et al., 2008). The conventional immobilization methods may cause the uncontrolled assembly and a decrease in protein activity (Kwon et al., 2006; Rusmini et al., 2007). Here, inorganic binding peptides were demosntrated for the controlled immobilization and patterning of GFPuv and MBP-GFPuv on silver and gold surface. The heterofunctionality of MBP-GFPuv-AuBP2c/AgBP2c and GFPuv-AuBP2c/AgBP2c genetically fused proteins were demonstrated fluorescence and noble metal binding characteristics using soft lithogpraghy techniques such as microcontact printing, self immobilization methods and fluorescence spectrophotometry.

Patterning and directed assembling of MBP-GFPuv-GEPI and GFPuv-GEPI fusion proteins has revealed that this multifunctional proteins may be used as a fluorescence ink for various applications in the field of bionanotechnology. Generally speaking, the specific and high-affinity binding of MBP-GFPuv-AgBP2c/AuBP2c and GFPuv-AgBP2c/AuBP2c heterofunctional proteins on the nanopatterned and flat surface indicate that several nanoplatforms may be fabricated using these fusion proteins.

Quenching of the fluorescence upon binding of the protein to nanoparticles was also evaluated. Fluorescent measurements have shown that the higher the total surface area of gold nanoparticles yielded the lower fluorescence intensity. This may indicates that the decrease in the intensity is proportional to the binding of the bifunctional protein to nanoparticle. Effects of binding GFPuv-AuBP fusion protein to gold, on fluorescence quenching/enhancement were tested on 2 nm, 5nm and 15 nm gold nanoparticles.

A difference in the fluorescence quenching level between GFPuv-AuBP and GFPuv was observed only in the case of 5 nm gold. In adition, binding of GFPuv-AgBP2c fusion protein to silver was demonstrated on 20 nm and 80 nm silver nanoparticles. The difference in the quenching level was observed only in the case of 80 nm silver nanoparticle. In a previous study, it has been shown that the fluorescence of the fluorescence protein is quenched by gold nanoparticle (Lapienc et al., 2010). A variety of mechanisms lead to quenching, therefore GFPuv and GFPuv-AuBP2c/AgBP2c may be quenched by different mechanisms. The specific binding of GFPuv-AuBP2c/AgBP2c bifunctional proteins may depend on physical characteristics of the nanoparticles. Further studies with different size and ratio of metal nanoparticles and with different GFPuv-GEPI constructs may provide a biologically controlled sensing moities based on fluorescence quenching/enhancement assays based on the binding of the fusion proteins to nanoparticles.

Taken together, based on the previous studies on the biocombinatorially-selected and characterized hydroxyapatite binding peptides (Gungormus et al., 2008), HABP1, HABP2, AgBP2c (Hnilova et al, unpuslished data) and AuBP2c (Hnilova et al., 2008) fusion proteins were created using GFP as a fluorescence protein partner. Throughout the study, various heterofunctional proteins were obtained: GFPuv-HABP1, MBP-GFPuv-AgBP2c, MBP-GFPuv-AuBP2c, GFPuv-AgBP2c and GFPuv-AuBP2c. These proteins have a potential for utilization in imaging studies, fabrication of new materials and systems for biotechnological and biomedical applications. In addition, the plasmid constructs encoding these heterofunctional proteins can be further engineered to add new functionalities to create technologically promising multifunctional proteins based platforms. Many biocombinatorially selected peptides can enable inorganic synthesis, such as gold,

silver, silica, calcium carbonate, and magnetite. Variuos GFPuv-GEPI constructs can be generated and therefore extended their applicability in the monitoring and probing the assembly and formation of materials.

REFERENCES

Addadi, L. and Weiner S., 1985. Interactions between acidic proteins and crystals - stereochemical requirements in biomineralization. *Proceedings of the National Academy of Sciences of the United States of America*, **82**, 4110-4114.

Adkins, H. J., Miller D. L. and Johnson, A. E., 1983. Changes in aminoacyl transfer ribonucleic-acid conformation upon association with elongation Factor-tu-guanosine 5'-triphosphate-fluorescence studies of ternary complex conformation and topology. *Biochemistry*, **22**, 1208-1217.

Agarwal, G., Naik R. R. and Stone, M. O., 2003. Immobilization of histidine-tagged proteins on nickel by electrochemical dip pen nanolithography. *Journal of the American Chemical Society*, **125**, 7408-7412.

Algar, W. R., Massey M. and Krull U. J., 2009. The application of quantum dots, gold nanoparticles and molecular switches to optical nucleic-acid diagnostics. *Trac-Trends in Analytical Chemistry*, **28**, 292-306.

Alivisatos, A. P., 1996. Semiconductor clusters, nanocrystals, and quantum dots. *Science*, **271**, 933-937.

Alivisatos, A. P., Gu W. W. and Larabell, C., 2005. Quantum dots as cellular probes. *Annual Review of Biomedical Engineering*, **7**, 55-76.

Anker, J. N., Hall, W. P., Lyandres, O., Shah, N. C., Zhao, J. and Van Duyne R. P., 2008. Biosensing with plasmonic nanosensors. *Nature Materials*, **7**, 442-453.

Bailey, L. E., Kambhampati, D., Kanazawa, K. K., Knoll, W. and Frank C. W., 2002. Using surface plasmon resonance and the quartz crystal microbalance to monitor in situ the interfacial behavior of thin organic films. *Langmuir*, **18**, 479-489.

Bailey, R. C., Kwong, G. A., Radu, C. G., Witte, O. N., and Heath, J. R., 2007. DNA-encoded antibody libraries: A unified platform for multiplexed cell sorting and detection of genes and proteins. *Journal of the American Chemical Society*, **129**, 1959-1967.

Ball, P., 2001. Life's lessons in design. *Nature*, 409, 413-416.

Barth, J. V., Costantini, G. and Kern, K., 2005. Engineering atomic and molecular nanostructures at surfaces. *Nature*, **437**, 671-679.

Belcher, A. M., Wu, X. H., Christensen, R. J., Hansma, P. K., Stucky, G. D. and Morse, D. E., 1996. Control of crystal phase switching and orientation by soluble mollusc-shell proteins. *Nature*, **381**, 56-58.

Benhar, I., 2001. Biotechnological applications of phage and cell display. *Biotechnology Advances*, **19**, 1-33.

Berman, A., Addadi, L. and Weiner, S., 1988. Interactions of sea-urchin skeleton macromolecules with growing calcite crystals-a study of intracrystalline proteins. *Nature*, **331**, 546-548.

Bernard, A., Delamarche, E., Schmid, H., Michel, B., Bosshard, H. R. And Biebuyck, H., 1998. Printing patterns of proteins. *Langmuir*, **14**, 2225-2229.

Bernard, A., Renault, J. P. , Michel, B., Bosshard, H. R. and Delamarche, E., 2000. Microcontact printing of proteins. *Advanced Materials*, **12**, 1067-1070.

Boonekamp, P. M., Vanderweepals, L. J. A., Vanwijkvanlennep, M. M. L., Thesing, C. W. and Bijvoet, O. L. M., 1986. 2 Modes of action of bisphosphonates on osteoclastic resorption of mineralized matrix. *Bone and Mineral*, **1**, 27-39.

Bornscheuer, U. T., 2003. Immobilizing enzymes: How to create more suitable biocatalysts. *Angewandte Chemie-International Edition*, **42**, 3336-3337.

Braun, R., Sarikaya, M. and Schulten, K., 2002. Genetically engineered gold-binding polypeptides: structure prediction and molecular dynamics. *Journal of Biomaterials Science-Polymer Edition*, **13**, 747-757.

Braux, J., Guillaume, C., Jallot, E., Nedelec, J. M., Laurent-Maquin, D. and Laquerriere, P., 2009. Effect of strontium treatment on human primary osteoblasts. Hydroxyapatite: A drug delivery system? *International Journal of Artificial Organs*, **32**, 458-458.

Brott, L. L., Naik, R. R., Pikas, D. J., Kirkpatrick, S. M., Tomlin, D. W., Whitlock, P. W., Clarson, S. J. and Stone, M. O., 2001. Ultrafast holographic nanopatterning of biocatalytically formed silica. *Nature*, **413**, 291-293.

Brown, S., 2001. Protein-mediated particle assembly. *Nano Letters*, 1, 391-394.

Brown, S., Sarikaya, M. and Johnson, E., 2000. A genetic analysis of crystal growth. *Journal of Molecular Biology*, **299**, 725-735.

Cady, N. C., Strickland, A. D. and Batt, C. A., 2007. Optimized linkage and quenching strategies for quantum dot molecular beacons. *Molecular and Cellular Probes*, **21**, 116-124.

Campbell, R. E., Tour, O., Palmer, A. E., Steinbach, P. A., Baird, G. S., Zacharias, D. A. and Tsien, R. Y., 2002. A monomeric red fluorescent protein. *Proceedings of the National Academy of Sciences of the United States of America*, **99**, 7877-7882.

M. A., Cariolou and Morse, D. E., 1988. Purification and characterization of calcium-binding conchiolin shell peptides from the mollusk, haliotis-rufescens, as a function of development. *Journal of Comparative Physiology B-Biochemical Systemic and Environmental Physiology*, **157**, 717-729.

Cha, J. N., Shimizu, K., Zhou, Y., Christiansen, S. C., Chmelka, B. F., Stucky, G. D. and Morse, D. E., 1999. Silicatein filaments and subunits from a marine sponge direct the polymerization of silica and silicones in vitro. *Proceedings of the National Academy of Sciences of the United States of America*, **96**, 361-365.

Chalfie, M., Tu, Y., Euskirchen, G., Ward, W. W. and Prasher, D. C., 1994. Green fluorescent protein as a marker for gene-expression. *Science*, **263**, 802-805.

Chen, Y., Munechika, K. and Ginger, D. S., 2007. Dependence of fluorescence intensity on the spectral overlap between fluorophores and plasmon resonant single silver nanoparticles. *Nano Letters*, **7**, 690-696.

Chen, Y., Munechika, K. and Ginger, D. S., 2008. Bioenabled nanophotonics. *Mrs Bulletin*, **33**, 536-542.

Cho, Y. and Ivanisevic, A., 2006. Peptides on GaAs surfaces: Comparison between features generated by microcontact printing and dip-pen nanolithography. *Langmuir*, **22**, 8670-8674.

Choe, W. S., Sastry, M. S. R., Thai, C. K., Dai, H., Schwartz, D. T. and Baneyx, F., 2007. Conformational control of inorganic adhesion in a designer protein engineered for cuprous oxide binding. *Langmuir*, **23**, 11347-11350.

Chudakov, D. M., Lukyanov, S. and Lukyanov, K. A., 2005. Fluorescent proteins as a toolkit for in vivo imaging. *Trends in Biotechnology*, **23**, 605-613.

Crameri, A., Whitehorn, E. A., Tate, E. and Stemmer, W. P. C., 1996. Improved green fluorescent protein by molecular evolution using DNA shuffling. *Nature Biotechnology*, **14**, 315-319.

Crowley, K. S., Reinhart, G. D. and Johnson, A. E., 1993. The signal sequence moves through a ribosomal tunnel into a noncytoplasmic aqueous environment at the ER membrane early in translocation. *Cell*, **73**, 1101-1115.

Dai, H. X., Choe, W. S., Thai, C. K., Sarikaya, M., Traxler, B. A., Baneyx, F. and Schwartz, D. T., 2005. Nonequilibrium synthesis and assembly of hybrid inorganic-protein nanostructures using an engineered DNA binding protein. *Journal of the American Chemical Society*, **127**, 15637-15643.

Daniel, M. C. and Astruc, D., 2004. Gold nanoparticles: Assembly, supramolecular chemistry, quantum-size-related properties, and applications toward biology, catalysis, and nanotechnology. *Chemical Reviews*, **104**, 293-346.

Dash, A. K. and Cudworth, G. C., 1998. Therapeutic applications of implantable drug delivery systems. *Journal of Pharmacological and Toxicological Methods*, **40**, 1-12.

Day, R. N. and Davidson, M. W., 2009. The fluorescent protein palette: tools for cellular imaging. *Chemical Society Reviews*, **38**, 2887-2921.

de Araujo, T. S., Macedo, Z. S., de Oliveira, P. A. S. C. and Valerio, M. E. G., 2007. Production and characterization of pure and Cr^{3+}-doped hydroxyapatite for biomedical applications as fluorescent probes. *Journal of Materials Science*, **42**, 2236-2243.

Deniz, A. A., Laurence, T. A., Dahan, M., Chemla, D. S., Schultz, P. G. and Weiss, S., 2001. Ratiometric single-molecule studies of freely diffusing biomolecules. *Annual Review of Physical Chemistry*, **52**, 233-253.

Dickerson, M. B., Jones, S. E., Cai, Y., Ahmad, G., Naik, R. R., Kroger, N. and Sandhage, K. H., 2008. Identification and design of peptides for the rapid, high-yield formation of nanoparticulate TiO_2 from aqueous solutions at room temperature. *Chemistry of Materials*, **20**, 1578-1584.

Drexler, K. E., 1994. Molecular nanomachines - physical principles and implementation strategies. *Annual Review of Biophysics and Biomolecular Structure*, **23**, 377-405.

Drexler, K. E., 1995. Molecular manufacturing: Perspectives on the ultimate limits of fabrication. *Philosophical Transactions of the Royal Society of London Series a-Mathematical Physical and Engineering Sciences*, **353**, 323-331.

Du, W., Wang, Y., Luo, Q. M. and Liu, B. F., 2006. Optical molecular imaging for systems biology: from molecule to organism. *Analytical and Bioanalytical Chemistry*, **386**, 444-457.

Dubertret, B., Calame, M. and Libchaber, A. J., 2001. Single-mismatch detection using gold-quenched fluorescent oligonucleotides. *Nature Biotechnology*, **19**, 365-370.

Dulkeith, E., Morteani, A. C., Niedereichholz, T., Klar, T. A., Feldmann, J., Levi, S. A., van Veggel, F., Reinhoudt, D. N., Moller, M. and Gittins, D. I., 2002. Fluorescence quenching of dye molecules near gold nanoparticles: Radiative and nonradiative effects. *Physical Review Letters*, **89**, 203002.

Dulkeith, E., Ringler, M., Klar, T. A., Feldmann, J., Javier, A. M. and Parak, W. J., 2005. Gold nanoparticles quench fluorescence by phase induced radiative rate suppression. *Nano Letters*, **5**, 585-589.

Evans, J. S., Samudrala, R., Walsh, T. R., Oren, E. E. and Tamerler, C., 2008. Molecular design of inorganic-binding polypeptides. *Mrs Bulletin*, **33**, 514-518.

Finney, N. S., 2006. Combinatorial discovery of fluorophores and fluorescent probes. *Current Opinion in Chemical Biology*, **10**, 238-245.

Fischer, A. J. and Lagarias, J. C., 2004. Harnessing phytochrome's glowing potential. *Proceedings of the National Academy of Sciences of the United States of America*, 101, 17334-17339.

Fong, H., White, S. N., Paine, M. L., Luo, W., Snead, M. L. and Sarikaya, M., 2003. Enamel structure properties controlled by engineered proteins in transgenic mice. *Journal of Bone and Mineral Research*, **18**, 2052-2059.

Gambetta, G. A. and Lagarias, J. C., 2001. Genetic engineering of phytochrome biosynthesis in bacteria. *Proceedings of the National Academy of Sciences of the United States of America*, **98**, 10566-10571.

Gao, X. H., Yang, L. L., Petros, J. A., Marshal, F. F., Simons, J. W. and Nie, S. M., 2005. In vivo molecular and cellular imaging with quantum dots. *Current Opinion in Biotechnology*, **16**, 63-72.

Gaskin, D. J. H., Starck, K. and Vulfson, E. N., 2000. Identification of inorganic crystal-specific sequences using phage display combinatorial library of short peptides: A feasibility study. *Biotechnology Letters*, **22**, 1211-1216.

Gell, C., Bormuth, V., Brouhard, G. J., Cohen, D. N., Diez, S., Friel, C. T., Helenius, J., Nitzsche, B., Petzold, H., Ribbe, J., Schaffer, E., Stear, J. H., Trushko, A., Varga, V., Widlund, P. O., Zanic, M. and Howard, J., 2010. Microtubule dynamics reconstituted in vitro and imaged by single-molecule fluorescence microscopy. *Methods in Cell Biology*, San Diego, Elsevier Academic Press Inc., **95**, 221-245.

Giepmans, B. N. G., Adams, S. R., Ellisman, H. and Tsien, R. Y., 2006. Review - The fluorescent toolbox for assessing protein location and function. *Science*, **312**, 217-224.

Ginger, D. S., Zhang, H. and Mirkin, C. A., 2004. The evolution of dip-pen nanolithography. *Angewandte Chemie-International Edition*, **43**, 30-45.

Glazer, A. N., 1989. Light guides - directional energy-transfer in a photosynthetic antenna. *Journal of Biological Chemistry*, **264**, 1-4.

Glimcher, M. and Nimni, M., 1992. Collagen cross-linking and biomineralization. *Connective Tissue Research*, **27**, 73-83.

Grant, G. A., 2002. *Synthetic peptides: a user's guide*, p. 3-8, New York: Oxford University Press.

Griffin, B. A., Adams, S. R. and Tsien, R. Y., 1998. Specific covalent labeling of recombinant protein molecules inside live cells. *Science*, **281**, 269-272.

Gronemeyer, T., Godin, G. and Johnsson, K., 2005. Adding value to fusion proteins through covalent labelling. *Current Opinion in Biotechnology*, **16**, 453-458.

Gungormus, M., Branco, M., Fong, H., Schneider, J. P., Tamerler, C., and Sarikaya, M., 2010. Self assembled bi-functional peptide hydrogels with biomineralization-directing peptides. *Biomaterials*, **31**, 7266-7274.

Gungormus, M., Fong, H., Kim, I. W., Evans, J. S., Tamerler, C. and Sarikaya, M., 2008. Regulation of in vitro calcium phosphate mineralization by combinatorially selected hydroxyapatite-binding peptides. *Biomacromolecules*, **9**, 966-973.

Guo, Y., Shi, D., Lian, L. J., Dong, Z. Y., Wang, W., Cho, H. S., Liu, G. K., Wang, L. M. and Ewing, R. C., 2008. Quantum dot conjugated hydroxylapatite nanoparticles for in vivo imaging. *Nanotechnology*, **19**, 175102.

Gurunathan, K. and Levitus, M., 2008. Applications of Fluorescence Correlation Spectroscopy to the Study of Nucleic Acid Conformational Dynamics. *Progress in Nucleic Acid Research and Molecular Biology*, San Diego, Elsevier Academic Press Inc., **82**, 33-69.

Hardman, R., 2006. A toxicologic review of quantum dots: Toxicity depends on physicochemical and environmental factors. *Environmental Health Perspectives*, **114**, 165-172.

Hart, S. J. and JiJi, R. D., 2002. Light emitting diode excitation emission matrix fluorescence spectroscopy. *Analyst*, **127**, 1693-1699.

Haugland, R. P., 2002. *Handbook of Fluorescent Probes and Research Products*, Molecular Probes, Invitrogen, Molecular Probes.

Herschel J. F. W., 1845. *On a case of superficial colour presented by a homogeneous liquid internally colourless*. Phil. Trans. R. Soc. London, **135**, 143–145.

Heuck, A. P., Hotze, E. M., Tweten, R. K. and Johnson, A. E., 2000. Mechanism of membrane insertion of a multimeric beta-barrel protein: Perfringolysin O creates a pore using ordered and coupled conformational changes. *Molecular Cell*, **6**, 1233-1242.

Hines, M. A. and Guyot-Sionnest, P., 1996. Synthesis and characterization of strongly luminescing ZnS-Capped CdSe nanocrystals. *Journal of Physical Chemistry*, **100**, 468-471.

Hnilova, M., Oren, E. E., Seker, U. O. S., Wilson, B. R., Collino, S., Evans, J. S., Tamerler, C. and Sarikaya, M., 2008. Effect of molecular conformations on the adsorption behavior of gold-binding peptides. *Langmuir*, **24**, 12440-12445.

Hoess, R. H., 2001. Protein design and phage display. *Chemical Reviews*, **101**, 3205-3218.

Hoffman, R. M., 2002. Green fluorescent protein imaging of tumour growth, metastasis, and angiogenesis in mouse models. *Lancet Oncology*, **3**, 546-556.

Hsieh, M. F., Li, J. K. J., Lin, C. A. J., Huang, S. H., Sperling, R. A., Parak, W. J. and Chang, W. H., 2009. Tracking of cellular uptake of hydrophilic CdSe/ZnS quantum dots/hydroxyapatite composites nanoparticles in MC3T3-E1 osteoblast cells. *Journal of Nanoscience and Nanotechnology*, **9**, 2758-2762.

Huang, Y., Chiang, C. Y., Lee, S. K., Gao, Y., Hu, E. L., De Yoreo, J. and Belcher, A. M., 2005. Programmable assembly of nanoarchitectures using genetically engineered viruses. *Nano Letters*, **5**, 1429-1434.

Inglis, W., Sanders, G. H. W., Williams, P. M., Davies, M. C., Roberts, C. J. and Tendler, S. J. B., 2001. A simple method for biocompatible polymer based spatially controlled adsorption of blood plasma proteins to a surface. *Langmuir*, **17**, 7402-7405.

Jaiswal, J. K. and Simon, S. M., 2004. Potentials and pitfalls of fluorescent quantum dots for biological imaging. *Trends in Cell Biology*, **14**, 497-504.

Jares-Erijman, E. A. and Jovin, T. M., 2003. FRET imaging. *Nature Biotechnology*, **21**, 1387-1395.

Johnson, A. E., 2005. Fluorescence approaches for determining protein conformations, interactions and mechanisms at membranes. *Traffic*, **6**, 1078-1092.

Jung, Y. W., Kang, H. J., Lee, J. M., Jung, S. O., Yun, W. S., Chung, S. J. and Chung, B. H., 2008. Controlled antibody immobilization onto immunoanalytical platforms by synthetic peptide. *Analytical Biochemistry*, **374**, 99-105.

Kacar, T., Ray, J., Gungormus, M., Oren, E. E., Tamerler, C. and Sarikaya, M., 2009a. Quartz Binding Peptides as Molecular Linkers towards Fabricating Multifunctional Micropatterned Substrates. *Advanced Materials*, **21**, 295-299.

Kacar, T., Zin, M. T., So, C., Wilson, B., Ma, H., Gul-Karaguler, N., Jen, A. K. Y., Sarikaya, M. and Tamerler, C., 2009b. Directed Self-Immobilization of Alkaline Phosphatase on Micro-Patterned Substrates Via Genetically Fused Metal-Binding Peptide. *Biotechnology and Bioengineering*, **103**, 696-705.

Kasaj, A., Willershausen, B., Reichert, C., Gortan-Kasaj, A., Zafiropoulos, G. G. and Schmidt, M., 2008. Human periodontal fibroblast response to a nanostructured hydroxyapatite bone replacement graft in vitro. *Archives of Oral Biology*, **53**, 683-689.

Kim, J. H., Shin, H. J., Cho, H., Kwak, S. M., Kim, T. S., Kang, J. Y. and Yang, E. G., 2006. A microfluidic protease activity assay based on the detection of fluorescence polarization. *Analytica Chimica Acta*, **577**, 171-177.

Kramer, R. M., Li, C., Carter, D. C., Stone, M. O. and Naik, R. R., 2004. Engineered protein cages for nanomaterial synthesis. *Journal of the American Chemical Society*, **126**, 13282-13286.

Krauland, E. M., Peelle, B. R., Wittrup, K. D. and Belcher, A. M., 2007. Peptide tags for enhanced cellular and protein adhesion to single-crystal line sapphire. *Biotechnology and Bioengineering*, **97**, 1009-1020.

Kulp, J. L., Sarikaya, M. and Evans, J. S., 2004. Molecular characterization of a prokaryotic polypeptide sequence that catalyzes Au crystal formation. *Journal of Materials Chemistry*, **14**, 2325-2332.

Kwon, Y., Coleman, M. A. and Camarero, J. A., 2006. Selective immobilization of proteins onto solid supports through split-intein-mediated protein trans-splicing. *Angewandte Chemie-International Edition,* **45**, 1726-1729.

Lakowicz, J. R., 2006. *Principles of fluorescence spectroscopy.* New York: Springer.

Lange, S. A., Benes, V., Kern, D. P., Horber, J. K. H. and Bernard, A., 2004. Microcontact printing of DNA molecules. *Analytical Chemistry,* **76**, 1641-1647.

Lapienc, V., Kukolka, F., Kiko, K., Arndt, A. and Niemeyer, C. M., 2010. Conjugation of Fluorescent Proteins with DNA Oligonucleotides. *Bioconjugate Chemistry,* **21**, 921-927.

Lavis, L. D. and Raines, R. T., 2008. Bright ideas for chemical biology. Acs *Chemical Biology,* **3**, 142-155.

Lee, K. B., Lim, J. H. and Mirkin, C. A., 2003. Protein nanostructures formed via direct-write dip-pen nanolithography. *Journal of the American Chemical Society*, **125**, 5588-5589.

Lee, K. B., Park, S. J., Mirkin, C. A., Smith, J. C. and Mrksich, M., 2002. Protein nanoarrays generated by dip-pen nanolithography. *Science,* **295**, 1702-1705.

Lee, K. J., Nallathamby, P. D., Browning, L. M., Osgood, C. J. and Xu, X. H. N., 2007. In vivo imaging of transport and biocompatibility of single silver nanoparticles in early development of zebrafish embryos. *Acs Nano,* **1**, 133-143.

Lee, S. W., Mao, C. B., Flynn, C. E. and Belcher, A. M., 2002. Ordering of quantum dots using genetically engineered viruses. *Science,* **296**, 892-895.

Lewin, M., Carlesso, N., Tung, C. H., Tang, X. W., Cory, D., Scadden, D. T. and Weissleder, R., 2000. Tat peptide-derivatized magnetic nanoparticles allow in vivo tracking and recovery of progenitor cells. *Nature Biotechnology,* **18**, 410-414.

Li, Y. J., Xie, W. H. and Fang, G. J., 2008. Fluorescence detection techniques for protein kinase assay. *Analytical and Bioanalytical Chemistry*, **390**, 2049-2057.

LiCata, V. J. and Wowor, A. J., 2008. *Applications of fluorescence anisotropy to the study of protein-DNA interactions*. Biophysical tools for biologists: Vol 1 in vitro Techniques. San Diego, Elsevier Academic Press Inc., **84**, 243-262.

Lichtman, J. W. And Conchello, J. A., 2005. Fluorescence microscopy. *Nature Methods*, **2**, 910-919.

Lilie, H., 2003. Designer proteins in biotechnology. *EMBO reports*, **4**, 347-351.

Liou, Y. C., Tocilj, A., Davies, P. L. and Jia, Z. C., 2000. Mimicry of ice structure by surface hydroxyls and water of a beta-helix antifreeze protein. *Nature*, **406**, 322-324.

Lipman, H., 1935. Staining the skeleton of cleared embryos with Alizarin red S. *Stain Technol*, **10**, 61-63.

Lippincott-Schwartz, J. and Patterson, G. H., 2003. Development and use of fluorescent protein markers in living cells. *Science*, **300**, 87-91.

Liu, T. Y., Chen, S. Y., Liu, D. M. and Liou, S. C., 2005. On the study of BSA-loaded calcium-deficient hydroxyapatite nano-carriers for controlled drug delivery. *Journal of Controlled Release*, **107**, 112-121.

Loo, C., Lowery, A., Halas, N. J., West, J. and Drezek, R., 2005. Immunotargeted nanoshells for integrated cancer imaging and therapy. *Nano Letters*, **5**, 709-711.

Lowenstam, H. A., 1981. Minerals Formed by Organisms. *Science*, **211**, 1126-1131.

Lowenstam, H. A., Traub, W. and Weiner, S., 1984. Nautilus hard parts - a study of the mineral and organic constitutents. *Paleobiology*, **10**, 268-279.

Ma, H., Zin, M. T., Zareie, M. H., Kang, M. S., Kang, S. H., Kim, K. S., Reed, B. W., Behar, C. T., Sarikaya, M. and Jen, A. K. Y., 2007. Assembly of nanomaterials through highly ordered self-assembled monolayers and peptide-organic hybrid conjugates as templates. *Journal of Nanoscience and Nanotechnology*, **7**, 2549-2566.

Ma, M. Y., Zhu, Y. J., Li, L. And Cao, S. W., 2008. Nanostructured porous hollow ellipsoidal capsules of hydroxyapatite and calcium silicate: preparation and application in drug delivery. *Journal of Materials Chemistry*, **18**, 2722-2727.

Maina, C. V., Riggs, P. D., Grandea, A. G., Slatko, B. E., Moran, L. S., Tagliamonte, J. A., McReynolds, L. A. and Diguan, C., 1988. An escherichia-coli vector to express and purify foreign proteins by fusion to and separation from maltose-binding protein. *Gene*, **74**, 365-373.

Mann, S., 1993. Molecular tectonics in biomineralization and biomimetic materials chemistry. *Nature*, **365**, 499-505.

Mann, S., 1996. *Biomimetic Materials Chemistry*. New York, Wiley-VCH.

Masi, A., Cicchi, R., Carloni, A., Pavone, F. S. and Arcangeli, A., 2010. *Optical methods in the study of protein-protein interactions. Integrins and ion channels: molecular complexes and signaling*. Berlin, Springer-Verlag Berlin, **674,** 33-42.

Mayer, G. and Sarikaya, M., 2002. Rigid biological composite materials: Structural examples for biomimetic design. *Experimental Mechanics*, **42**, 395-403.

Meloan, S., Puchtler, H., 1985. Chemical mechanisms of staining methods: von Kossas technique. What von Kossa really wrote and a modified reaction for selective demonstration of inorganic phosphate. *J Histotechol*, **8**, 11-13.

Mercola, D. A., Morris, J. W. S. and Arquilla, E. R., 1972. Use of resonance interaction in study of chain folding of insulin in solution. *Biochemistry*, **11**, 3860.

Michalet, X., Pinaud, F. F., Bentolila, L. A., Tsay, J. M., Doose, S., Li, J. J., Sundaresan, G., Wu, A. M., Gambhir, S. S. And Weiss, S., 2005. Quantum dots for live cells, in vivo imaging, and diagnostics. *Science*, **307**, 538-544.

Miyawaki, A., Nagai, T. and Mizuno, H., 2005. Engineering fluorescent proteins. *Microscopy Techniques*, **95**, 1-15.

Mrksich, M., Dike, L. E., Tien, J., Ingber, D. E. and Whitesides, G. M., 1997. Using microcontact printing to pattern the attachment of mammalian cells to self-assembled monolayers of alkanethiolates on transparent films of gold and silver. *Experimental Cell Research*, **235**, 305-313.

Mrksich, M. and Whitesides, G. M., 1996. Using self-assembled monolayers to understand the interactions of man-made surfaces with proteins and cells. *Annual Review of Biophysics and Biomolecular Structure*, **25**, 55-78.

Murphy, J. T. and Lagarias, J. C., 1997. The phytofluors: a new class of fluorescent protein probes. *Current Biology*, **7**, 870-876.

Nagai, K. and Thogersen, H. C., 1987: Synthesis and sequence-specific proteolysis of hybrid proteins produced in escherichia-coli. *Methods in Enzymology*, **153**, 461-481.

Naik, R. R., Stringer, S. J., Agarwal, G., Jones, S. E. and Stone, M. O., 2002. Biomimetic synthesis and patterning of silver nanoparticles. *Nature Materials*, **1**, 169-172.

Nam, J. M., Thaxton, C. S. and Mirkin, C. A., 2003. Nanoparticle-based bio-bar codes for the ultrasensitive detection of proteins. *Science*, **301**, 1884-1886.

Nam, K. T., Lee, Y. J., Krauland, E. M., Kottmann, S. T. and Belcher, A. M., 2008. Peptide-mediated reduction of silver ions on engineered biological scaffolds. *Acs Nano*, **2**, 1480-1486.

Nath, N. and Chilkoti, A., 2002. A colorimetric gold nanoparticle sensor to interrogate biomolecular interactions in real time on a surface. *Analytical Chemistry*, **74**, 504-509.

Niemeyer, C. M., 2001. Nanoparticles, proteins, and nucleic acids: Biotechnology meets materials science. *Angewandte Chemie-International Edition*, **40**, 4128-4158.

Noy, A., Miller, A. E., Klare, J. E., Weeks, B. L., Woods, B. W. and DeYoreo, J. J., 2002. Fabrication of luminescent nanostructures and polymer nanowires using dip-pen nanolithography. *Nano Letters*, **2**, 109-112.

Oh, S. H., Finones, R. R., Daraio, C., Chen, L. H. and Jin, S. H., 2005. Growth of nano-scale hydroxyapatite using chemically treated titanium oxide nanotubes. *Biomaterials*, **26**, 4938-4943.

Oi, V. T., Glazer, A. N. and Stryer, L., 1982. Fluorescent phycobiliprotein conjugates for analyses of cells and molecules. *Journal of Cell Biology*, **93**, 981-986.

Oren, E. E., Tamerler, C., Sahin, D., Hnilova, M., Seker, U. O. S., Sarikaya, M. and Samudrala, R., 2007. A novel knowledge-based approach to design inorganic-binding peptides. *Bioinformatics*, **23**, 2816-2822.

Oren, E. E., Tamerler, C. and Sarikaya, M., 2005. Metal recognition of septapeptides via polypod molecular architecture. *Nano Letters*, **5**, 415-419.

Ostuni, E., Yan, L. and Whitesides, G. M., 1999. The interaction of proteins and cells with self-assembled monolayers of alkanethiolates on gold and silver. *Colloids and Surfaces B-Biointerfaces*, **15**, 3-30.

Paine, M. L. and Snead, M. L., 1997. Protein interactions during assembly of the enamel organic extracellular matrix. *Journal of Bone and Mineral Research*, **12**, 221-227.

Park, T. J., Hyun, M. S., Lee, H. J., Lee, S. Y. and Ko, S., 2009. A self-assembled fusion protein-based surface plasmon resonance biosensor for rapid diagnosis of severe acute respiratory syndrome. *Talanta*, **79**, 295-301.

Park, T. J., Lee, S. Y., Lee, S. J., Park, J. P., Yang, K. S., Lee, K. B., Ko, S., Park, J. B., Kim, T., Kim, S. K., Shin, Y. B., Chung, B. H., Ku, S. J., Kim, D. H. and Choi, I. S., 2006. Protein nanopatterns and biosensors using gold binding polypeptide as a fusion partner. *Analytical Chemistry*, **78**, 7197-7205.

Pender, M. J., Sowards, L. A., Hartgerink, J. D., Stone, M. O. and Naik, R. R., 2006. Peptide-mediated formation of single-wall carbon nanotube composites. *Nano Letters*, **6,** 40-44.

Petrounia, I. P. and Arnold, F. H., 2000. Designed evolution of enzymatic properties. *Current Opinion in Biotechnology*, **11**, 325-330.

Piston, D. W. and Kremers, G. J., 2007. Fluorescent protein FRET: the good, the bad and the ugly. *Trends in Biochemical Sciences*, **32**, 407-414.

Pla-Roca, M., Fernandez, J. G., Mills, C. A., Martinez, E. and Samitier, J., 2007. Micro/nanopatterning of proteins via contact printing using high aspect ratio PMMA stamps and NanoImprint apparatus. *Langmuir*, **23**, 8614-8618.

Pons, T., Medintz, I. L., Sapsford, K. E., Higashiya, S., Grimes, A. F., English, D. S. and Mattoussi, H., 2007. On the quenching of semiconductor quantum dot photoluminescence by proximal gold nanoparticles. *Nano Letters*, **7**, 3157-3164.

Prasher, D. C., Eckenrode, V. K., Ward, W. W., Prendergast, F. G. and Cormier, M. J., 1992. Primary structure of the aequorea-victoria green-fluorescent protein. *Gene*, **111**, 229-233.

Ramachandran, R., Tweten, R. K. and Johnson, A. E., 2004. Membrane-dependent conformational changes initiate cholesterol-dependent cytolysin oligomerization and intersubunit beta-strand alignment. *Nature Structural & Molecular Biology*, **11**, 697-705.

Reichman, J., 2007. *Handbook of Optical Filters for Fluorescence Microscopy*. Chroma Technology Corp.

Revzin, A., Russell, R. J., Yadavalli, V. K., Koh, W. G., Deister, C., Hile, D. D., Mellott, M. B. and Pishko, M. V., 2001. Fabrication of poly(ethylene glycol) hydrogel microstructures using photolithography. *Langmuir*, **17**, 5440-5447.

Rosander, A., Bjerketorp, J., Frykberg, L. and Jacobsson, K., 2002. Phage display as a novel screening method to identify extracellular proteins. *Journal of Microbiological Methods*, **51**, 43-55.

Roy, M. D., Stanley, S. K., Amis, E. J. and Becker, M. L., 2008. Identification of a highly specific hydroxyapatite-binding peptide using phage display. *Advanced Materials*, **20**, 1830.

Ruiz, S. A. and Chen, C. S., 2007. Microcontact printing: A tool to pattern. *Soft Matter*, **3**, 168-177.

Rusmini, F., Zhong, Z. Y. and Feijen, J., 2007. Protein immobilization strategies for protein biochips. *Biomacromolecules*, **8**, 1775-1789.

Ryu, D. D. Y. and Nam, D. H., 2000. Recent progress in biomolecular engineering. *Biotechnology Progress*, **16**, 2-16.

Sanchez, F. and Sobolev, K., 2010. Nanotechnology in concrete - A review. *Construction and Building Materials*, **24**, 2060-2071.

Sano, K., Sasaki, H. and Shiba, K., 2006. Utilization of the pleiotropy of a peptidic aptamer to fabricate heterogeneous nanodot-containing multilayer nanostructures. *Journal of the American Chemical Society*, **128**, 1717-1722.

Sano, K. I., Sasaki, H. and Shiba, K., 2005. Specificity and biomineralization activities of Ti-binding peptide-1 (TBP-1). *Langmuir*, **21**, 3090-3095.

Sano, K. I. and Shiba, K., 2003. A hexapeptide motif that electrostatically binds to the surface of titanium. *Journal of the American Chemical Society*, **125**, 14234-14235.

Santra, S., Zhang, P., Wang, K. M., Tapec, R. and Tan, W. H., 2001. Conjugation of biomolecules with luminophore-doped silica nanoparticles for photostable biomarkers. *Analytical Chemistry*, **73**, 4988-4993.

Sarikaya, M., 1999. Biomimetics: Materials fabrication through biology. *Proceedings of the National Academy of Sciences of the United States of America*, **96**, 14183-14185.

Sarikaya, M., Aksay, I. A., 1995. *AIP Series in Polymers and Complex Materials*. NY, AIP Press: Woodbury.

Sarikaya, M., Tamerler, C., Jen, A. K. Y., Schulten, K. and Baneyx, F., 2003. Molecular biomimetics: nanotechnology through biology. *Nature Materials*, **2**, 577-585.

Sarikaya, M., Tamerler, C., Schwartz, D. T. and Baneyx, F. O., 2004. Materials assembly and formation using engineered polypeptides. *Annual Review of Materials Research*, **34**, 373-408.

Schmid, J. A. and Neumeier, H., 2005. Evolutions in science triggered by green fluorescent protein (GFP). *Chembiochem*, **6**, 1149-1156.

Schultz, S., Smith, D. R., Mock, J. J. and Schultz, D. A., 2000. Single-target molecule detection with nonbleaching multicolor optical immunolabels. *Proceedings of the National Academy of Sciences of the United States of America*, **97**, 996-1001.

Seeman, N. C. and Belcher, A. M., 2002. Emulating biology: Building nanostructures from the bottom up. *Proceedings of the National Academy of Sciences of the United States of America*, **99**, 6451-6455.

Seker, U. O. S., Wilson, B., Dincer, S., Kim, I. W., Oren, E. E., Evans, J. S., Tamerler, C. and Sarikaya, M., 2007. Adsorption behavior of linear and cyclic genetically engineered platinum binding peptides. *Langmuir*, **23**, 7895-7900.

Shaner, N. C., Campbell, R. E., Steinbach, P. A., Giepmans, B. N. G., Palmer, A. E. and Tsien, R. Y., 2004. Improved monomeric red, orange and yellow fluorescent proteins derived from Discosoma sp red fluorescent protein. *Nature Biotechnology*, **22**, 1567-1572.

Sharma, A., Shulman, S. G., 1999. *Introduction to fluorescence spectroscopy*. Wiley-interscience.

Shimomura, O., Johnson, F. H. and Saiga, Y., 1962. Extraction, purification and properties of aequorin, a bioluminescent protein from the luminous hydromedusan, Aequorea. *J. Cell. Comp.Physiol*, **59,** 223–239

Slocik, J. M. and Naik, R. R., 2006. Biologically programmed synthesis of bimetallic nanostructures. *Advanced Materials*, **18**, 1988-1992.

Smith, G. P., 1985. Filamentous fusion phage - novel expression vectors that display cloned antigens on the virion surface. *Science*, **228**, 1315-1317.

Smith, G. P. and Petrenko, V. A., 1997. Phage display. *Chemical Reviews*, **97**, 391-410.

Sprague, B. L. and McNally, J. G., 2005. FRAP analysis of binding: proper and fitting. *Trends in Cell Biology*, **15**, 84-91.

Stanley, C. M., 2003. *Filters and mirrors for applications in fluorescence microscopy*. Biophotonics, Pt A. San Diego, Academic Press Inc., **360**, 394-415.

Stokes G. G., 1852. *On the change of refrangibility of light*. Phil. Trans. R. Soc. London, **142**:463–562.

Tamerler, C., Duman, M., Oren, E. E., Gungormus, M., Xiong, X. R., Kacar, T., Parviz, B. A. and Sarikaya, M., 2006a. Materials specificity and directed assembly of a gold-binding peptide. *Small*, **2**, 1372-1378.

Tamerler, C., Kacar, T., Sahin, D., Fong, H. and Sarikaya, M., 2007a. Genetically engineered polypeptides for inorganics: A utility in biological materials science and engineering. *Materials Science & Engineering C-Biomimetic and Supramolecular Systems*, **27**, 558-564.

Tamerler, C., Khatayevich, D., Gungormus, M., Kacar, T., Oren, E. E., Hnilova, M. and Sarikaya, M., 2010. Molecular Biomimetics: GEPI-Based Biological Routes to Technology. *Biopolymers,* **94**, 78-94.

Tamerler, C., Oren, E. E., Duman, M., Venkatasubramanian, E. and Sarikaya, M., 2006b. Adsorption kinetics of an engineered gold binding peptide by surface plasmon resonance spectroscopy and a quartz crystal microbalance. *Langmuir*, **22**, 7712-7718.

Tamerler, C. and Sarikaya, M., 2007b. Molecular biomimetics: Utilizing naturels molecular ways in practical engineering. *Acta Biomaterialia*, **3**, 289-299.

Tamerler, C. and Sarikaya, M., 2008. Molecular biomimetics: Genetic synthesis, assembly, and formation of materials using peptides. *Mrs Bulletin*, **33**, 504-510.

Tamerler, C. and Sarikaya, M., 2009a. Genetically Designed Peptide-Based Molecular Materials. *Acs Nano*, **3**, 1606-1615.

Tamerler, C. and Sarikaya, M., 2009b. Molecular biomimetics: nanotechnology and bionanotechnology using genetically engineered peptides. *Philosophical Transactions of the Royal Society a-Mathematical Physical and Engineering Sciences*, **367**, 1705-1726.

Tan, J. L., Tien, J. and Chen, C. S., 2002. Microcontact printing of proteins on mixed self-assembled monolayers. *Langmuir*, **18**, 519-523.

Tan, K., Cheang, P., Ho, I. A. W., Lam, P. Y. P. and Hui, K. M., 2007. Nanosized bioceramic particles could function as efficient gene delivery vehicles with target specificity for the spleen. *Gene Therapy*, **14**, 828-835.

Thai, C. K., Dai, H. X., Sastry, M. S. R., Sarikaya, M., Schwartz, D. T. and Baneyx, F., 2004. Identification and characterization of Cu2O- and ZnO-binding polypeptides by Escherichia coli cell surface display: Toward an understanding of metal oxide binding. *Biotechnology and Bioengineering*, **87**, 129-137.

Tinnefeld, P. and Sauer, M., 2005. Branching out of single-molecule fluorescence spectroscopy: Challenges for chemistry and influence on biology. *Angewandte Chemie-International Edition*, **44**, 2642-2671.

Tomasio, S. D. and Walsh, T. R., 2007. Atomistic modelling of the interaction between peptides and carbon nanotubes. *Molecular Physics*, **105**, 221-229.

Trugnan, G., Fontanges, P., Delautier, D. and Ait-Slimane, T., 2004. FRAP, FLIP, FRET, BRET, FLIM, PRIM... new techniques for a colourful life. *M S-Medecine Sciences*, **20**, 1027-1034.

Truskett, V. N. and Watts, M. P. C., 2006. Trends in imprint lithography for biological applications. *Trends in Biotechnology*, **24**, 312-317.

Waggoner, A., 2006. Fluorescent labels for proteomics and genomics. *Current Opinion in Chemical Biology*, **10**, 62-66.

Walla P. J., 2009. Modern Biophysical Chemistry p 62-98, Wiley-VCH Verlag GmbH & Co. KGaA, Weinheim, Germany.

Wang, L., Jackson, W. C., Steinbach, P. A. and Tsien, R. Y., 2004. Evolution of new nonantibody proteins via iterative somatic hypermutation. *Proceedings of the National Academy of Sciences of the United States of America*, **101**, 16745-16749.

Wei, J. H., Kacar, T., Tamerler, C., Sarikaya, M. and Ginger, D. S., 2009. Nanopatterning peptides as bifunctional inks for templated assembly. *Small*, **5**, 689-693.

Weinstein, R. S., Roberson, P. K. and Manolagas, S. C., 2009. giant osteoclast formation and long-term oral bisphosphonate therapy. *New England Journal of Medicine*, **360**, 53-62.

Wessels, J. T., Yamauchi, K., Hoffman, R. M. and Wouters, F. S., 2010. Advances in cellular, subcellular, and nanoscale imaging in vitro and in vivo. *Cytometry Part A*, **77**, 667-676.

Whaley, S. R., English, D. S., Hu, E. L., Barbara, P. F. and Belcher, A. M., 2000. Selection of peptides with semiconductor binding specificity for directed nanocrystal assembly. *Nature*, **405**, 665-668.

Wiedenmann, J., Oswald, F. and Nienhaus, G. U., 2009. Fluorescent Proteins for Live Cell Imaging: Opportunities, Limitations, and Challenges. *Iubmb Life*. **61**, 1029-1042.

Wiley, B. J., Im, S. H., Li, Z. Y., McLellan, J., Siekkinen, A. and Xia, Y. A., 2006. Maneuvering the surface plasmon resonance of silver nanostructures through shape-controlled synthesis. *Journal of Physical Chemistry B*, **110**, 15666-15675.

Wilson, D. L., Martin, R., Hong, S., Cronin-Golomb, M., Mirkin, C. A. and Kaplan, D. L., 2001. Surface organization and nanopatterning of collagen by dip-pen nanolithography. *Proceedings of the National Academy of Sciences of the United States of America*. **98**, 13660-13664.

Wittrup, K. D., 2001. Protein engineering by cell-surface display. *Current Opinion in Biotechnology*, **12**, 395-399.

Woodbury, R. G., Wendin, C., Clendenning, J., Melendez, J., Elkind, J., Bartholomew, D., Brown, S. and Furlong, C. E., 1998. Construction of biosensors using a gold-binding polypeptide and a miniature integrated surface plasmon resonance sensor. *Biosensors & Bioelectronics*, **13**, 1117-1126.

Woolhead, C. A., McCormick, P. J. and Johnson, A. E., 2004. Nascent membrane and secretory proteins differ in FRET-detected folding far inside the ribosome and in their exposure to ribosomal proteins. *Cell*, **116**, 725-736.

Xi, X. G. and Deprez, E., 2010. Monitoring helicase-catalyzed DNA unwinding b1y fluorescence anisotropy and fluorescence cross-correlation spectroscopy. *Methods*, **51**, 289-294.

Xia, Y. N. and Whitesides, G. M., 1998. Soft lithography. *Annual Review of Materials Science*, **28**, 153-184.

Yang, P., Quan, Z., Li, C., Kang, X., Lian, H., and Lin, J., 2008. Bioactive, luminescent and mesoporous europium-doped hydroxyapatite as a drug carrier. *Biomaterials*, **29**, 4341-4347.

Yang, Z. P. and Chilkoti, A., 2000. Microstamping of a biological ligand onto an activated polymer surface. *Advanced Materials*, **12**, 413-417.

Yokoo, N., Togashi, T., Umetsu, M., Tsumoto, K., Hattori, T., Nakanishi, T., Ohara, S., Takami, S., Naka, T., Abe, H., Kumagai, I. and Adschiri, T., 2010. Direct and selective immobilization of proteins by means of an inorganic material-binding peptide: Discussion on functionalization in the elongation to material-binding peptide. *Journal of Physical Chemistry B*, **114**, 480-486.

Yonzon, C. R., Jeoungf, E., Zou, S. L., Schatz, G. C., Mrksich, M. and Van Duyne, R. P., 2004. A comparative analysis of localized and propagating surface plasmon resonance sensors: The binding of concanavalin a to a monosaccharide functionalized self-assembled monolayer. *Journal of the American Chemical Society*, **126**, 12669-12676.

Zaheer, A., Lenkinski, R. E., Mahmood, A., Jones, A. G., Cantley, L. C. and Frangioni, J. V., 2001. In vivo near-infrared fluorescence imaging of osteoblastic activity. *Nature Biotechnology*, **19**, 1148-1154.

Zhang, Y., Yuan, Y. and Liu, C. S., 2008. Fluorescent labeling of nanometer hydroxyapatite. *Journal of Materials Science & Technology*, **24**, 187-191.

Zimmer, M., 2002. Green fluorescent protein (GFP): Applications, structure, and related photophysical behavior. *Chemical Reviews*, **102**, 759-781.

Zin, M. T., Ma, H., Sarikaya, M. and Jen, A. K. Y., 2005. Assembly of gold nanoparticles using genetically engineered polypeptides. *Small*, **1**, 698-702.

Zin, M. T., Munro, A. M., Gungormus, M., Wong, N. Y., Ma, H., Tamerler, C., Ginger, D. S., Sarikaya, M. and Jen, A. K. Y., 2007. Peptide-mediated surface-immobilized quantum dot hybrid nanoassemblies with controlled photoluminescence. *Journal of Materials Chemistry*, **17**, 866-872.

Url-1 <*http://www.clontech.com/images/pt/PT3055-5.pdf*>, accessed at 12.05.2008.

Url-2 <*http://www.fermentas.com/en/products/all/molecular-cloning/kits/k123-clonejet-pcr-cloning*>, accessed at 05.04.2010.

Url-3 <*http://www.qiagen.com/literature/render.aspx?id=136*>, accessed at 09.05.2009.

Url-4 <*http://expasy.org/tools/protparam.html*>, accessed at 10.08.2008.

Url-5 <*http://tools.invitrogen.com/content/sfs/manuals/topota_man.pdf*>, accesed at 12.10.2009.

Url-6 <*http://www.neb.com/nebecomm/ManualFiles/manualE8200.pdf*>, accessed at 22.12.2009.

Url-7 <*http://www.neb.com/nebecomm/products/productE8200.asp*>, accessed at 10.02.2009.

APPENDICES

APPENDIX A.1 : DNA Markers (Fermentas).
APPENDIX A.2 : Protein molecular weight marker (Fermentas).

APPENDIX A.1

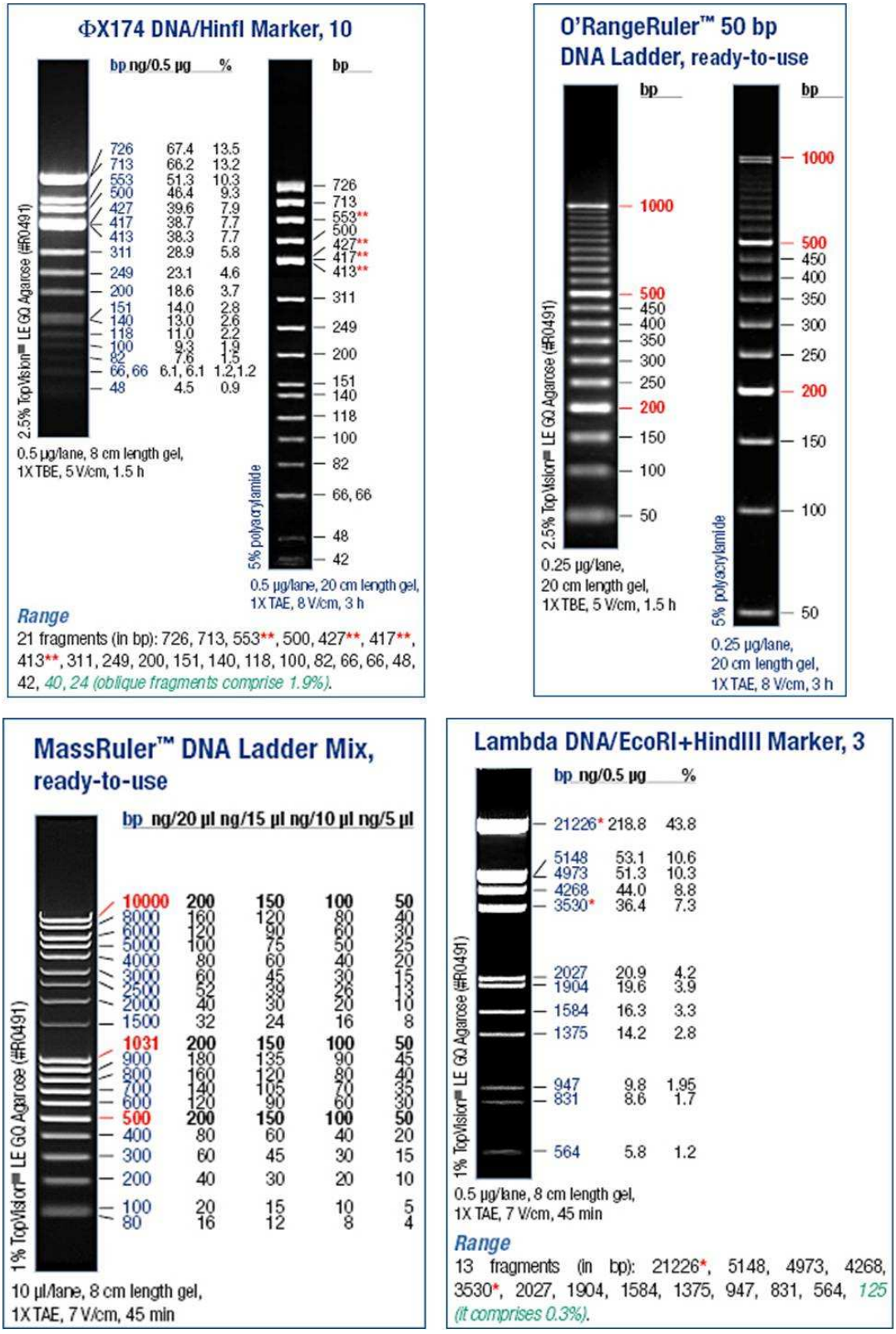

Figure A.1 : DNA Markers (Fermentas).

APPENDIX A.2

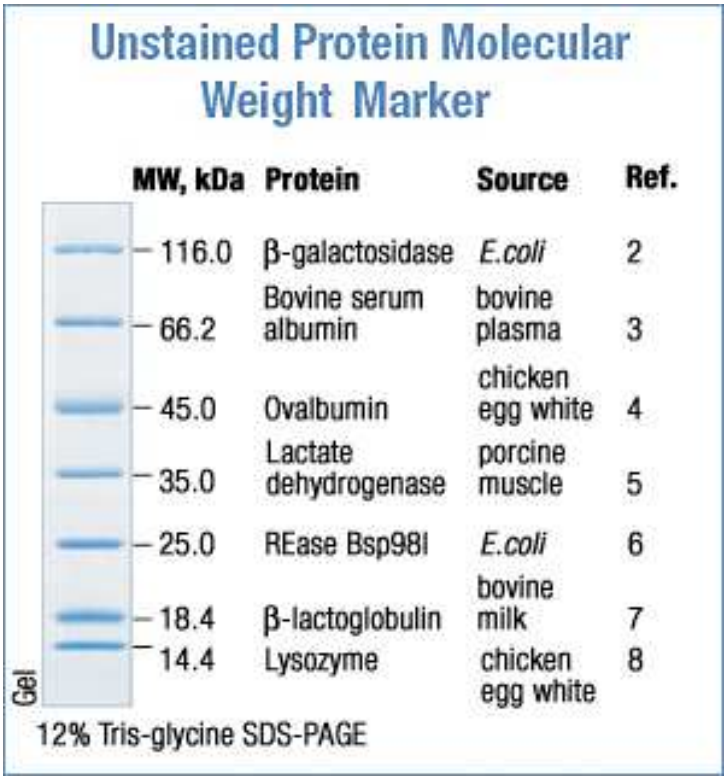

Figure A.2 : Protein Molecular Weight Marker (Fermentas).

CURRICULUM VITAE

Candidate's full name: Esra YÜCA

Place and date of birth: İstanbul 1980

Permanent Address: İstanbul

Universities and Colleges attended:
I.T.U Molecular Biology-Genetics and Biotechnology (Ph.D.)
Y.T.U Molecular Biology (M.Sc.)
İ.Ü Biology Department (B.Sc.)
Ataköy Cumhuriyet College

Publications:

- Yuca E., Yazgan Karatas A., Seker U. O. S., Gungormus M., Dinler-Doganay G., Sarikaya M., Tamerler C., "In vitro labeling of hydroxyapatite minerals by an engineered protein". Biotechnology & Bioengineering. DOI: 10.1002/bit.23041.

Abstracts:

- Yuca, E., Seker, U. O. S., Gungormus, M., Yazgan Karatas A., Sarikaya, M. and Tamerler, C.; "Hydroxyapatite Fused-GFP Protein: Towards a Biomineralization Monitoring System" 2009 MRS Fall Meeting, 30 November-3 December 2009, Boston USA.

- Tayran, H., Yuca, H., Alkan, B., Goller, G., Yazgan Karatas, A., "Chemiluminescence Resonance Energy Transfer Between Immobilized Aequorin and GFP Proteins." International Symposium on Biotechnology: Developments and Trends, METU, 27-30 September 2009, Ankara.

- Yuca, E., Seker, U. O. S., Gungormus, M., Yazgan Karatas A., Sarikaya, M. and Tamerler, C.; "Inorganıc Binding Peptide As Fusion Patner to Autofluorescent Proteins Monitoring Mineral Formation'' Molecular Biomimetics and Bionanotechnology-4, 24-28 Agustos, 2009, University of Washington, Seattle, USA.

- Karaca, E., Yuca, E., Hnilova, M., Yazgan Karatas, A., Sarikaya, M., Tamerler, C., "Red Fluorescent Protein with Genetically Fused Metal Binding Activity" 24-28 Agustos, 2009, University of Washington, Seattle, USA.

- Tayran, H., Yuca, H., Alkan, B., Goller, G., Yazgan Karatas, A., "Investigation of Chemiluminescence Resonance Energy Transfer Between The Photoproteins and Fluorescent Proteins" International Conference on Nanomaterials and Nanosystems, 10-13 August 2009, İstanbul NanoMat2009.

▪ Karaca, E., Yuca, E., Hnilova, M., Yazgan Karatas, A., Sarikaya, M., Tamerler, C., "DsRed Fluorescent Protein with Genetically Fused Metal Binding Activity" International Conference on Nanomaterials and Nanosystems, 10-13 August 2009, Istanbul, NanoMat 2009.

▪ Yüca, E., Seker, U. O. S., Güngörmüş, M., Yazgan Karataş, A., Sarikaya, M., Tamerler, C., "Hidroksiapatite Özgün Peptid İçeren GFP Füzyon Proteinin Biyomineralizasyonun Görüntülenmesinde Kullanımı" 14. Biyomedikal Mühendisliği Ulusal Toplantısı Biyomut2009, 20-24 Mayıs 2009 İzmir.

▪ Yüca, E., Seker, U. O. S., Güngörmüş, M., Yazgan Karataş, A., Sarikaya, M., Tamerler, C., "Biyomineralizasyonun Görüntülenmesinde Kullanılabilecek Nanoyapılı GFP-GEPI Bifonksiyonel Proteinlerinin oluşturulması ". ITU-nanobilim ve nanoteknoloji çalıştayı 12-13 Şubat 2009, Istanbul.

▪ Karaca, E., Yüca, E., Yazgan Karatas, A., Sarikaya, M., Tamerler, C., "Metal Biyosensörü Olarak Altın Bağlı Kırmızı Floresans Füzyon Proteini". ITU-nanobilim ve nanoteknoloji çalıştayı 12-13 Şubat 2009, Istanbul.

▪ Utku, F. S., Yüca, E., Şeker, U. Ö. Ş., Güngörmüş, M., Yazgan Karataş, A., Sarikaya, M., Tamerler, C., "Anorganiklere Bağlanan Peptidlerce İndüklenen Kalsiyum Fosfat Mineralizasyonunun Çevresel Taramalı Elektron Mikroskopuyla İncelenmesi". ITU-nanobilim ve nanoteknoloji çalıştayı 12-13 Şubat 2009, Istanbul.

▪ Yuca, E., Seker, U. O. S., Gungormus, M., Yazgan Karatas, A., Sarikaya, M., Tamerler, C., "HABP-GFP Bifunctional Proteins: Towards a Biomineralization Marker System'' Molecular Biomimetics and Bionanotechnology-3 University of Washington, Seattle, USA, 10-12 September 2008.

▪ Yuca E, Karatas A., Mustafa G, Sarikaya M, Tamerler C, Jun 2008. GFP based bifunctional proteins for real time monitoring of biomineralization. Joint Conference of the 33rd FEBS Congress/11th IUBMB Conference, JUN 28-JUL 03, 2008 Athens, GREECE, FEBS JOURNAL 275 ,374.

▪ Yuca E, Karatas A., Gungormus M, Sarikaya M, Tamerler C, GEPI-GFP Bifunctional Proteins for Detection and Monitoring of Biomineralization. S 141, 4. Nanobilim ve Nanoteknoloji Konferansı. Haziran 2008 Istanbul.

▪ Yuca, E., Yazgan Karatas, A., Sarikaya, M., Tamerler, C., "Symbiosis-13th European Congress on Biotechnology"."GFP Based Designer Proteins As Molecular Sensory Systems" 16-19 September 2007, Barcelona, Spain.

▪ Yuca, E., Yazgan Karatas, A., Gungormus, M., Sarikaya, M., Tamerler, C.,. "GFP Based Designer Proteins as Sensory Systems for Detection and Monitoring of Mineral Formation" 13. Biyomedikal Bilim ve Teknoloji Sempozyumu (BIOMED 2007). 26-28 Ağustos 2007, Yeditepe Üniversitesi.

▪ Yuca, E., Yazgan Karatas, A., Gungormus, M., Sarikaya, M., Tamerler, C., "GFP Based Designer Proteins as Sensory Systems for Detection and Monitoring of Mineral Formation Towards Tissue Engineering" Molecular Biomimetics and Bionanotechnology-II Workshop, 23-25 May 2007, MOBGAM, ITU.

▪ Yuca, E., Yazgan Karatas, A., Sarikaya, M., Tamerler, C., "Construction of Green Fluorescent Protein Based Designer Proteins". Uluslararası Molecular Biomimetics and Bionanotechnology-I Workshop, 12-14 November 2006, MOBGAM, ITU.

▪ Tamerler, C., Oren, E. E., Gungormus, M., Fong, H., Sahin, D., Seker, U. O. S.,

Kacar, T., Cetinel, S., Yuca, E., Yazici, H., Kondu, P., Selcuki, C., Karatas, A., Bermek, H., Gul Karaguler, N., Sarikaya, M.,. "Biomolecular Design for Bionanotechnology". Molecular Biomimetics and Bionanotechnology-I Workshop, 12-14 November 2006, MOBGAM, ITU.

- Yuca, E., Memon, A.R., Cevher Keskin, B., 2004, Role of ARF1 and SAR1 in *Medicago truncatula.* 2rd National Molecular Diagnosis Symposium. İzmir/Turkey.

- Cevher Keskin, B., Yüca, E., Memon, A.R., 2003. Regulation of ARF1 and SAR1 GTP-Binding Proteins at Different Developmental Stages in Pea. 13rd National Biotechnology Congress. Çanakkale/Turkey.

- Yüca, E., Memon, A.R., Cevher Keskin, B., 2003, Factors Regulating The Expression and Function of The ARF and SAR families of GTP-Binding Proteins in *Medicago truncatula.* Membrane Trafficking in Plants, Society for Experimental Biology, University of Glasgow/UK.

- Cevher Keskin, B., Memon, A.R., Yüca, E., 2003, Expression of ARF1 and SAR1 Low Molecular Weight GTP-Binding Proteins at Different Developmental Stages in Pea. European Plant Endomembrane Meeting. University of Glasgow/UK.

- Memon, A. R., Cevher Keskin, B., Yüca, E., 2003, Expression of ARF1 and SAR1 GTP- Binding Proteins at Different Developmental Stages in *Pisum sativum.* Annual Meeting, American Society of Plant Biology. USA.

- Memon, A. R., Cevher Keskin, B., Yüca, E., 2003, Tissue Specific Expression of ARF1 and SAR1 GTP-Binding Proteins in Pea. Federation of European Biochemical Societies 28th International Meeting. Istanbul/Turkey.